VEÐURSTOFA ÍSLANDS

Report
05007

Ragnar Stefánsson, Françoise Bergerat, Maurizio Bonafede, Reynir Böðvarsson, Stuart Crampin, Páll Einarsson, Kurt L. Feigl, Christian Goltz, Ágúst Guðmundsson, Frank Roth, Ragnar Sigbjörnsson, Freysteinn Sigmundsson, Peter Suhadolc, Max Wyss, Jacques Angelier, Þóra Árnadóttir, Maria Elina Belardinelli, Amy Clifton, Loïc Dubois, Gunnar B. Guðmundsson, Páll Halldórsson, Sigurlaug Hjaltadóttir, Björn Lund, Símon Ólafsson, Sandra Richwalski, Christoph Sens-Schönfelder, Ragnar Slunga, Ari Tryggvason, Kristín S. Vogfjörð, Barði Þorkelsson

PREPARED – second periodic report

February 1, 2004 - January 31, 2005

VÍ-ES-05
Reykjavík
May 2005

Contents

AUTHORS 4

WP 1 OVERALL COORDINATION OF THE PROJECT 5

WP 2 ANALYSIS OF MULTIPARAMETER GEOPHYSICAL DATA APPROACHING THE JUNE 2000 EARTHQUAKES, ASSESSING STATE OF STRESS 8

WP 2.1 PATTERN SEARCH IN MULTIPARAMETER SEISMIC DATA 11

WP 2.2 POSSIBLE PRECURSORY SEISMIC QUIESCENCE AND B-VALUE CHANGES 15

WP 2.3 LONG-TERM DEFORMATION IN THE SOUTH ICELAND SEISMIC ZONE (SISZ) INFERRED BY JOINT INTERPRETATION OF GPS, INSAR AND BOREHOLE STRAIN DATA 20

WP 2.4 SPACE AND TIME VARIATIONS IN CRUSTAL STRESS USING MICROEARTHQUAKE SOURCE INFORMATION FROM THE SOUTH ICELAND SEISMIC ZONE 23

WP 2.5 USING SHEAR-WAVE SPLITTING ABOVE SMALL EARTHQUAKES TO MONITOR STRESS IN SISZ 28

WP 3 SHORT-TERM CHANGES/PRECURSORS 33

WP 3.1 FORESHOCKS AND DEVELOPMENT OF NEW WARNING ALGORITHMS 36

WP 3.2 RADON ANOMALIES 38

WP 4 A MODEL OF THE RELEASE OF THE TWO JUNE 2000 EARTHQUAKES BASED ON ALL AVAILABLE OBSERVATIONS 42

WP 4.1 SOURCE MECHANISM AND FAULT DIMENSIONS OF THE JUNE 17 AND JUNE 21 EARTHQUAKES DETERMINED FROM MAPPING OF AFTERSHOCKS 49

WP 4.2 WAVEFORM INVERSIONS FOR MOMENT DISTRIBUTION ON THE FAULT 51

WP 4.3 SURFACE FRACTURES IN THE SOURCE REGION OF THE JUNE 2000 EVENTS 58

WP 4.4 DEFORMATION MODEL FOR THE JUNE 2000 EARTHQUAKES FROM JOINT INTERPRETATION OF GPS, INSAR AND BOREHOLE STRAIN DATA 62

WP 5 NEW HAZARD ASSESSMENT/NEW METHODS FOR IMPROVING ASSESSMENT OF PROBABLE EARTHQUAKE EFFECTS 66

WP 5.1 MAPPING SUBSURFACE FAULTS IN SOUTHWESTERN ICELAND WITH THE MICROEARTHQUAKES INDUCED BY THE JUNE 17TH AND JUNE 21ST EARTHQUAKES 68

WP 5.2 MAPPING AND INTERPRETATION OF EARTHQUAKE RUPTURE IN THE REYKJANES PENINSULA AND OTHER SURFACE EFFECTS THERE AND IN THE SISZ 70

WP 5.3 STUDY OF THE STRONG GROUND MOTION, ACCELERATION AND INTENSITIES OF THE TWO LARGE EARTHQUAKES 78

WP 5.4 REEVALUATION OF THE HISTORICAL EARTHQUAKES IN LIGHT OF THE NEW OBSERVATIONS 81

WP 5.5 HYDROGEOLOGICAL CHANGES ASSOCIATED WITH THE JUNE 2000 EARTHQUAKES 82

WP 5.6 PALEO-STRESS FIELDS AND MECHANICS OF FAULTING 86

WP 6 MODELLING AND PARAMETERIZING THE SW ICELAND EARTHQUAKE RELEASE AND DEFORMATION PROCESSES 90

WP 6.1 EARTHQUAKE PROBABILITY CHANGES DUE TO STRESS TRANSFER 92

WP 6.2 MODEL STRESS IN THE SOLID MATRIX AND PRESSURES IN FLUIDS PERMEATING THE CRUST 96

APPENDIX 1 101

APPENDIX 2 105

Authors

WP1	Ragnar Stefánsson and Bardi Thorkelsson, IMOR
WP2	Ragnar Stefánsson and Gunnar B. Gudmundsson, IMOR
WP2.1	Christian Goltz and Christoph Sens-Schönfelder, CAU
WP2.2	Max Wyss, WAPMERR
WP2.3	Thóra Árnadóttir, NVI
WP2.4	Reynir Bödvarsson, Björn Lund and Ari Tryggvason, UU
WP2.5	Stuart Crampin, UEDIN
WP3	Ragnar Stefánsson, IMOR
WP3.1	Ragnar Slunga, UU
WP3.2	Páll Einarsson, SIUI
WP4	Ragnar Stefánsson, IMOR
WP4.1	Kristín S. Vogfjörd, IMOR
WP4.2	Peter Suhadolc, UNIVTS-DST
WP4.3	Páll Einarsson, SIUI
WP4.4	Thóra Árnadóttir, NVI
WP5	Ragnar Stefánsson, IMOR
WP5.1	Sigurlaug Hjaltadóttir and Kristín S. Vogfjörd, IMOR
WP5.2	Amy Clifton, NVI
WP5.3	Símon Ólafsson and Ragnar Sigbjörnsson, UI
WP5.4	Páll Halldórsson, IMOR
WP5.5	Ágúst Gudmundsson, UGOE
WP5.6	Francoise Bergerat and Jacques Angelier, UPMC
WP6	Ragnar Stefánsson, IMOR
WP6.1	Frank Roth and Sandra Richwalski, GFZ POTSDAM
WP6.2	Maurizio Bonafede and Maria Elina Belardinelli, DF.UNIBO
ANNEX 1	Kurt Feigl and Loïc Dubois, CNRS.DTP
ANNEX 2	Sigurlaug Hjaltadóttir and Kristin S. Vogfjörd, IMOR

WP 1 Overall coordination of the project

Objectives

Scientific coordination and management of the PREPARED project.

Methodology and scientific achievements related to workpackages including contribution from partners

The input is reporting on scientific progress in the various workpackages and management reports from the contractors.

Through organizing workshops/coordinator meetings and special meeting sessions the coordinator organizes this multidisciplinary, multinational project towards results expressed in the PREPARED objectives. A PREPARED website organized by the coordinator is a significant tool for this.

The coordinator compiled 6, 12 and 18 months Management Reports about the progress of the project. After the first year of the project the coordinator published an Executive Publishable Summary and a Periodic Progress Report. The present report is the Second Periodic Progress Report but not a Final Report as originally planned after 24 months. With a special amendment 6 months extension was granted for fulfilling the objectives of the project. The Final Report which will be published in due time after the 30 months duration of the project will in addition to Final Scientific Report and Cost Statement Summary, etc., contain a Technical Implementation Plan (TIP).

The coordinator, which also provides a significant part of the data, ensures that the other participants in the consortium can easily access data and results of other participants, as well as giving advices in carrying out the various parts of the project.

The coordinator which has warning duties in Iceland and which also operates and develops an Early Information and Warning System (EWIS) ensures that results of the project will be implemented into the EWIS database, for risk-mitigating purposes in Iceland and be demonstrated for risk-mitigating organizations elsewhere (Roberts et al. 2004, Stefánsson and Guðmundsson 2005).

The end of the first year period of the project and the start of the second year was signified by a two day workshop, i.e. the PREPARED Mid-Term Meeting, held in Reykjavík, January 30-31, 2004. The minutes of the meeting can be found on the URL *http://hraun.vedur.is/ja/prepared.* This meeting was a summing up of the progress of the project. Lead contractors of the various workpackages gave presentations about the status of the work and laid the lines for the second part of the project. Detailed description of this meeting can be found in the First Periodic Report.

Informal meetings of several PREPARED partners were organized during the EGU General Assembly in Nice France, 25-30 April, 2004. Papers relevant for the PREPARED project were presented at the assembly by IMOR staff. These papers, which are referred elsewhere in the report, describe how time-dependent hazard assessments and earthquake warnings are realized in Iceland through joint work in the PREPARED and EWIS projects.

On June 24-25, 2004, the coordinator visited the EC in Brussel to have discussions with Denis Peter and Maria Yeroyanni, the present and the former programme officers of the PREPARED

project, about the status of and possible modifications in carrying out the PREPARED project. Discussions were also with other parts of EC about future cooperation.

Ragnar Stefánsson and Matthew J. Roberts from IMOR participated in the FORESIGHT Kick-Off meeting in Istanbul, September 11-13, 2004. The FORESIGHT project which takes to volcanic eruptions, landslides and tsunamis besides seismic hazard and risk is related to the PREPARED project in its objectives and to the Icelandic EWIS project, which is a common application tool for PREPARED as well as for FORESIGHT.

The PREPARED project results were presented at the XXIX ESC General Assembly in Potsdam, September 10-15, 2004 by IMOR staff (Ragnar Stefánsson and Steinunn S. Jakobsdóttir) and some other partners of the project, as referred to in other WP reports.

The project leader, Ragnar Stefánsson, was invited to an international workshop organized by CRdC AMRA, the University of Napoli and the EU NaRA on Seismic Early Warning for European Cities - towards a coordinated effort to improve the level of basic knowledge, held in Napoli, Italy, September 23-25, 2004, to present there the paper Realization of time dependent earthquake warnings in Iceland and the development of an Early Information and Warning System for geologic hazards (Stefánsson and Roberts 2004). The coordinator participated also in discussion, forming of a consortium and recommendations to EC on seismic early warning activities.

A proposal of the coordinator for a special session on the PREPARED project at the EGU General Assembly in Vienna, Austria, April 24-29, 2005, was accepted. The participants in the project will describe the outcome and progress of the PREPARED project in 30 presentations in this special session (Natural hazard session, NH 4.04). Several presentations related to PREPARED will also be held at other sessions of EGU 2005.

Socio-econimic relevance and policy implication

The social and economic impact of a destructive earthquake is enormous. Well established prognosis of what can be expected is a basis for decision on how and where man-made structures are built may lead to strengthening or removal of existing vulnerable buildings. It is a basis for various technical and social precautions and preparedness, that can mitigate the impact of earthquake hazards in various ways.

The PREPARED project is based on the experiences of the two M=6.6 earthquakes in the South Iceland lowland in year 2000. Earlier earthquake prediction research projects, like the SIL project 1988-1995 and the two PRENLAB projects 1996-2000, aimed at by monitoring and research to prepare for that such an earthquake would occur. The successes in providing long-term hazard assessments for this region before the earthquakes as well as the success during these two earthquakes in providing useful warnings and earthquake information has fostered the hopes among scientists and the public that further progress is possible and the faith in science to be able to mitigate risk by warnings and information. A significant and useful short-term warning was possible shortly before the second earthquake. In the ongoing work there are signs that practical short-term warnings for a “first earthquake” will be possible in the future in Iceland. The faith in science for mitigating earthquake risk is already of enormous socio-economic significance and for the quality of life in this area. The experiences gained in PREPARED in Iceland can be applied in other parts of the world for encouraging work in this field and will create hopes that it is possible to obtain good results in earthquake prediction.

Discussion and conclusions

The project as a whole consists of applying variety of methods for revealing processes leading to earthquakes, and finally of multidisciplinary group work for developing tools that are applicable in early information and warnings. The final outcome of the project thus is very depending on the outcome of all the individual workpackages. Delays in preparation of some basic data and of some workpackages, made it necessary to apply for a 6 months extension of the project. The project is progressing well towards a good outcome and in fulfilling its objectives at the end of the project period on July 31, 2005.

Plan and objectives for the next period

The project is ongoing in accordance with the original work plan and the revised work plan as accepted with the 6 months extension. During the last 6 month period the focus on merging together results from the various workpackages is planned.

References

Roberts, M.J., R. Stefánsson & P. Halldórsson 2004. Internet-based platform for real-time geoscience during tectonic crises in Iceland. EGU General Assembly, Nice, France, April 25-30, 2004.

Stefánsson, R. & M.J. Roberts 2004. Realization of time-dependent earthquake warnings in Iceland and the development of an early information and warning system for geologic hazards. Workshop organized by CRdC AMRA, the University of Napoli and the EU NaRAs on Seismic early warning for European cities, Napoli, Italy, September 23-25, 2004.

Stefánsson, R. & G.B. Guðmundsson 2005. About the state-of-the-art in providing earthquake warnings in Iceland. *Icelandic Meteorological Office - Report*. In press.

WP 2 Analysis of multiparameter geophysical data approaching the June 2000 earthquakes, assessing state of stress

Objectives

Analysis and linking together multiparameter geophysical observations expressing stress or strain induced variations with time approaching the June 2000 earthquakes and after these. Explain the possibly common source for these variations. Explain them physically. Formulate procedures to assess increase or decrease in probability of earthquake hazard on basis of observable multiparameter observations.

Methodology and scientific achievements related to workpackages including contribution from partners

The input is observations and results of evaluations in WP2.1-2.5, and evolving models and evolving crustal parameters in various other workpackages.

Lead contractors from WP2.1-2.5 work with the coordinator in analyzing the multidisciplinary observations. They work also in close cooperation with other groups, especially the modellers. Within WP1 we try to focus the multidisciplinary results of the various WP´s to create tools to help to discover patterns in observations that would help to access time-dependent hazard probability or closeness in time and space to an impending large earthquake, in accordance with the basic objectives of PREPARED.

The work of the lead contractor here has been concentrated on analyzing large amount of seismic data available at IMOR, to create a necessary database for the work of the various WP2.x´s.

During September 2003 this enormous database could be made available for applications. Since then there have been much contacts about applying the data and exchange of data among the partners. All the WP2.x´s have obtained data from the coordinator and discussion has been about the data and an interpretation of them, and modifications made in the database to make more information accessible and to constrain it. Special discussion was arranged among all the partners in connection with the PREPARED Mid-Term Meeting as well as with many of the participants at the EGU General Assembly in Nice 2004.

Analysis of patterns in the seismic data
The coordinator has also carried out analysis of the seismic data, to search for patterns, especially long-term patterns in approaching the two large earthquakes of year 2000, and made this analysis accessible to the partners and workshops, and in reports (see list of reports).

Providing GPS continuous data, strain data and basic analysis of these
The coordinator carries out continuous GPS measurements and strain measurements and these data are significant for the WP2.x´s. Evaluations of these have also been made available to the consortium.

Merging the results of various workpackages into useful assessment tools
In the outcome of the various workpackages several types of patterns and changes are indicated that may be useful for creating a generic long-term assessment or warning tool.

It remains to compare these results in a concerted way, analyze better their physical significance and how well they comply with the emerging models of the PREPARED project. Among suggested patterns for understanding long-term build-up of conditions leading to earthquake are:

● Simple time evolution of seismicity/number of earthquakes with time as well as patterns in spacial distribution of the activity. Also horizontal compressions of individual microearthquake mechanisms (Stefánsson and Guðmundsson 2005).
● Spectral amplitude grouping (SAG) (WP2.4 of this report).
● Stress tensor inversion of microearthquake mechanisms (WP2.4 of this report).
● SRAM analysis (described in WP2.4 of the MT report).
● Analysis of GPS measurements since 1992 show distribution of strain rates in accordance with what would be expected prior to the June 2000 earthquakes (WP2.3 of the MT report, and Árnadóttir et al. 2005).
● Analysis of b-values did not reveal changes as a function of time during a decade before the earthquakes, however spacial variations in their values are significant for detecting a large earthquake asperity (WP2.2 of this report, and Wyss & Stefánsson 2005).
● Analysis of the pre-earthquake seismic pattern by PCA (WP2.1 of this report).
● Analysis of SWS, shear-wave splitting time (WP2.5 of this report).

Merging together these results involves understanding the physical process which they express, both to understand better their significance and generality as well as to plan for observational methods and infrastructures which can make use of the finding for future long-term and medium-term assessments and warnings.

Socio-economic relevance and policy implication

Being able to assess in a qualified scientific way that a large earthquake is approching, its location and size is very significant. It creates background for concentration of various risk-mitigating efforts in the area, like that of civil protection groups, strengthening of structures, etc. It also creates a basis for increased monitoring, earth watch and research to prepare for more definitie short-term warnings.

Discussion and conclusions

Several observable changes are observed in geophysical data in approaching the two June 2000 earthquakes in the SISZ. It remains to explain these changes in light of the general outcome and models emerging in the PREPARED project.

High pore fluid pressures near the bottom of the seismogenic crust appear as a central element in building up conditions for the release of the earthquakes. The earthquake preparation and nucleation process involves build-up of stresses in an area around the fault where fluids from below play a significant role. Approach in the release time of the earthquake the high pore fluid pressures within the system move from a volume distribution at depth within the crust towards the becoming fault and weakening it. The possibility for median-term or short-term predictions may probably be based on observing these changes in real-time.

Plan and objectives for the next period

The last period involves comparing the various observed patterns to each other, explaining them in light of the modelling work of various workpackages of the project.

References

Árnadóttir, Þ., S. Jónsson, F. Pollitz, W. Jiang & K.L. Feigl 2005. Post-seismic deformation following the June 2000 earthquake sequence in the South Iceland seismic zone. Submitted to *J. Geophys. Res*.

Stefánsson, R. & G.B. Guðmundsson 2005. About the state-of-the-art in providing earthquake warnings in Iceland. *Icelandic Meteorological Office - Report.* In press.

Wyss, M. & R. Stefánsson 2005. Nucleation points of main shocks in southern Iceland, mapped by b-value. Submitted.

WP 2.1 Pattern search in multiparameter seismic data

1. Objectives

The occurrence of earthquakes is a complex and highly variable process coupled in space and time. The resulting difficulty to separate superimposed seismicity patterns stemming from different causes impedes the search for anomalies possibly preceding large earthquakes. Within the ideal setting of the PREPARED project the objectives were twofold: confirmation and enhancement of the method on the one hand, application to seismicity in the SISZ on the other to detect long- term premonitory changes before the large events in 2000 and to search for precursors of impending events.

2. Methodology and scientific achievements related to Work Package 2.1 including contribution from partners

Principle Components Analysis (PCA) is a rotational transformation that eliminates correlation in multi-dimensional data. Figure 1 illustrates the properties of PCA: the axes of the outer box A, B and C correspond to the values of the pixels in the time slices (gridded seismicity rates during a given period of time), i.e. the values of a certain pixel in the three time slices represented by a certain point in the figure are given by the coordinates of the point. PCA rotates the coordinate system into the axes plotted in the center of the point cloud. In this new system, which represents the so-called components, the data points are uncorrelated. Applying this transformation to seismicity data, we hope to unveil possibly subtle but physically important constituents of seismicity which are otherwise hidden.

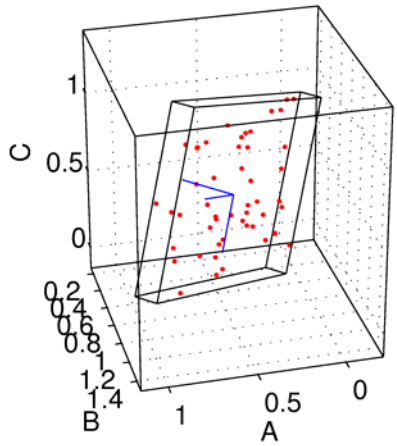

Figure 1. *Principle of PCA for three-dimensional data. Data originally sampled in the A,B,C-coordinate system is transformed such that it is de-correlated in the new coordinate system shown in the center of the point cloud.*

One goal was to assess the physical significance of the components obtained with PCA and to test the dependence on gridding parameters. Such analysis was necessary to establish the stability of our approach after we had previously shown that it works in principle (cf. First Periodic Report). We used three approaches to this problem: 1) the analysis is repeated on a catalogue with events shuffled in time, 2) decompositions obtained using time slices of different length are compared, 3) decompositions obtained using time slices of equal length but different transition dates are compared.

The simplest way of destroying the structure of the events in the catalogue (i.e., the logic of earthquake dynamics) is to shuffle their occurrence times. In so doing, the spatial structure is retained and only temporal relations are changed. Component 1 (C1) is unaffected by this

randomization as it contains the average activity which is the same in the shuffled catalogue. All other components are completely distorted. Figure 2 shows C2 as an example: it contains only random fluctuations now. We measure the significance of the components in terms of the spatial auto-correlation function (ACF). We plot the ACF for C2 of the original and the shuffled data in Figure 3: in the shuffled dataset, the spatial coherence is completely destroyed whereas the original data exhibits correlations on a range up to 40 km. The maximum length of detectable correlation decreases in the higher order components but even in the highest there is some spatial coherence. This confirms that the higher components contain more subtle patterns which tend to have smaller spatial extend. The fact that the spatial structure in the components is destroyed by changing the temporal relation in the data is good evidence that the coherent patterns in the components can neither be generated by chance nor by any step of the decomposition. This means that the coherent patches in the component must be related to physical processes that cause the spatio-temporal structure in the earthquake data. It is these coherent patterns that we expect to emerge and grow prior to large earthquakes.

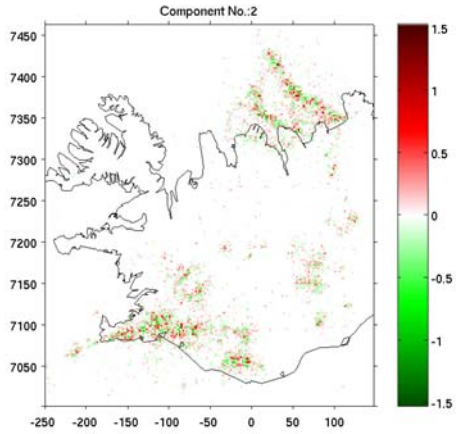

Figure 2. *PCA component 2 represents random fluctuations after the original seismicity data has been shuffled in time, giving evidence that the coherent patches found when transforming original data represent physical patterns. It is these coherent patterns that are expected to grow prior to large events*.

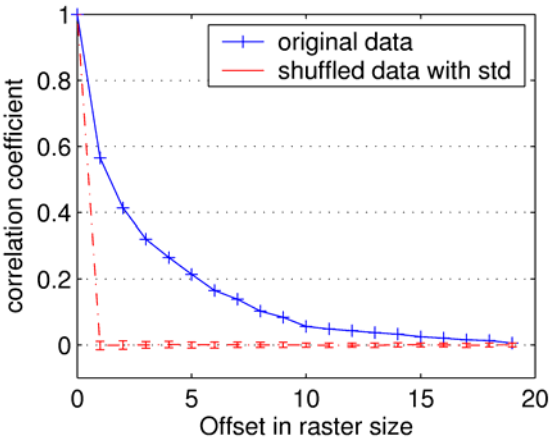

Figure 3. *Spatial auto-correlation function for C2 as obtained from original and shuffled data. Temporally shuffled data thus leads to the destruction of spatial coherence in components as well.*

The effect of the gridding parameters is a minor one and here we only state that the first 30% of the components are not affected by changes in these parameters. Only higher components may experience alteration. This gives us confidence that PCA as applied here is successful in identifying geological processes by their seismicity.

Knowing the physical processes which generate the observed seismicity, it is possible to study subtle patterns which are normally hidden in the dominant background seismicity. Since PCA is a rotational transformation there is an inverse transformation which can be used to reconstruct the time slices (seismicity rates during a given period of time) from the components. This makes it possible to modify the data in the component representation and study the resulting time slices after back transformation. The most useful application is the removal of the first component, i.e. the

background activity. What remains should be anomalous activity, anomalous with respect to the activity that persists during all time slices. These anomalies may be excess seismic activity as well as unusual quiescence.

The example in Figure 4 shows the background reduced activity of the six month before June 2000. The color scale can be understood as excess activity compared to background level while negative values mean that the activity is unusually low. For the decomposition we used only data until June 2000. Seismicity in this period is obviously dominated by an area at the eastern edge of the SISZ. This earthquake sequence accompanied the eruption of the Hekla volcano in February 2000. Otherwise, the activity of Iceland did not differ much from the background level. The ability of this method to isolate accelerated activity by elimination of background seismicity can be used to reconstruct the preparatory phase of the earthquakes in June 2000. Again we only used events that occurred before June 2000. After eliminating the background activity as described above, a threshold is applied to isolate the areas of accelerated activity. The areas of accelerated activity are plotted in Figure 5 with times mapped on a color scale.

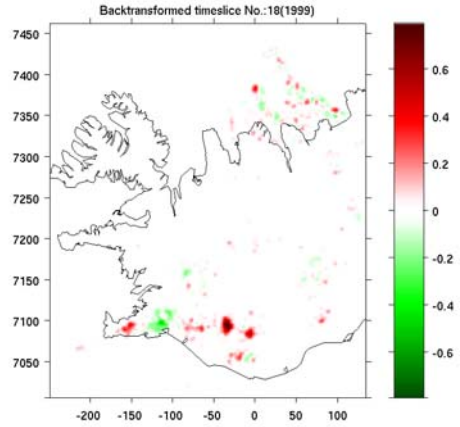

Figure 4. *Seismicity rates during the six months preceding the large events of June 2000 after background activity has been removed by removal of C1 and back-transformation. Positive values represent excess activity with respect to background activity, negative ones signify relative quiescence.*

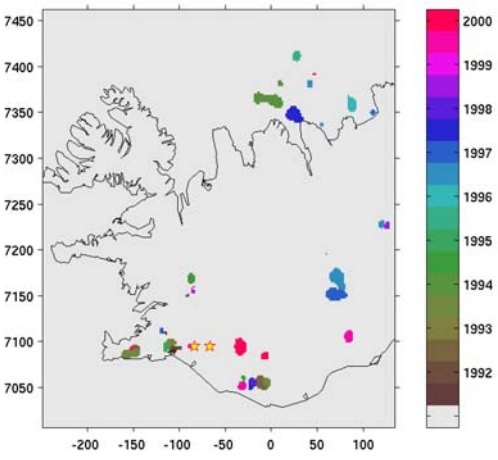

Figure 5. *Coherent regions of activity elevated with respect to average (background) activity prior to the June 2000 events (stars) as obtained by thresholding the back-transformed data. The scale indicates the temporal occurrence of the patterns.*

Several observations can be made from Fig. 5: before 1994 (brownish colors), only areas in SW Iceland exhibited activity well above the background level. This changed in 1994 because of the network expansion. Greenish and bluish colors are spread all over Iceland. In contrast, pinkish colors and red, which mark the activity of the two years before the June 2000 earthquakes, can only be found in South Iceland. Red, indicating the 6 month before the earthquakes, is limited to the close vicinity of the SISZ.

Another objective of the reporting period was to test the temporal resolution of the method. A fundamental constraint to the length of the time slices, which describes the temporal resolution, is given by the number of recorded earthquakes. To ensure a sufficient number of events in the grid of the times slices, there is a trade-off between the temporal and the spatial resolution. A length of the time slices of 6 month appeared to be the optimal choice in order to retain a useful spatial resolution.

3. Socio-economic relevance and policy implications

We further justified our approach by showing that it is able to successfully isolate (subtle) coherent patterns in Icelandic seismicity. These patterns have physical meaning and we are confident that our method can be a valuable contribution to the monitoring of earthquake hazard in Iceland. We have developed and tested a software package which may be used by IMO on a regular basis. The socio-economic relevance of a method for the assessment of time-dependant earthquake hazard is of great importance not only in Iceland but also elsewhere. The main implication of our results is that the method must now be tested in real time.

4. Discussion and conclusions

The analysis of Icelandic seismicity by means of PCA provided insight into how to deal with this complex data and into the dynamics of seismicity patterns. Seismic sequences associated with main shocks on tectonic faults or with volcanic events can clearly be separated very well by our method. This allows studying the temporal evolution of these and more subtle patterns independently of other, possibly dominant, features of seismicity. Our final goal was to identify significant coherent patterns emerging before the earthquakes in June 2000. On the basis of the six-month discretization, we find one dominant feature which emerges in the last time slice before the June events. However, this feature reflects the Hekla volcano eruption in February 2000. Apart from this we do not find patterns that could be unambiguously identified as precursory. We have to point out that our work is one single case study in the application of a new statistical approach to seismicity in Iceland. Clearly, further cases are required before we will be able to ultimately judge the success of our method. It might well be that the strong seismic activity due to Hekla made it impossible to detect a clearer preparatory signal in the statistical sense. Geophysically, we may of course speculate that the unusual activity at Hekla indeed reflects a process that played a role in the stress accumulation which finally caused the earthquakes in June. A continuous application including possible future enhancements of the method at IMO (and elsewhere) seems desirable because PCA proved valuable in studying the space-time dynamics of the complicated seismicity dynamics of Iceland.

5. Plan and objectives for the next period

It is hoped that the regular application of our method/software at IMO will ultimately lead to the identification of precursors for future events. During the use of our software we hope to be able to continuously enhance our method and the software by maintaining a close exchange with IMO. A detailed comparison of results obtained by our approach with that of recent other proposals from statistical physics will also be carried out.

WP 2.2 Possible precursory seismic quiescence and b-value changes

a) Objectives

The ratio of the occurrence of small to large earthquakes in a seismogenic volume is measured by the b-value of the frequency-magnitude distribution (FMD) log N = a – bM (1) (N is the cumulative number, a and b are constants, and M is the magnitude, (Ishimoto and Iida, 1939)). This power law is closely approximated by the observations in the vast majority of volumes other authors and we have investigated, regardless of size. If enough events are available (usually, we use 100 events for b-estimates), even the data from the smallest volumes resolvable (approximately 1 km dimensions) obey equation (1).

Spatial variations of b, ranging from 0.5 to 1.5, are observed ubiquitously over distances of 1 to tens of kilometers (Imoto et al., 1990; Ogata et al., 1991; Ogata and Katsura, 1993; Wiemer and Wyss, 2002). Beneath volcanoes, anomalously high b-values map magma chambers (e.g., (Wiemer and McNutt, 1997), (Sanchez et al., 2003)); along fault zones, anomalously low b-values map asperities (Wiemer and Wyss, 1997; Wyss, 2001). A corollary of the latter observation is that the rupture initiation points of main shocks may be mapped by low b-value volumes (Wyss et al., 2000), and that recurrence times are estimated more correctly, if local b-values are used, rather than averages, derived by mixing seismicity from asperity with those from non-asperity volumes (Wyss and Matsumura, 2002; Zuniga and Wyss, 2001).

Evaluating the stationarity of b-value patterns is difficult in the presence of spatial heterogeneity. In a first rigorous search for violation of stationarity of local b-variations, it was found that in 85% of the volumes investigated, b-values were stationary over three decades at Parkfield, California (Schorlemmer et al., 2004).

Because b-value is inversely proportional to the mean size of earthquakes, as measured by their magnitude (Aki, 1965), b = 2.3/(Mmean-Mmin) (2) (Mmin is the minimum magnitude used and Mmean is the mean magnitude in the sample), mapping b-values is equivalent to mapping mean magnitude. The cited evidence that great differences exist in mean magnitude between adjacent seismogenic volumes, means that the probability for a rupture to reach a given size, once initiated, is different in different volumes. Asperities, with their characteristically low b-values, produce more than average medium magnitude earthquakes, and main shocks are more likely to emanate from these volumes.

One of the main points of this paper is to determine whether or not the hypothesis of the correlation of main shock initiation points with low b-value volumes, holds for southern Iceland. An associated question we investigated is: what are the dimensions of the b-value heterogeneity in southern Iceland? From these dimensions, we propose to derive the dimensions of the seismo-tectonic fabric.

We also seek more information on the possible association of high b-value anomalies with elevated pore pressure. Because fluids are known to play an important role in the tectonics and energy supply of Iceland, this data set offers an opportunity to investigate this question.

The two main shocks of June 2000 constituted a major tectonic event in southern Iceland. Therefore, information is of interest that could contribute to understanding them, and possibly

preparing for future such occurrences. Thus, the target for this study is the seismogenic zone of southern Iceland that generated these two main shocks.

b) Methodology and data

The heterogeneity of reporting as a function of time, space and magnitude is a major problem in all earthquake catalogs. Before studying seismicity patterns, we must define the part of any catalog that is homogeneous in reporting. Because we need as many events as possible for statistical resolution power, we seek to define the largest extent of the homogeneous part in the catalog as a function of time, space and magnitude.

The earthquake catalog for Iceland produced by the Meteorological Office of Iceland offers a version with moment magnitudes, Mw, and one with local magnitudes, ML (Jakobsdóttir et al., 2002). Here, we used Mw because this magnitude, being derived from moments, is physically more meaningful.

First, we determined the onset of the high resolution catalog, using the assumption that the seismicity rate is stationary, except for swarms and aftershock sequences. This assumption is usually well fulfilled, even in relatively small volumes (Wyss and Toya, 2000). In southern Iceland, a strong increase of reported events in small magnitude bands is seen in 1994. However, this increase, and the associated evidence for magnitude changes at that time, is restricted to the Reykjanes peninsula. Magnitude shifts, inadvertent changes of magnitude scale, are a common problem in earthquake catalogs that can introduce errors in studies of seismicity rate and b-value (e. g. (Wyss, 1991; Zuniga and Wiemer, 1999)). To detect these, we scanned the catalog with the algorithm GENAS (Habermann, 1983) and applied magnitude signatures to evaluate the nature of reporting rate changes as a function of magnitude band (Habermann, 1987). In the area surrounding the 2000 main shocks, we found no signals that could be interpreted as magnitude shifts.

The spatial limits of the high-quality catalog depend on the distribution of seismograph stations. By mapping the minimum magnitude of complete reporting, Mc, (Wiemer and Wyss, 2000), we can simultaneously determine the range of magnitudes we can use and the spatial extent over which these magnitudes are reported completely. Using the catalog from 1991 on, Mc in the target area is approximately 0, whereas in the western part of southern Iceland it is substantially higher (Fig. 1). In this Mc-map, the data are averaged over time. Thus, one needs estimates of Mc as a function of time to verify that Mc = 0 is approximately valid from 1991 through the beginning of 2000. This is found to be the case (Fig. 2).

If we use the data from 1994 onward to map Mc, the same pattern as seen for the 1991-2000.46 data in Figure 1 emerges. Thus, one would not gain coverage of additional space, if one sacrificed the pre 1994 data.

Therefore, we define the high-quality catalog since 1991 as covering the southern Iceland seismogenic zone between 20.25°W and 21.3°W, and the magnitude range we used for the study is $Mw \geq -0.1$. This minimum limit, a little lower than the average minimum seen in Figure 2, is selected because, in the analysis to be carried out, the b-value is estimated from magnitudes $M \geq Mc$ for the sample at hand.

The seismicity studied in this paper is restricted to the time before June 2000 because we are interested in determining to what extent the main shocks in that year could have been anticipated.

The few events with depths greater than 20 km are excluded because their hypocenter locations are suspect. The catalog used (Fig. 3) includes 6902 events.

c) Socio-economic relevance and policy implication

This important to understand the tectonic fabric of the earthquake source area.

d) Discussion and conclusion

With $Mc = 0$ in the core area (Fig. 1), the earthquake catalog for southern Iceland shows a lower level of completeness than any other catalog we have analyzed (Wiemer and Wyss, 2000). This level of complete reporting is outstanding and provides an order of magnitude more events for detailed statistical analysis than the best regional catalogs worldwide.

An argument has surfaced on occasion that the power law of the FMD may not continue to hold to arbitrarily small magnitudes (e.g. (Rydelek and Sacks, 1989; Taylor et al., 1990). However, the nearly 7000 earthquakes from southern Iceland show that in this area the power law holds down to magnitude 0.1, at least (Fig. 4). This agrees with the results of Abercrombie and Brune (1994), who showed the same to be true for data recorded in a borehole experiment in southern California. In our opinion, deviations from the power law at small magnitudes is usually due to incomplete reporting of events or mixing of datasets with different *Mc*, as shown by Wiemer and Wyss (2003) for the work of Taylor et al. (1990) and Heimpel and Malin (1998).

As a function of space, the *b*-values vary strongly over distances of only 2 km (Figs. 4 and 5), suggesting that the tectonic fabric is heterogeneous on a small scale. The same small scale heterogeneity is observed when inverting fault plane solutions for stress directions. Unless volumes with radii of about 1 km are used, the inversions show large misfits, indicating that stress directions are heterogeneous. Others have also come to the conclusion that southern Iceland is heterogeneous on a small scale (Einarsson, 1991; Hackman et al., 1990; Stefansson et al., 1993; Stefansson and Halldórsson, 1988), mainly based on detailed fault mapping and on the observation that historical large earthquakes occur on parallel faults, separated by only a few kilometers.

As a function of depth, *b*-values increase in California (Gerstenberger et al., 2001) and Japan (Wyss and Matsumura, 2002). In Iceland this trend also exists (Fig. 6A), but is obscured by pockets of high *b*-values at shallow depth (Figs. 5 and 6B). The method of Gerstenberger et al. (2001) to systematically evaluate the increase of *b* with depth cannot be used here, because the thickness of the seismogenic crust increases from W to E in the middle of our study area (double line in Fig. 6A). However, the close tracking of the bottom of the seismogenic layer with high *b*-values (Fig. 6A) shows that smaller than average earthquakes are preferentially produced along the bottom of the seismogenic crust. This observation can be interpreted as being due to the presence of fluids under pressure.

What is the evidence that high pore pressures correlate with an excess production of small earthquakes (anomalously high *b*-values)? The following list also contains evidence that *b* depends on stress, because the stress level can be reduced by pore pressure. (1) In the seismicity around the waste disposal well near Denver, the *b*-values correlated directly with the strongly fluctuating pressure with which fluids were injected (Wyss, 1973). (2) In laboratory experiments without fluids it was found that *b*-values correlated inversely with stress (Scholz, 1968). This can be interpreted to support the idea that high pore pressures lead to high *b*-values, because ruptures can occur under lower tectonic stresses when the pore pressure is elevated. (3) Inverse correlation of *b* with known stress levels in underground mines (Urbancic et al.). (4) The observation that *b*-values

are anomalously high around magma chambers, which can sometimes be a function of time (e. g. (Wyss et al., 1997)), is also best interpreted as due to high fluid pressure. The most convincing observation supporting this view was made in connection with a magmatic intrusion (Wiemer et al., 1998). These authors mapped the strong increase of *b*-values that occurred instantaneously with the intrusion, within the resolution of the data (a few months), most strongly at the tip of the intrusion, but to a diminished extent at distances of up to 6 km. This observation strongly suggests that an increase of pore pressure caused the increase in *b*-value. (5) The observation of anomalously high *b*-values at about 100 km depth in subduction zones below the volcanic arc suggests that the liberation of water from subducting hydrous minerals may generate at the same time high *b*-values and magma for arc volcanism (Wiemer and Benoit, 1996) (Wiemer and McNutt, 1997) (Wyss et al., 2001). (6) The observation that $b(\text{thrusts}) < b(\text{strike-slip}) < b(\text{normal faults})$ also is interpreted to demonstrate that *b* depends inversely on stress level (Schorlemmer et al, 2004).

The brittle ductile boundary in the SISZ near the two large earthquakes of the year 2000 is at 8-9 km depth beneath the first, 17 June earthquake, and at 7-8 km depth beneath the earthquake of June 21. The second hypocenter was located about 17 km to the west of the first. The temperature at the boundary is estimated to be in the 580°-750° C temperature range (Stefansson et al., 1993; Tryggvason et al., 2002). In the westward prolongation of the SISZ, i.e. 30-40 km to the west of the main shocks of 2000, the Hengill volcanic system, 20 by 20 km in size, exhibits low seismic velocities at 4-10 km depth, and significantly more reduction in the P-velocities than in the S velocities. This is interpreted as indicating that supercritical fluids (of meteoric or magmatic origin) are present in the greatly fractured crust. Slight reduction in the *Vp/Vs* ratio is also observed in the SISZ, below the June 17 earthquake *Vp/Vs* at 4-5 km depth, and below the June 21 earthquake at 6-7 km depth (Tryggvason et al., 2002). The *Vp/Vs* ratio could only be resolved down to 7-8 km depth in the cited study. These low velocity ratios could point to high pore fluid pressures within the 10-20 km wide seismic zone. Interplay between tectonic strain and fluid intrusions from below, within the SISZ, has earlier been suggested on various grounds, most significantly as a possible explanation of the earthquake fault arrangements in space and time within the SISZ e.g., (Stefansson and Halldórsson, 1988).

The interpretation that high *b*-value anomalies are due to local high pore pressure in the Icelandic crust is our preferred choice. This choice is plausible because liquids under high pore pressure are known to be abundant in the study area. Thus, we interpret the patterns of high *b*-value anomalies seen in Figures 6A especially, but also in Figures 5 and 6B and 6C, as due to liquids that penetrate the crust from below and establish pockets of high pore pressure at mid-crustal levels.

The main topic of this paper, the possible correlation of low *b*-values with the source volumes of the two *Ms*6.6 main shocks, seems to support clearly the hypothesis, in spite of the otherwise choppy variations of *b* (Fig. 6). The comparison of the FMDs (Fig. 7) from the volumes surrounding the hypocenter of the three main shock (including the *M*4.5 event of September 1999), also show the contrast clearly. The way one samples around the hypocenter for FMD data does not influence the results much. One can select the nearest 100 to 150 earthquakes in a circle or one can select them by a rectangle parallel to the aftershock zone, the result is about the same. For the definition of the *b*-value in the main shock source volumes, only events that occurred prior to the respective main shocks were used, because the main shocks themselves and their aftershocks would introduce a bias favoring low *b*-values, if they were used. The Utsu test (Utsu, 1992) judges the contrasts to be highly significant.

The idea of calculating local recurrence times is a refinement of the method of probabilistic estimates of recurrence time. In the standard method, the *b*-value is calculated for earthquakes

from a volume recognized as a tectonic volume. Such volumes are often defined as a zone along a particular fault. Recognizing that along such a fault not only the *a*-values, but also the *b*-values can vary strongly it was proposed that the choice of volumes from which to draw samples should be further restricted to those fault segments with uniform *b*-values (Wiemer and Wyss, 1997). From the point of view of statistical analysis, this restriction is required because otherwise the *b*-value of the mixed population does not measure the correct power law relationship of either part of the sample (assuming for simplicity that the fault is made up of a low and a high *b*-value part). From the point of view of fault physics, the separation of sampling is required because the asperities (low *b*-value sections) control the return time of rupture because this is where the accumulation of stress is concentrated.

The map of local recurrence time in cross section shows that very large values (more than 5000 years) are calculated for the majority of samples (brown in Fig. 8), suggesting that main shocks rarely emanate from these locations. The two fault zones are mapped by the lowest *TL*-values. The main shock of 17 June emanated from a low *TL* volume. The June 21 shock, which was triggered by the first one that occurred four days earlier, was located adjacent to the low *TL* zone on that fault. We interpret this to support the hypothesis that main shocks generally emanate from volumes with low *TL* since the first main shock emanated from a low *TL* volume. It is, of course, also possible that ruptures initiated near the major asperity (1 km from the shallow blue zone along the same fault but above the hypocenter of the western main shock in Fig. 8) and manages to propagate into the asperity for generation of the main rupture. The location of the second main shock may not conform exactly to the hypothesis because this was a rupture triggered by the nearby main shock 4 days earlier.

The absolute values of *TL* depend on the selection of the volume size (here R = 2 km) and the expected main shock magnitude (here M6.6). Therefore, they are not necessarily accurate. However, the short values calculated, 500 to 2000 years, are not unreasonable. Direct observations of recurrence times are not available because the same fault segments have not re-ruptured since 1700 (Einarsson and Eiríksson, 1982). The faults that have ruptured strike approximately NS, at distances of about 5 km from each other (Einarsson, 1991; Stefansson and Halldórsson, 1988). Thus, it is likely that recurrence times on individual faults are larger than 300 years.

We conclude that after the fact it is clear that main shocks in southern Iceland emanate from low *b*-value volumes with radii of approximately 2 km, and that both faults that ruptured were mapped by the lowest values for *TL*. These observations agree with the hypothesis that asperities, as preferred main shock initiation points, can be mapped by anomalies of short recurrence time, which are mostly controlled by low *b*-values (larger than average mean magnitude). This has been documented in California (Wiemer and Wyss, 1997), Japan (Wyss and Matsumura, 2002) and Mexico (Zuniga and Wyss, 2001). However, it may be difficult to identify such spots before the main shocks occur because of the small-scale *b*-value heterogeneity (Figs. 4 and 6) and because of the small dimensions of these asperities.

e) Plan and objectives for the next period

Publish the work performed.

WP 2.3 Long-term deformation in the South Iceland seismic zone (SISZ) inferred by joint interpretation of GPS, InSAR and borehole strain data

a) Objectives

The objective of the work package is to evaluate the long term 3D deformation in S Iceland prior to the June 2000 earthquakes, using existing geodetic data. The 3D deformation map will be used to derive a strain map for S Iceland prior to the June 2000 earthquakes, and to search for long-term precursors in geodetic signal.

b) Methodology and scientific achievements related to work packages including contribution from partners

We have analysed all campaign and continuous GPS data collected on Reykjanes Peninsula and in South Iceland from 1992-2004, using the GAMIT/GLOBK software (King and Bock, 2003; Herring, 2003), in collaboration with P10 (Kurt Feigl). The GAMIT/GLOBK solution is in the ITRF2000 reference frame. The GAMIT/GLOBK software estimates velocities and offsets due to different sources during the time period. The velocities represent the average "pre-seismic" (1992-2000) and "post-seismic" (2000-2004) velocity field in SW Iceland. The displacements represent the instantaneous co-seismic offsets in position estimated at the epochs of the two earthquakes on June 17 and June 21, 2000.

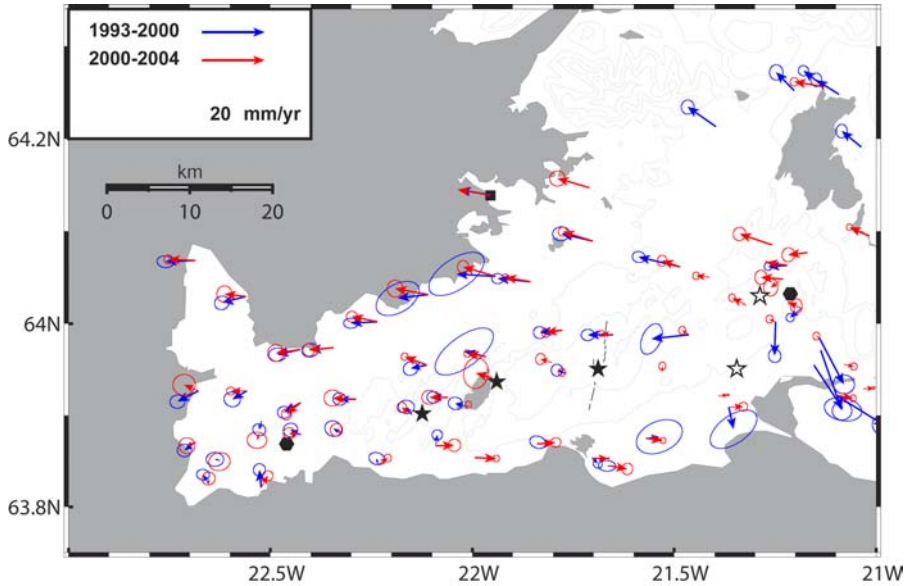

Figure 1. *Horizontal velocity field on Reykjanes Peninsula obtained from GAMIT/ GLOBK analysis, assuming that REYK moves with half REVEL2000 rate (Sella et al, 2002). The pre-seismic (1992-1999) velocities are shown with blue vectors, and the average post-seismic velocity field (2000-2004) with red vectors. The black stars show locations of triggered M~5 earthquakes on June 17, 2000. White stars show locations of M~5 earthquakes in 1998. The black hexagon indicates the location of the Mogi point source from Feigl et al. (2000).*

The horizontal velocity field on Reykjanes Peninsula for the pre and post-seismic period, derived using GAMIT/GLOBK, shown in Figure 1. The figure shows some slight changes in velocities on Reykjanes Peninsula between the two time intervals, 1992-2000 and 2000-2004. The most

significant change in velocities is in the region of the Hengill volcano (black hexagon in Figure 1). From 1993-1998 the Hengill triple junction experienced an increase in seismicity and a rate of uplift of about 20 mm/yr (*Sigmundsson et al.,* 1997; *Feigl et al*., 2000). The effect of the inflation at Hengill is observed by high GPS station velocities in the area from 1992-1999 (blue arrows) compared to lower velocities from 2000-2004 (red arrows). The velocity perturbation seems to extend out to about 15 km west of Hengill. Another area showing a small change of velocities is near the epicenter of the Kleifarvatn 2000 event. At least two stations south of Kleifarvatn seem to have higher eastward component of motion after the June 2000 earthquakes than before.

A comparison between the pre-seismic (1992-1999) and post-seismic (2000-2004) velocity field in the south Iceland seismic zone is shown in Figure 2.

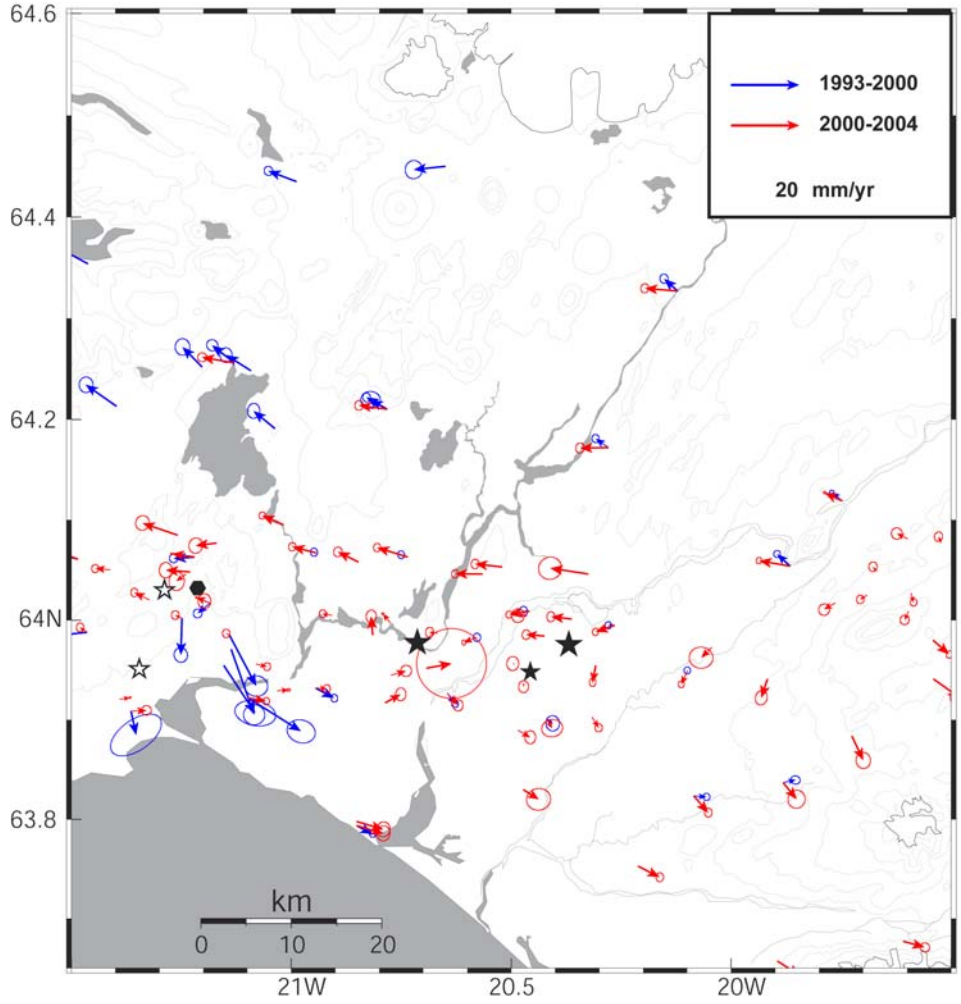

Figure 2. *Horizontal velocity field in the SISZ obtained from GAMIT/GLOBK analysis, assuming that REYK moves with half REVEL2000 rate (Sella et al, 2002). The pre-seismic (1992-1999) velocities are shown with blue vectors, and the average post-seismic velocity field (2000-2004) with red vectors. The large black stars show locations of the June 17 and June 21, 2000, mainshocks.*

The post-seismic velocities are higher than the pre-seismic velocities in the SISZ, in particular at stations north of the June 2000 earthquakes. The velocities can be explained by afterslip at 8-14 km depth below the coseismic ruptures, or by viscoelastic relaxation. The preferred viscoelastic models have lower crustal viscocities of 0.5-1.0 x 10^{19} Pa s and upper mantle viscosity of about 3 x 10^{18} Pa s. The details of the post-seismic velocity field and modelling are described in a manuscript submitted to *J. Geophys. Res* (Árnadóttir et al., submitted 2005).

c) Socio-economic relevance and policy implication

The velocity field during the pre-seismic time interval has been used to estimate the pre-seismic strain field. The post-seismic velocity field in the SISZ has been used to estimate source of post seismic deformation and estimate stress changes due to the post seismic deformation.

d) Discussion and conclusions

This work package is on schedule and will produce the post-seismic as well as the pre-seismic velocity field in SW Iceland

e) Plan and objectives for the next period

In the next period we plan to complete a manuscript describing the results of the GAMIT/GLOBK analysis of the pre- co- and post-seismic GPS data, and submit to J. Geophys. Res. for publication.

References

Árnadóttir, Th., S. Jónsson, F. Pollitz, W. Jiang, and K. L. Feigl, Post-seismic deformation following the June 2000 earthquake sequence in the south Iceland seismic zone, submitted to *J. Geophys. Res*, 2005.

Feigl, K.L., J. Gasperi, F. Sigmundsson, and A. Rigo (2000), Crustal deformation near Hengill volcano, Iceland 1993-1998: Coupling between magmatic activity and faulting inferred from elastic modeling of satellite radar interferograms, *J. Geophys. Res*, 105, 25655-25670.

Herring, T.A. (2003), GLOBK: Global Kalman filter VLBI and GPS analysis program version 4.1, Mass. Inst. Technol., Cambridge.

King, R.W., and Y. Bock (2003), Documentation for the GAMIT Analysis Software release 10.1, Mass. Inst. Technol., Cambridge.

Sella, G., T. Dixon, and A. Mao (2002), REVEL: A model for recent plate velocities from space geodesy, *J. Geophys. Res.,* 107, ETG 11-1-31, doi:10.1029/2000JB000033.

Sigmundsson, F., P. Einarsson, S. Th. Rögnvaldsson, G. Foulger, K. Hodgkinsson, and G. Thorbergsson (1997), The 1994-1995 seismicity and deformation at the Hengill triple junction, Iceland: Triggering of earthquakes by minor magma injection in a zone of horizontal sher stress, *J. Geophys. Res*, 102, 15151-15161.

WP 2.4 Space and time variations in crustal stress using microearthquake source information from the South Iceland seismic zone

1 Objectives

The main purpose of the WP 2.4 is to utilize the unique data set provided by the SIL-network to analyze the SISZ using various type methods and algorithms. In this report we will show results from four type of methods and algorithms: a) Spectral Amplitude Grouping, b) Stress Tensor Inversion and d) Earthquake waiting time distributions and scaling law analysis.

2 Methodology and scientific achievements

2.1 Spectral Amplitude Grouping

The variations in Spectral Amplitude Grouping (SAG) (Lund and Bödvarsson, 2002) temporal grouping results for the SIL area reported earlier (PREPARED, First periodic report), prompted us to revisit the grouping algorithm in order to confirm the results and gain further insight into the grouping processes.

The algorithm described in Lund and Bödvarsson (2002) has been complemented by a number of standard hierarchical cluster linkage algorithms (Murtagh and Heck, 1987), such as single, complete, average, median, centroid and minimum variance linkage. We find, as expected, that the original Lund and Bödvarsson (2002) algorithm performs similar to the complete (furthest neighbor) and minimum variance linkage methods, i.e. the clusters formed are relatively small with a very high degree of correlation among all group members. In comparison, the single (nearest neighbor) and centroid linkage algorithms form clusters with a large number of events of less homogeneity. Preliminary investigations of the temporal grouping pattern indicates that for homogeneous clusters, the pattern reported earlier remains. If clusters, however, are allowed to expand on the patterns is distorted. Detailed studies of the SAG grouping pattern in the SIL area will be reported later in the project, here we conclude that the large scale SAG anomaly in 1996 seems to be a very stable feature, as is the anomaly associated with the June 2000 events.

2.2 Stress Tensor Inversion of Earthquake Focal Mechanisms

Stress Tensor Inversion of Earthquake Focal Mechanisms. In order to investigate the temporal evolution of stress in the source areas of the two large earthquakes of June 2000, we used the SAG method to form groups of 50 events that do not have similar mechanisms. The groups are formed in time order, with each group having 50% event overlap with the preceding group. The events' focal mechanisms were then inverted for the causative state of stress using the method of Lund and Slunga (1999). As the state of stress might vary both in time and space, it is important to assess both the temporal and spatial distribution of the groups intended for inversion. We show here an example from the source area of the June 21 earthquake, a continuation of the work reported in the first report. In Fig. 1 we plot the events used in the present study, and the division of the source region into four study areas approximately according to the focal mechanism quadrants of the June 21 event. These areas are on the order of 5 km by 7 km large, encompassing between 650 (A) and 1800 (D) events usable for this study. As can be seen in Fig. 1, the events are not evenly distributed in space throughout the four areas and we can, therefore, expect small spatial shifts in the locations of the groups in the temporal inversions.

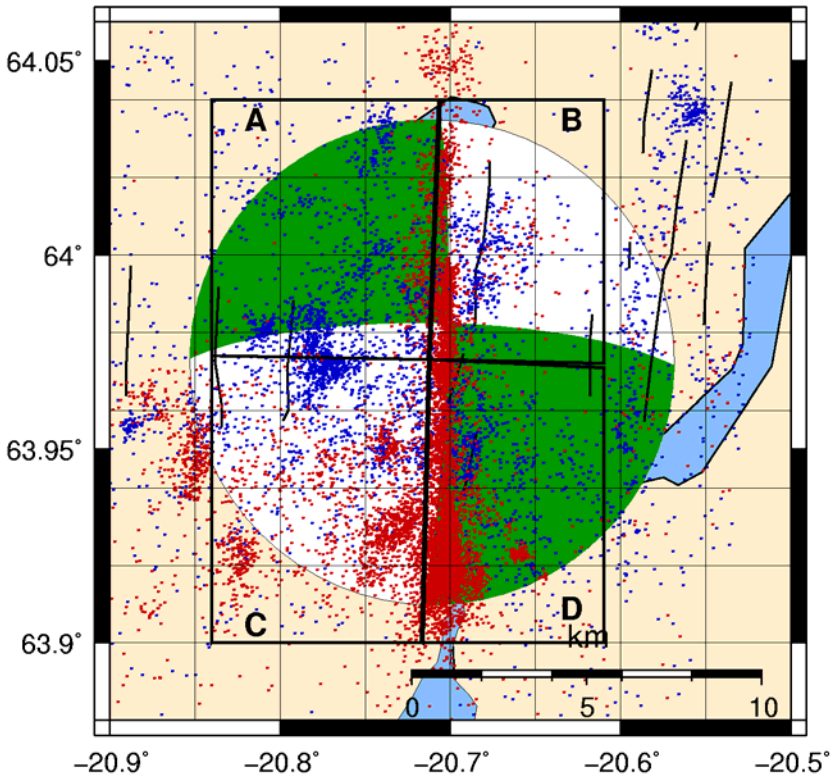

Fig. 1. *Map of the June 21, 2000, source area in southern Iceland. Blue dots are events from Jan 1, 1991 to June 16, 2000. Red dots are earthquakes from June 17, 2000 to December 31, 2002. The black squares indicate the areas from which we used data in the stress study.*

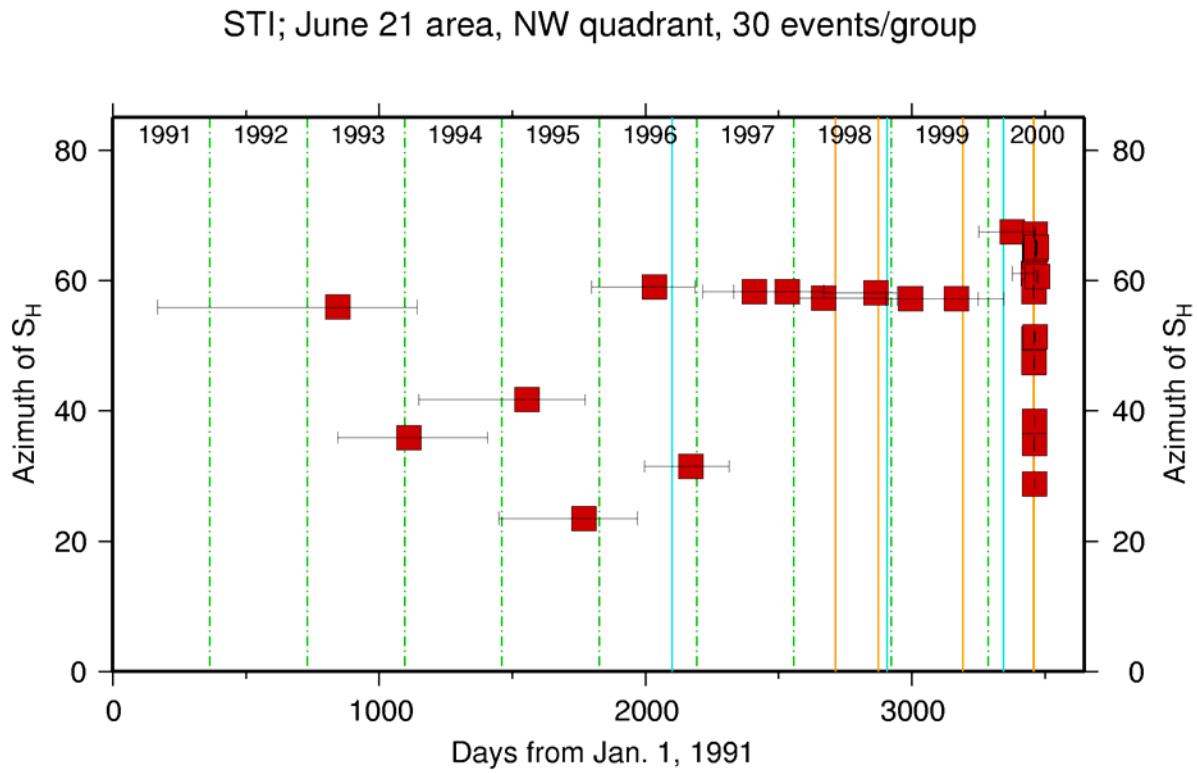

Fig. 2. *Direction of the maximum horizontal stress, with respect to north, versus the number of days since Jan1, 1991, in the NW quadrant of the June 21 earthquake. Horizontal bars on the data points show the time period of the data, vertical orange lines indicate larger earthquakes in the SISZ and light blue lines show volcanic eruptions in South Iceland. Vertical dashed lines delineate the years.*

In Fig. 2 we show the result of the inversions, in terms of the direction of the maximum horizontal stress, SH, in the NW quadrant, area B. The most interesting feature of Fig. 2 is perhaps the remarkable stability in the direction of SH from 1997 through 1999. We also see that that, with the exception of the mid 1996 value, there seems to be an east-west ward shift in the directions of SH from 1996 to 1997. Examining the mid-1996 inversion more closely, most of SH directions in the two-sigma confidence interval cluster around N35W with only a few solutions, albeit the best fitting one, at N60W. The misfits on all inversions in Fig. 2 are very low, supporting the notion of a shift in SH in the NW quadrant (B) to a more steady N60W direction after 1996. Looking instead at Fig. 3, the SE quadrant (C), we see no evidence of a constant SH direction between 1997 and 1999. There is an overall tendency toward a north-south ward shift overall between 1991 and 1998, but with large variations. There was a magnitude 4.3 earthquake in this area in 1999, which is the cause of the many data points in late 1999. The examples of Fig. 2 and 3 show how varying the stress tensor estimates are with just a 5-10 km shift in study location. Some of the variance in the estimates within the study areas may also e due to spatial averaging. We are currently investigating statistical methods to help us assess the uncertainty in the stress estimates, along with more detailed stress studies in the whole of the South Iceland Seismic Zone.

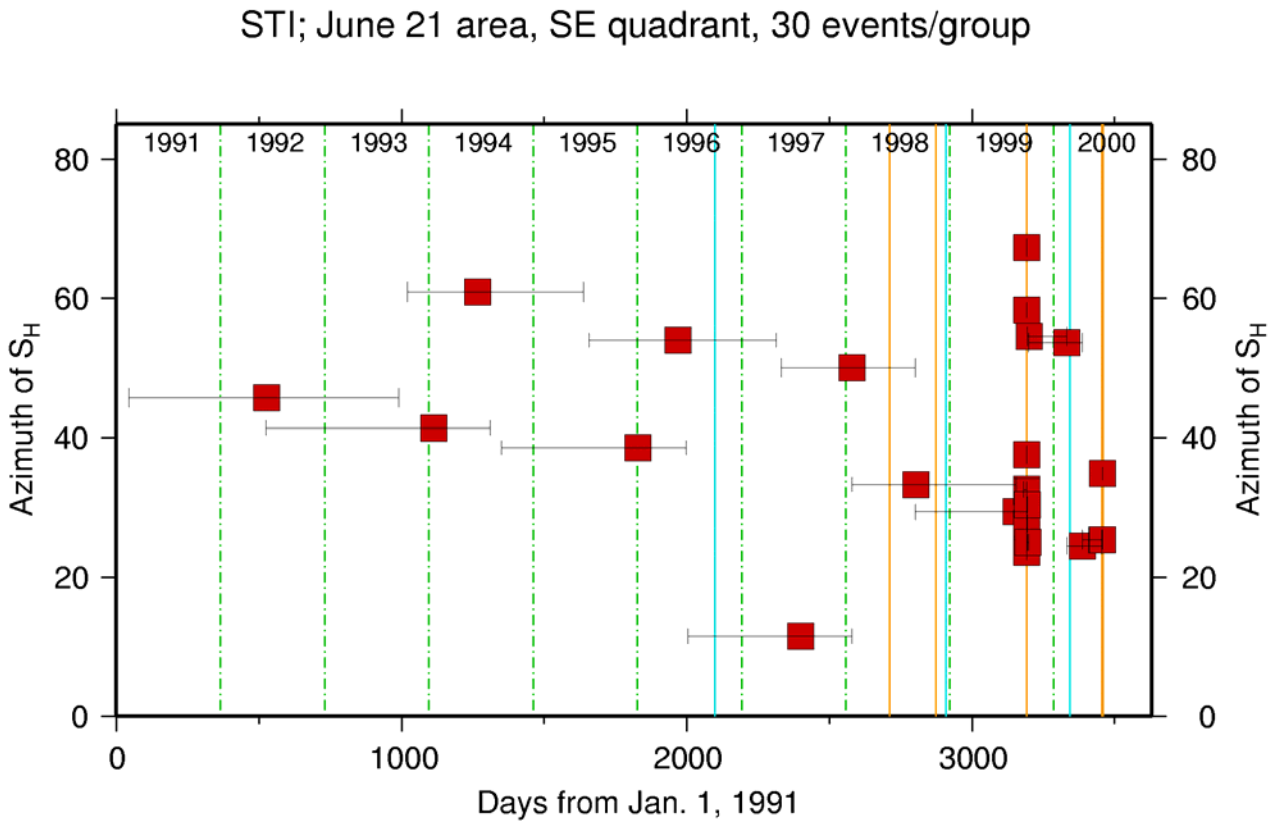

Fig. 3. *Direction of the maximum horizontal stress, with respect to north, versus the number of days since Jan1, 1991, in the SE quadrant of the June 21 earthquake. Lines as in Fig 2.*

2.3 Earthquake waiting time distributions and scaling laws

Recently, several authors (Bak et al. (2002); Christensen et al. (2002); Corral (2003); Corral (2004a); Corral (2004b)), have used waiting time distributions for large earthquake datasets to study the temporal and spatial scaling behaviour of earthquakes and draw conclusions regarding the physics of earthquake processes.

In a region dominated by aftershock activity a typical waiting time distribution is dominated by power law behaviour, but with significant deviation at the longest and the shortest waiting times. The power law regime reflects the Omori law for the decay of the rate of aftershocks while the deviations at short and long waiting times have been interpreted differently. At short waiting times the deviation is often assumed to reflect "data loss" while at long waiting times the deviation has been considered to be due to a regime of uncorrelated earthquakes.

Rescaling waiting time distributions from analyses using different magnitude thresholds and spatial ranges leads to a "collapse" of the data onto a single curve. This "data collapse" has been interpreted by some previous authors as evidence that we observe a self-organised critical system and that the position of a change in gradient demarks a change from correlated to uncorrelated behaviour, of great physical significance.

We show, theoretically and by simulation, that the deviation from power law behaviour at long waiting times is simply due to an effectively finite aftershock sequence. This implies that: 1) the position of a change of gradient in rescaled waiting time distributions does not have the physical significance of separating correlated and uncorrelated earthquakes and 2): the "data collapse" cannot be taken as evidence of earthquakes being a self-organised critical phenomena.

The basic theory of distributions in the waiting time domain has been shown and, illustrated using numerical simulations and some examples of real data from Iceland.

The following papers have been submitted:

Modelling earthquake temporal occurrence; Poisson and Omori delay time distributions. Kristin Jonsdottir, Mattias Lindman, Roland Roberts, Björn Lund, Reynir Bödvarsson. Submitted to Geophys. J. Int.

Earthquakes Descaled: On Waiting Time Distributions and Scaling Laws. Mattias Lindman, Kri stin Jonsdottir, Roland Roberts, Böjrn Lund, Reynir Bödvarsson. Submitted to Physical Review Letters, accepted 2005-02-14.

3 Socio-economic relevance

This research is a contribution to a better understanding of the deformation processes in the SISZ and other seismic areas in general. This can be of importance for possible future earthquake predictions which would be of important value for the society.

4 Discussion and conclusion

In this report we have tried to give information on the ongoing research and the very preliminary results that we have available. We feel that the preliminary results from the various methods described above are promising and will contribute to a better understanding of the ongoing processes in the seismogenetic crust in SISZ.

5 Plan and objectives for the next period

We will continue working according to our original plans and implement some of the algorithms for real-time use at Icelandic Met. Office. We will participate in the PREPARED meetings and some international meetings.

References

Lund, B and R. Bödvarsson, Correlation of microearthquake body-wave spectral amplitudes, Bull. Seis. Soc. Am., 92, 2410-2433, 2002.

Lund, B and R. Slunga, Stress tensor inversion using detailed microearthquake information and stability constraints: Application to Ölfus in southwest Iceland, J. Geophys. Res., 104, 14947-14964, 1999.

Murtagh, F. and A. Heck, Multivariate Data Analysis, D. Reidel Publishing Company, Dordrecht, Holland, 1987.

Bak, P., Christensen, K., Danon, L. & Scanlon, T., 2002. Unified scaling law for earthquakes, Phys. Rev. Lett., 88, 178501.

Christensen, K., Danon, L., Scanlon, T. & Bak, P., 2002. Unified scaling law for earthquakes, Proc. Natl. Acad. Sci. USA, 99, 2509-2513.

Corral, A., 2003, Local distributions and rate fluctuations in a unified scaling law for earthquakes, Phys. Rev. Lett., 68, 035102.

Corral, A., 2004a, Long-term clustering, scaling, and universality in the temporal occurrence of earthquakes, Phys. Rev. Lett., 92, 108501.

WP 2.5 Using shear-wave splitting above small earthquakes to monitor stress in SISZ

a) Objectives

Overall objectives are to develop the technology and understanding of shear-wave splitting to stress-forecast earthquakes.

Specific Objectives (from Description of Work, September 2004)

A1) Continue monitoring shear-wave splitting (SWS) above small earthquakes in SISZ and elsewhere.
A2) Evaluation of stress-induced SWS changes in SIL-data since 1991, to be correlated with other methods for improved stress-forecasting.
A3) Identify the build-up of stress (from 1) as a basis for stress-forecasts.
A4) Develop automatic analysis of shear-wave splitting by artificial neural networks (ANN) techniques.
A5) Develop training sets for ANN that preserve interpreter's experience for individual seismic stations.

b) Methodlogy and scientific achievements

B1) ***Referring to Objective A1: Continue monitoring shear-wave splitting***

We have continued monitoring shear-wave splitting (SWS) at the eight stations (BRE, BJA, FLA, GRI, HED, KRI, SAN, SAU) where there is sufficient seismic activity (more than one event each month, say, within the shear-wave window) to monitor temporal changes in SWS (see B2 and B3, below). We are currently up-to-date as of 31st January, 2005.

Originally, measurements were made from hard-copy playouts of three-component seismograms rotated into preferred orientations where the orientations were derived from three-dimension sections of particle-motion diagrams (hodograms).

We have now developed a semi-automatic Shear-Wave Analysis System for measuring SWS parameters which can then be optimised by user-friendly processes (see B4, below). This greatly speeds up measuring SWS without resorting to hard-copies.

B2) ***Referring to Objective A2*: *Evaluation of stress-induced SWS since 1991***

Previously, we were could not identify changes in shear-wave splitting before the three large earthquakes in SISZ in June 2000 (two over *Ms* 6.6), because there was a 6-week gap in shear-wave source earthquakes at Station SAU at the beginning of a 6-month increase in time-delays. This increase of time-delays in Band-1 of the shear-wave window is the primary phenomenon for forecasting the time and magnitude of impending earthquakes, see Figure 1 of Volti & Crampin (2003).

There have been three advances in data and data analysis since Figure 1 was drawn.

1) The Iceland seismic catalogue was extended (courtesy of the PREPARED project) to lower magnitude events down to M 0.0. This greatly enlarges the number of time-delay data, which is now reasonably adequate for the whole of 2000.
2) We now use a newly developed Shear-Wave Analysis System (SWAS) for semi-automated measuring of time-delays and polarisations (see B4, below).

3) The third advance lessens the impact of clustering in the plots of time-delay variations. Earthquakes frequently cluster in time and space and, if such swarms occur within the shear-wave window, as at the ends of February and March, 2000, in Figure 1, the swarm activity tends to dominate the least-squares fit to the data (Fig. 1). We now lessen the impact of data clustering by only plotting the daily-average of time-delays.

These improvements lead to clear definition of both the increase in Band-1 time-delays (interpreted as imaging stress-accumulation) and the precursory decrease at Station SAU and now also at BJA in Figure 1.

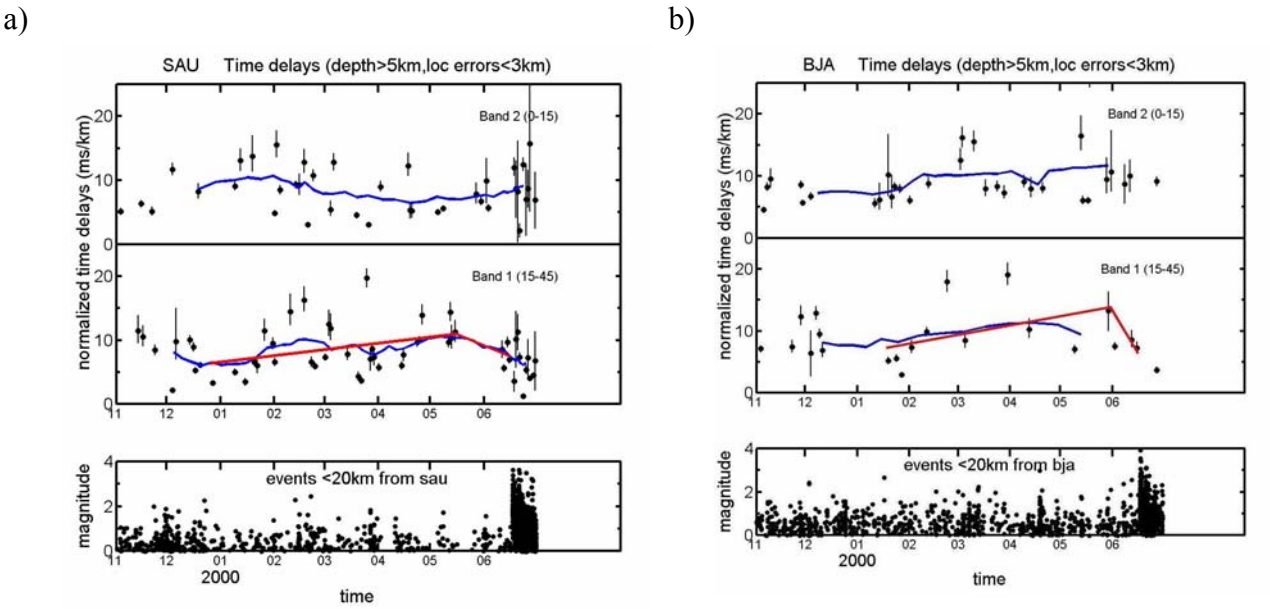

Figure 1. *Temporal increases and decreases before the Ms 6.6 June, 2000, earthquakes.*

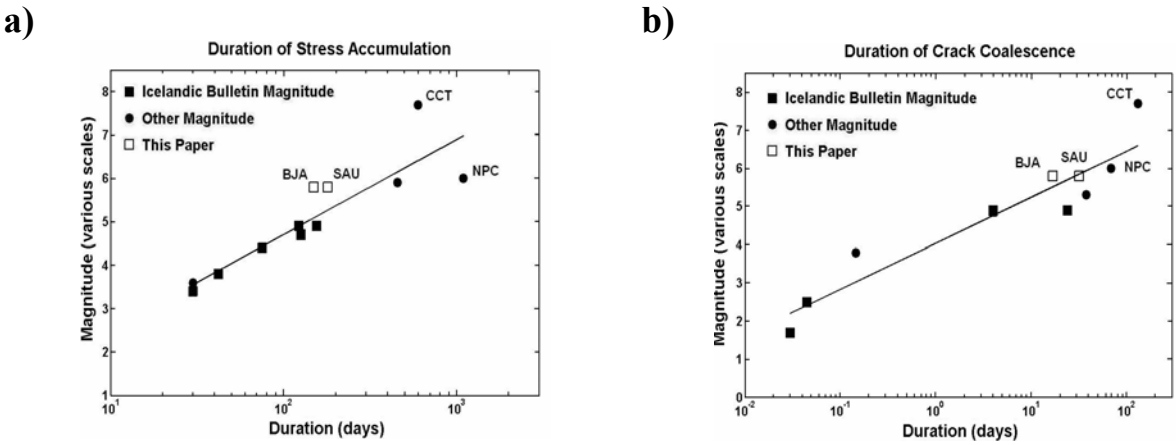

Figure 2. *Duration-magnitude relationships for (a) increases of time-delays and (b) precursory decreases before earthquakes in Iceland (solid squares) and worldwide (solid circles) (Wu & Crampin 2005). The June. 2000, events are open squares for stations BJA and SAU (Figure 1). Points marked CCT and NPS refer to the 1988 North Palm Springs Earthquake, on the San Andreas Fault in California, and the 1999 Chi-Chi Earthquake in Taiwan. CCT and NPS are in subduction zones and strike-slip tectonics and rates of strain accumulation are likely to be different from the spreading centre tectonics of Iceland.*

Both increases and decreases have the typical magnitude-duration relationships (Figure 2) seen in Iceland and elsewhere.

B3) ***Referring to Objective A3: Identify the build-up of stress as a basis for stress-forecasts.*** A stress-forecast (SF102) has been issued in confidence to IMO where the increase in time-delays has continued for some three years.

B4) ***Referring to Objective A4. Develop automatic analysis of shear-wave splitting by artificial neural networks (ANN) techniques.***
Extensive investigation of Artificial Neural Networks by ourselves and others did not produced useful results. Elsewhere, Liu *et al.* (2004) have developed a wholly automatic-correlation technique of Silver and Chen (19) cross for measuring shear-wave splitting. They claim it is successful, but only by eliminating some 70% of the earthquake signals. Such reduction in data points is seldom useful in evaluating changes before earthquakes, as can be seen by eliminating 70% of the points in Figures 1a and 1b. Liu *et al.* (2004) claimed they did not see changes in shear-wave splitting during the *aftershock* sequence of the 1999, Chi-Chi Earthquake, Taiwan. Crampin & Gao (2005) showed that the figure in Liu *et al.* (2004) showing variations *before* the earthquake showed exactly the same variations as we see elsewhere in Figure 1, for example. These are the "CCT" points in Figures 2a and 2b.

We have developed a semi-automatic Shear-Wave Analysis System (SWAS) - a separate report on SWAS is one of the main priorities before the end of the project. In summary, SWAS uses an Expert Analysis System to determine initial values of time-delays and polarisations, usually obtaining values are within few sample points of best estimates. The advantage of SWAS is that it has a user-friendly format for rapidly adjusting time-delays and polarisations by comparing three images:

(i) EW, NS, vertical, horizontal-radial and horizontal-transverse seismograms;
(ii) Particle-motion diagrams (hodograms) for sagittal, transverse, and vertical planes, where picked sample points can be 'stepped' along the record until effects are optimised; and
(iii) EW, NS, vertical, and horizontal-fast and horizontal-slow seismograms rotated parallel and perpendicular to the selected polarisation.

The ease of adjusting, evaluating, updating files, and plotting diagrams makes optimisation of shear-wave splitting measurements rapid and comparatively effortless.

We suggest that SWAS is a major break through in measuring polarisations and time-delays of shear-wave splitting. We intend to make SWAS available, of course, to PREPARED Partners, but also to seismologists elsewhere.

B5) ***Referring to Objective A5: Develop training sets for ANN***
Since ANN is not a useful concept for measuring shear-wave splitting, there is no need for training sets, and this objective of the Workpackage is abandoned.

c) Socio-economic relevance and policy implication

We consider the advances in understanding fluid-rock deformation developed during the EC PRENLAB, SMSITES, and PREPARED Projects allow us to stress-forecasting the time and magnitudes of impending large earthquakes. The SMSITES Project was the development of a prototype Stress-Monitoring Site (SMS) for controlled-source monitoring of shear-waves. SMITES showed spectacular sensitivity to equivalent energy to a M 3.5 earthquake at 70km-distance, confirming that SMS would be able to recognise stress accumulation, and reliably forecast, all damaging earthquakes ($M > 5$, say) within ~400km of the SMS.

This gives the opportunity for GEMS: a global network of SMSs, both onshore and offshore (~70% of earthquakes are offshore), on a grid of ~400km in seismic areas and ~1000km in stable continental shields and oceanic basins (Crampin *et al.* 2005).

Benefits of GEMS:

- Forecast all damaging earthquakes worldwide, with warnings from a week, say, before *M* 5 earthquakes to a year or more before *M* 8 events.
- Provide a stress-forecasting service analogous to the weather forecasting service for a longer-term overall monitoring of variations in the stress field of the dynamic Earth.
- Monitor release of stress by massive hydraulic fracturing when vulnerable cities are threatened by stress accumulation.
- Provide borehole sites for other geophysical measurements currently disturbed by surface noise.
- Provide for the first time data about the dynamic evolution of the earth, about which we know surprisingly little. Richard Feynman wrote that "*Strange as it may seem, we understand the distribution of matter in the interior of the sun much better than we understand the interior of the earth*." GEMS would help to eliminate Feynman's anomaly at the beginning of the 21st century.

Once GEMS had been set up, staff trained, and background stress-levels established, in principle, no one need ever die in an earthquake (or tsunami) again. (Stress-accumulation offshore would indicate the possibility of tsunamis.)

It is suggested that GEMS is of great Socio-Economic Relevance, and that setting up GEMS should be an EC policy objective.

d) Discussion and conclusion

The new understanding fluid-rock deformation developed, tested, and proved during the EC PRENLAB, SMSITES, and current PREPARED Projects appears to be a fundamental advance in understanding how *in situ* rock behaves. Variations in shear-wave splitting are directly correlated with low-deformation, so that comparatively simple analysis of shear-wave splitting above small earthquakes can monitor the accumulation of stress before larger earthquakes. The time and magnitude of the impending event can be estimated from the time and duration, respectively, that levels of fracture criticality (at the percolation threshold) are reached. Unfortunately, swarms of earthquakes are far too scarce for routine forecasting and a forecasting service requires networks of borehole stress-monitoring sites (SMSs). It suggested that a global network of SMSs could forecast the times and magnitudes of all damaging earthquakes worldwide.
The importance of other earthquake studies is identifying the likely source zone by precursor studies, such as was done in the successful stress-forecast (Crampin *et al.* 1999).

e) Plan and objectives for the next period

Further optimisation and availability of SWAS and monitoring of stress-forecast SF102. Complete papers Gao & Crampin (2005) and Wu & Crampin (2005).

References

Crampin, S., Volti, T. & Stefánsson, R., 1999b. A successfully stress-forecast earthquake, *Geophys. J. Int.,* **138,** F1-F5.

Crampin, S. & Gao, Y., 2005. Comment on "Systematic Analysis of Shear-Wave Splitting in the Aftershock Zone of the 1999 Chi-Chi, Taiwan, Earthquake: Shallow Crustal Anisotropy and Lack of Precursory Changes," by Liu, Teng, and Ben-Zion: Temporal Variations Confirmed, *Bull. Seism. Soc. Am.,* in press.

Crampin, S., Zatsepin, S. V., Browitt, C. W. A., Keilis-Borok, V. I., Suyehiro, K., Gao, Y. and Walter, L., 2005. GEMS: the opportunity for forecasting all damaging earthquakes worldwide, *Bull. Seism. Soc. Am.,* submitted.

Gao, Y. & Crampin, S., 2004. A further stress-forecast earthquake (with hindsight), where migration of source earthquakes causes anomalies in shear-wave polarisations*, Geophys. J. Int.,* **Fast Track,** in preparation.

Liu, Y., Teng, T.-L. & Ben-Zion Y., 2004. Systematic analysis of shear-wave splitting in the aftershock zone of the 1999 Chi-Chi earthquake: Shallow crustal anisotropy and lack of precursory variations, *Bull. Seism. Soc, Am*., **94,** 2330-2347.

Liu, Y., Ben-Zion, Y. & Teng T.-L., 2005. Reply to Comment by Crampin and Gao on "Systematic analysis of shear-wave splitting in the aftershock zone of the Chi-Chi, Taiwan, Earthquake: Shallow crustal anisotropy and lack of precursory changes," by Liu, Teng, and Ben-Zion, *Bull. Seism. Soc. Am*. **95,** in press.

Volti, T. & Crampin, S., 2003. A four-year study of shear-wave splitting in Iceland: 2. Temporal changes before earthquakes and volcanic eruptions, in *New insights into structural interpretation and modelling,* ed. Nieuwland, D. A., *Geol. Soc. Lond., Spec. Publ.,* **212,** 135-149.

Wu, J. & Crampin, S., 2005. Smaller source earthquakes and improved measuring techniques allow the largest earthquake in Iceland to be stress-forecast (with hindsight), *Geophys. J. Int.,* **Fast Track,** in preparation.

WP 3 Short-term changes/precursors

Objectives

Analysis of observed short-term changes in various measurements, especially before the large earthquakes. Test and develop multidisciplinary short-term warning algorithms.

Methodology and scientific achievements related to workpackages including contribution from partners

The input here is basically analysis and deliverables, warning algorithms/detection of short-term anomalies of WP3.1 and WP3.2, as well as analysis of seismic patterns carried out by the coordinator within WP3 (Stefánsson and Gudmundsson 2005). Also related deliverables from several other workpackages of the project which provide results applicable for developing new warning algorithms, such as WP2.1, 2.2, 2.3, 2.5, 4.1, 5.5 and 6.2.

Automatic warning procedures of different types are already operated by the coordinator, IMOR. An alert system based mainly on seismicity rate has been operated there for 10 years. New algorithms based on work in the PRENLAB projects have been in operation for test purposes during the last two years. They are based on, besides the character of the seismicity, microearthquake source information and wave path information. These warning procedures have shown to be significant, especially for activating and assisting the seismologists in evaluation of signs of possible impending hazards.

WP3 is a forum for integration of all results of the PREPARED project which can help in developing and testing enhanced short-term warnings.

A sceme is in development for short-term warnings and information. It contains two main components:

1) An automatic alert system, which provides the seismologists with alert information of time changes/anomalies

In various seismic observations, various seismicity patterns, fault plane solutions and stresses based on microearthquakes. Such information is also integrated in the automatic earthquake warning algorithm, EQWA (Stefánsson and Guðmundsson 2005; WP3.1 in this report; Slunga 2004).

In radon observations in geothermal wells (WP3.2 in this report; Hjartardóttir et al. 2005; Theódórsson and Guðjónsson 2003).

In water height in boreholes, and other related information. (Jónsson et al. 2003).

In observations of stress build-up and short-term stress relaxation by shear-wave splitting (WP2.5 in this report, Gao and Crampin 2005; Wu and Crampin 2005).

2) Real-time research, i.e. scientific/manual real-time evaluations and investigations

Automatic warning algorithms are based on models of the earthquake process, which are incomplete and related to different conditions in time and space. During observed pre-earthquake process understanding can be improved on the crustal conditions that make it more likely that the process can be understood possibly resulting in useful warnings. Therefore it is significant to develop algorithms and software tools for fast evaluations and visualization of the real-time observations, for the scientists to have a profound basis for fast and well based assessments.

The methods for automatic alerting as well as for fast evaluations and visualization is imbedded in the Early Warning and System (EWIS) developed and operated by the coordinator (Roberts et al. 2004, Stefánsson and Roberts 2004).

Socio-economic relevance and policy implication

It is of economic and social significance to be able to provide short-term warnings before earthquakes. It makes it possible to prepare people and rescue infrastructure before the event.

The warning does not only include saying that an earthquake is probably impending within hours or days. Short-term warnings are provided on various levels when real-time monitoring and investigations reach high-level of probability. Shortly before the earthquake it can be expected that knowledge on the exact fault position and intensity will have clarified, which is of a great significance even if warning of the exact time of rupture fails. Fast information on distribution of earthquake effects and possible aftershocks is very significant, even if the short-term warning before the earthquake fails.

Knowledge of progress in this field increases the quality of life in any earthquake-prone area.

Discussion and conclusions

Progress in the various involved WP´s, provides various examples of observable processes approaching the 2000 earthquakes. Modelling work emphasizes that understanding of fluid migration and of high porous fluid pressures is of fundamental significance in providing the observed forerunning signals.

Plan and objectives for the next period

The main activity in WP3 in the next period is to test the indications obtained in the qualitative seismic analysis described shortly above and to merge together the results of the various other WP´s providing short-term indicators or adequate modelling into overall short-term warning and information scheme.

References

Gao, Y. & S. Crampin 2005. A further stress-forecast earthquake (with hindsight), where migration of source earthquakes causes anomalies in shear-wave polarisations. *Geophys. J. Int*. In preparation.

Hjartardóttir, Á.R., P. Einarsson, P. Theodórsson & G. Jónsson 2005. Radon data from the South Iceland Seismic Zone, 1977-1993 and 1999-2003. Report and CD, Science Institute, University of Iceland.

Jónsson, S., P. Segall, R. Pedersen & G. Björnsson 2003. Post-earthquake ground movements correlated to pore-pressure transients. *Nature* 424, 179-183.

Roberts, M.J., R. Stefánsson & P. Halldórsson 2004. Internet-based platform for real-time geoscience during tectonic crises in Iceland. In. Abstracts from the I EGU General Assembly, Nice, France, April 25-30, 2004.

Slunga, R. 2004. Rock-water interaction in the crust. In: Abstracts from the 26th Nordic Geological Winter Meeting, Uppsala, Sweden, January 6-9, 2004.

Stefánsson, R. & M.J. Roberts 2004. Realization of time-dependent earthquake warnings in Iceland and the development of an early information and warning system for geologic hazards. Workshop organized by CRdC AMRA, the University of Napoli "Federico II" and the EU NaRAs on: "Seismic early warning for European cities", Napoli, Italy, September 23-25, 2004.

Stefánsson, R. & G.B. Guðmundsson 2005. About the state-of-the-art in providing earthquake warnings in Iceland. *Icelandic Meteorological Office - Report.* In press.

Theodórsson, P. & G.I. Guðjónsson 2003. A simple and sensitive liquid scintillation counting system for continuous monitoring of radon in water. *Advances in Liquid Scintillation Spectrometry*, 249-252.

Wu, J. & S. Crampin 2005. Smaller source earthquakes and improved measuring techniques allow the largest earthquake in Iceland to be stress-forecast (with hindsight). *Geophys. J. Int.* In preparation.

WP 3.1 Foreshocks and development of new warning algorithms

a) Objectives

During the PRENLAB projects an earthquake warning algorithm, EQWA, based on the statistics of the microearthquakes was designed. The following microearthquake parameters were included: hypocenter location, origin time, seismic moment, slip size, static stress drop, and fault radius. The EQWA is described by Slunga (2003a). Within PREPARED there is an intention to go into a more physical analysis of the microearthquakes preceeding an earthquake which possibly will increase the predictive value of the EQWA. The improved EQWA will then be made operational and implemented within the routine system.

b) Methods and achievements

In the search for not only statistical but more clearly physical precursors the work has been concentrated to checking the behaviour of the absolute crustal stresses. As pointed out in a paper submitted to GRL it is possible to estimate the complete stress tensor if two approximate assumptions are made: first the vertical stress is assumed to equal the lithostatic pressure, second the shear stresses are assumed to be as large as Coulomb failure criterion allows. The Coulomb failure criterion adds the water pressure to the unknowns. However, at shallow depths the water pressure is known to be hydrostatic and at larger depths there will be a transition to lithostatic pressure at depths and temperatures where the rock strength is reduced. Rock mechanics indicate that basalt may contain hydrostatic water down to 3-3.5 km depth. At larger depths the water pressure will be increased. A simple model for the water pressure is achieved if it is related to the smallest principal compression by accounting for the rock strength. Based on Bott's criterion four close microearthquake with different fracture orientation and for which the auxiliary plane has been eliminated is then enough to allow an estimate of all the six parameters of the rock stress tensor. This estimate pertains to the volume of the four microearthquakes and the time window of their occurancies. The presently used microearthquake fault plane solution algorithm is based on the far field impulses (Slunga 1981) which cannot discriminate the fault plane and the auxiliary plane. If the number of available microearthquakes is large the method of high accuracy multievent location by wave form correlation eliminates the auxiliary plane for some of the microearthquakes (in Iceland typically about 30 per cent). This allowed a test of monitoring the stress before the largest erathquake in the active Hengill area. The results (which are not very dependent on the water pressure estimate) showed increased compressional stresses within about 1 km of the nucleation point of the June 4 1998 earthquake and also at the nucleation point of the preceeding foreshock a few hours before. The area studied was about 10*10 sqkm. Very low compressive stresses were found in the quadrants of tension. This is a very promising result. Unfortunately the paper was not accepted and unfortunately no scientific reasons were given (one argument was based on the believe that granite and basalt behaves in a similar way which is contradicting rock mechanical results). However, these positive scientific results showed the need of improving the fault plane solution method in such a way that the auxiliary planes more often can be eliminated. As the earlier found microearthquake precursors are based on observations independent of the fault plane solutions (seismicity rate, b-value, and distributions of the fault radius and the static stress drops and peak slips) there is a real chance that the stress monitoring based on fault plane solutions may improve the performance of the earthquake warning algorithm (EQWA).

c) Social and economic effects

If the promising resukts can be utilized in a well working EQWA it means that life can be saved and also some economical losses can be reduced. The value can be compared to the meteorological storm warnings even if storms normally affects larger areas.

d) Discussion and conclusions

The absolute stress level is a new aspect on the EQ warning and is independent of the previous EQ parameters used. This can possibly lead to a significant improvement of the EQWA. The preliminary investigations are promising.

e) Plan and objectives for the remaining time period

The detailed study of the foreshocks before all larger EQ in the area will continue. The potential value of the stress level monitoring will be evaluated during this work. The results of these investigations will be incorporated in the coming version of the EQWA.

Reference

Slunga R. (1981), Earthquake source mechanism by use of body-wave amplitudes – an application to Swedish earthqakes, *Bull. Seism. Soc. Am*., 25-35.

WP 3.2 Radon anomalies

a) Objectives

To establish the significance of the radon anomalies that occurred prior to the June 2000 earthquakes by comparing them to earlier results of the radon monitoring program in South Iceland and other results world-wide. Characteristics of the anomalies will be determined with the aim of developing a warning algorithm.

Deliverables

1. Time series of radon at all measuring stations in South Iceland since 1977 are now available on a CD (Hjartardóttir et al., 2005).
2. Paper in a refereed journal on the radon anomalies identified. A manuscript is under revision.
3. Presentation of the radon results at 2 international meetings.
4. Warning algorithm.

b) Methodology and scientific achievements:

The relationship between radon and earthquakes in this area has been studied since 1977 when Egill Hauksson of the Lamont-Doherty Earth Observatory installed the first equipment for this purpose (Hauksson, 1981, Hauksson and Goddard, 1981). The instruments were operated until 1993. A summary of the results until then was given by Jónsson and Einarsson (1996). A very clear relationship could be established and a number of premonitory radon anomalies were identified. A sample of a time-series is given in Fig. 1.

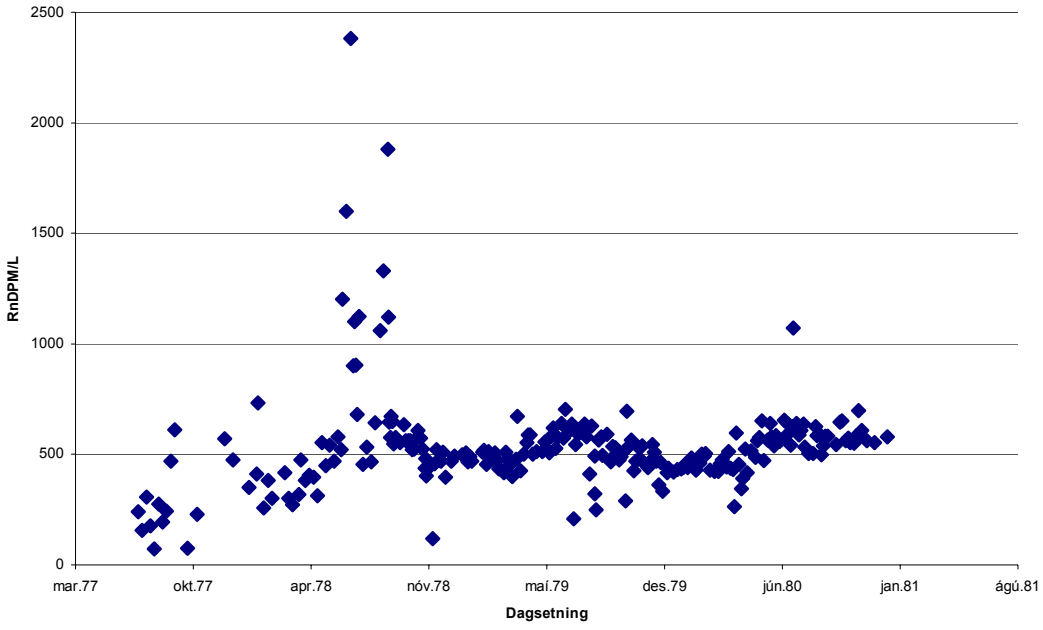

Fig. 1. *Sample time-series of radon at the Flúðir station in South Iceland for the years 1977-1980. The large excursions in 1978 preceded earthquakes, as reported by Hauksson and Goddard (1981). The positive results spurred further work and a new instrument was designed and tested for the purpose of radon monitoring. The instrument is based on a novel liquid scintillation technique where counting only Bi-218/Po-218 pulse pairs gives high sensitivity with a simple construction.*

The system represents a significant progress in the radon measuring technique (Theodórsson, 1996, Theodórsson and Guðjónsson, 2004).

A new program of sampling from geothermal wells in the South Iceland Seismic Zone was initiated in 1999, a year before the destructive earthquakes of June 2000 occurred. The two M6.5 earthquakes originated in the middle of the sampling network. These events were preceded by clear anomalies at six out of seven stations (Theodórsson et al. 2000, Kerr, 2001, Einarsson et al., 2005, Hjartardóttir, 2003). Four types of change could be identified in the radon time series in association with the earthquake sequence of June 2000:

1. Pre-seismic decrease of radon. Anomalously low values were measured in the period 101-167 days before the earthquakes.
2. Pre-seismic increase. Spikes appear in the time series 40-144 days prior to the earthquakes.
3. Co-seismic step. The radon values decrease at the time of the first earthquake. This is most likely related to the co-seismic change in ground water pressure observed over the whole area (Björnsson et al., 2001).
4. Post-seismic return to pre-seismic levels about 3 months after the earthquakes, probably also linked with the pressure change in the geothermal systems reported by Jónsson et al. (2003).

A paper on these results was submitted for publication in a refereed journal (Einarsson et al., 2005). A revised manuscript is in the final stages of preparation.

In view of the positive results of the project we are developing and testing a new, automatic radon instrument, Auto-Radon, based on the same design, that continuously monitors the radon concentration in the geothermal ground water (Theodórsson and Guðjónsson, 2004). The instruments are situated at the drill hole stations, taking 4 radon readings each day. Four stations have been installed so far. A sample time-series is shown in Fig. 2.

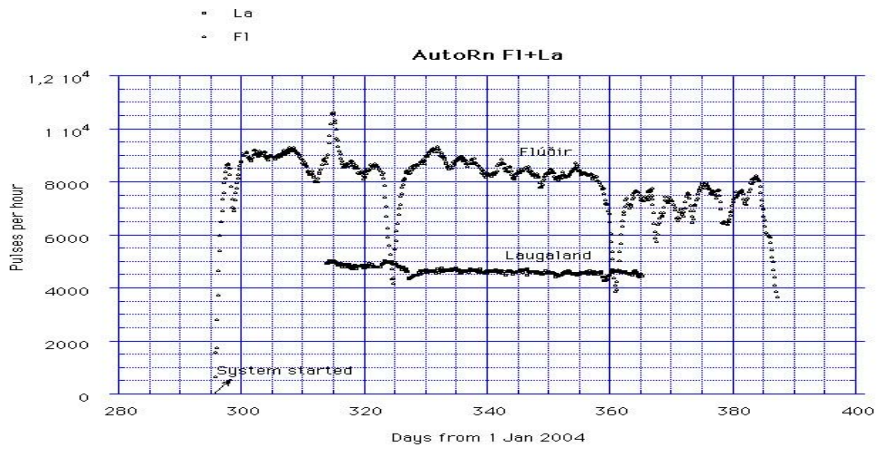

Fig. 2. *Samples of time-series for radon activity in water from geothermal drill-holes at Flúðir and Laugaland in the South Iceland Seismic Zone. Measurements are done automatically by the Autoradon instrument (Theodórsson and Guðjónsson, 2003).*

c) Socio-economic relevance and policy implication

So far the radon program is a purely scientific endeavour. Its socio-economic relevance and policy implications are impossible to judge at this time.

d) Discussion and conclusion

The most significant finding of this study is the high correlation between the radon time series over the entire area in the time period 1999-2001. Stations that are tens of kilometres apart show very similar fluctuations in the concentration of radon. Considering the short half-life of radon these fluctuations can hardly be ascribed to material transport between the stations. A common origin of the fluctuations must be assumed. Two significant events occurred in the crust of South Iceland during this time, the Hekla eruption of February 26 – March 8 and the earthquake sequence of June. It must be considered very likely that these events were the causal agents for the radon fluctuations. This conclusion is further strengthened by the temporal correlation of the post-earthquake radon recovery with the pore-pressure recovery and its poro-elastic response observed by Jónsson et al. (2003). We believe these observations are of crucial importance for the understanding of the physical mechanism of premonitory radon anomalies.

e) Plan and objectives for the next period

1. Find a statistics test for significance of correlation between the radon and the earthquake time series.

2. Work on an algorithm that detects radon anomalies in a time series.

References:

Björnsson, G., Ó. Flóvenz, K. Sæmundsson, E. M. Einarsson. Pressure changes in Icelandic geothermal reservoirs associated with two earthquakes in June 2000, in: Proceedings of the Twenty-Sixth Workshop on Geothermal Reservoir Engineering, Stanford University, Stanford, CA, 2001.

Einarsson, P., P. Theodórsson, G. I. Guðjónsson. Radon anomalies prior to the earthquakes sequence in June 2000 in the South Iceland Seismic Zone. Manuscript under revision 2005.

Hauksson, E., Radon content of groundwater as an earthquake precursor: Evaluation of worldwide data and physical basis. J. Geophys. Res., 86, 9397-9410, 1981.

Hauksson, E., and J. Goddard, Radon earthquake precursor studies in Iceland. J. Geophys. Res., 86, 7037-7054, 1981.

Hjartardóttir, Á. R. Radonfrávik sem fyrirboðar Suðurlandsskjálftanna 2000. (Radon anomalies occurring before the earthquakes of 2000 in South Iceland, in Icelandic). BS-thesis, Department of Natural Sciences, University of Iceland, 35 pp and Tables, 2003.

Hjartardóttir, Á. R., P. Einarsson, P. Theodórsson and G. Jónsson. Radon Data from the South Iceland Seismic Zone, 1977-1993 and 1999-2003. Report and CD, Science Institute, University of Iceland, 2005.

Jónsson, S., and P. Einarsson. Radon anomalies and earthquakes in the South Iceland Seismic Zone 1977-1993. In: Seismology in Europe (Ed. B. Thorkelsson et al.), European Seismological Commission, Reykjavík, p. 247-252, 1996.

Jónsson, S., P. Segall, R. Pedersen, G. Björnsson. Post-earthquake ground movements correlated to pore-pressure transients. Nature, 424, 179-183, 2003.

Kerr, R. A. Predicting Icelandic fire and shakes. Science, Jan. 26, 2001.

Theodórsson, P., Improved automatic radon monitoring in ground water. In: Seismology in Europe (Ed. B. Thorkelsson et al.), European Seismological Commission, Reykjavík, p. 253-257, 1996.

Theodórsson, Páll, Páll Einarsson, Guðjón I. Guðjónsson. Radon anomalies prior to the earthquake sequence in South Iceland in June 2000. Am. Geophys. Union, Fall Meeting, Abstract in Eos, 81, p. 891, 2000.

Theodórsson, P. and Guðjónsson, G. I. A simple and sensitive liquid scintillation counting system for continuous monitoring of radon in water. *Advances in Liquid Scintillation Spectrometry*, 249-252, 2003.

WP 4 A model of the release of the two June 2000 earthquakes based on all available observations

Objectives

To model the source process in time and space of the two large earthquakes based on multidisciplinary information.

Methodology and scientific achievements related to workpackages including contribution from partners

The main input here are results and deliverables of WP4.1, WP4.2, WP4.3 and WP4.4., and results from other WP´s, like the modelling packages WP6.1 and WP6.2 as well as WP5.5.

Modelling based on deformation observations

Modelling has been carried out based on deformation data (GPS, InSAR), both as takes to the slip and fault size (WP4.4 of this report; Pedersen et al. 2003).

Table 1
Fault parameters for the June 2000 events estimated from different data sets

	Length (km)	Width (km)	Depth (km)	Dip (°E)	Strike (N°E)	Lon. (°)	Lat. (°)	Strike slip (m)	Dip slip (m)	Rake (°)	M_0 ($\times 10^{18}$ Nm)	M_w
June 17												
Uniform slip	10.6	7.9	0.0*	87*	1	−20.347	63.973	1.7	0	180	4.4	6.4
Distributed slip	~15	~10	0.0	87*	2*	−20.347	63.973	0.0–2.6	0*	180*	4.5	6.4
Árnadóttir et al. [17]	9.5	9.8	0.1	90*	3	−20.351	63.970	2.0	0.2	174	5.6	6.5
Pedersen et al. [18]	16.0	10.0*	0.0*	86*	5*	−20.342	63.979	0.3–2.4	0.0–0.2	175	5.4	6.5
NEIC [9]	–	–	–	75	−1	−20.487	63.966	–	–	173	4.3	6.4
Harvard CMT [33]	–	–	–	87	4	−20.47	63.99	–	–	−164	7.1	6.5
June 21												
Uniform slip	11.9	8.2	0.0*	90*	0	−20.705	63.987	1.8	0	180	5.3	6.4
Distributed slip	~15	~10	0.0	90*	0*	−20.705	63.987	0.0–2.9	0*	180*	5.0	6.5
Árnadóttir et al. [17]	12.3	8.0	0.0*	90*	0.5	−20.691	63.984	1.5	0	180	4.5	6.4
Pedersen et al. [18]	15.0	9.0*	0.0*	90*	0*	−20.703	63.982	0.5–2.2	0	180	5.1	6.4
NEIC [9]	–	–	–	79	−4	−20.758	63.980	–	–	−173	5.0	6.4
Harvard CMT [33]	–	–	–	85	2	−20.85	63.98	–	–	−167	5.4	6.5

Latitude and longitude are for the center of the fault plane at the upper edge.
*Parameter held fixed in the modeling.

Table 1. *Modelling resuls are summarized, i.e. fault parameters for the June 2000 earthquakes estimated from different datasets. Latitudes and longitudes which are given for the deformation models are valid for the center of the fault planes at the upper edge. (WP4.4 of this report; and Pedersen et al. 2003).*

The modelling marked in the table by Árnadóttir et al. is based on GPS repeated measuring net 1995, 1999 and 2000 (June 19-30). Rectangular dislocation in an elastic half space is assumed. The dip of the fault planes was in both cases fixed to vertical and the depth of the June 21 earthquake fault was fixed to the depth indicated by microearthquake aftershocks. Besides this model was not constrained by other information about location or surface faulting (Árnadóttir et al. 2001).

The modelling marked by Pedersen et al. in the table is based on 5 pairs of InSAR interferograms, the closest around the earthquakes from June 16 to July 21. Rectangular dislocation in an elastic halfspace was assumed and a double couple focal mechanism. For both earthquakes 3 slip patches were assumed along the fault plane referring to the dimensions of the aftershock distribution. For the June 17 earthquake, a 3-patch model based on preliminary results from volumetric strainmeters in the area was applied in the final search for best fit. The June 21 earthquake was also modelled by a three patch model along the fault plane. In the June 17 earthquake most slip is indicated in the central part and least in the southern part. In the June 21 earthquake most slip is inferred in the southern part and least in the central part. A more complex model is indicated to explain al the data for the June 21 earthquake (see table and other results in Pedersen et al. 2001).

The two uppermost models of the table, *uniform slip* and *distibuted slip* are results of Pedersen et al. (2003). The models comply with both the GPS measurements and the InSAR data, assuming elastic halfspace with rectangular dislocations. Poisson´s ratio is assumed 0.28 (undrained, no fluid flow). It is concluded that both earthquakes can be approximated by simple planar faults. Slip distribution (Figure 2) is estimated from the two earthquakes as seen in Figure 1. It is interesting that most of the slip takes place above the earthquake hypocenters.

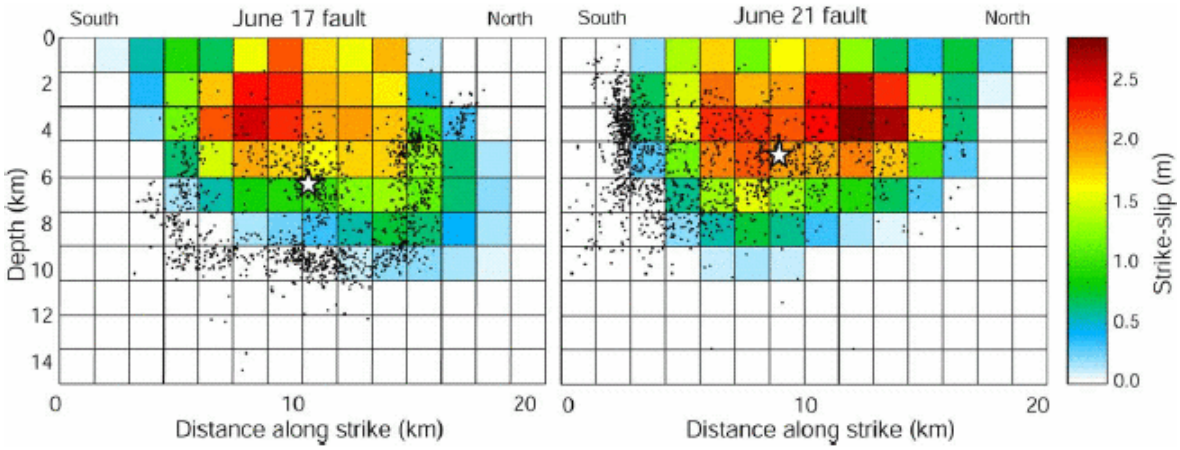

Figure 1. *Right-lateral strike slip distribution estimated for the June 17 and June 21 earthquakes. Hypocenters are showns with white stars, and aftershocks in the immediate vicinity of the modelled fault planes as black dots. Smoothing factor κexp2 =1.4 was used for this solution. Tests using different k values were carried out showing that the choise of κ does not significantly affect the estimated moment magnitude.*

The two bottom lines of the table for each earthquake are dynamic models based on amplitudes of seismograms at teleseismic distances around the world, NEIC (U.S.G.S.) and Harvard (Dziewonski et al. 2001).

Dynamic modelling, i.e. information from seismic waves
In WP4.2 model is also sought by waveform inversion of near field strong motion data for moment distribution on the fault. The results are given in WP4.2 of this report.

Information from microearthquakes
WP 4.1 contains new information based on microseismicity near the faults of the two earthquakes. In the following some older information is reviewed.

The June 17 earthquake

According to the Icelandic Meteorological Office (IMO) the origin time of the June 17 earthquake was 15:40:40.94 GMT, the hypocenter at 63.97°N, 20.37°W, and a hypocentral depth of 6.3 km. The aftershocks indicate an 11-12 km long rupture extending from the surface to 10 km depth. The assumed fault strikes N7°E and dips 86° towards the east.

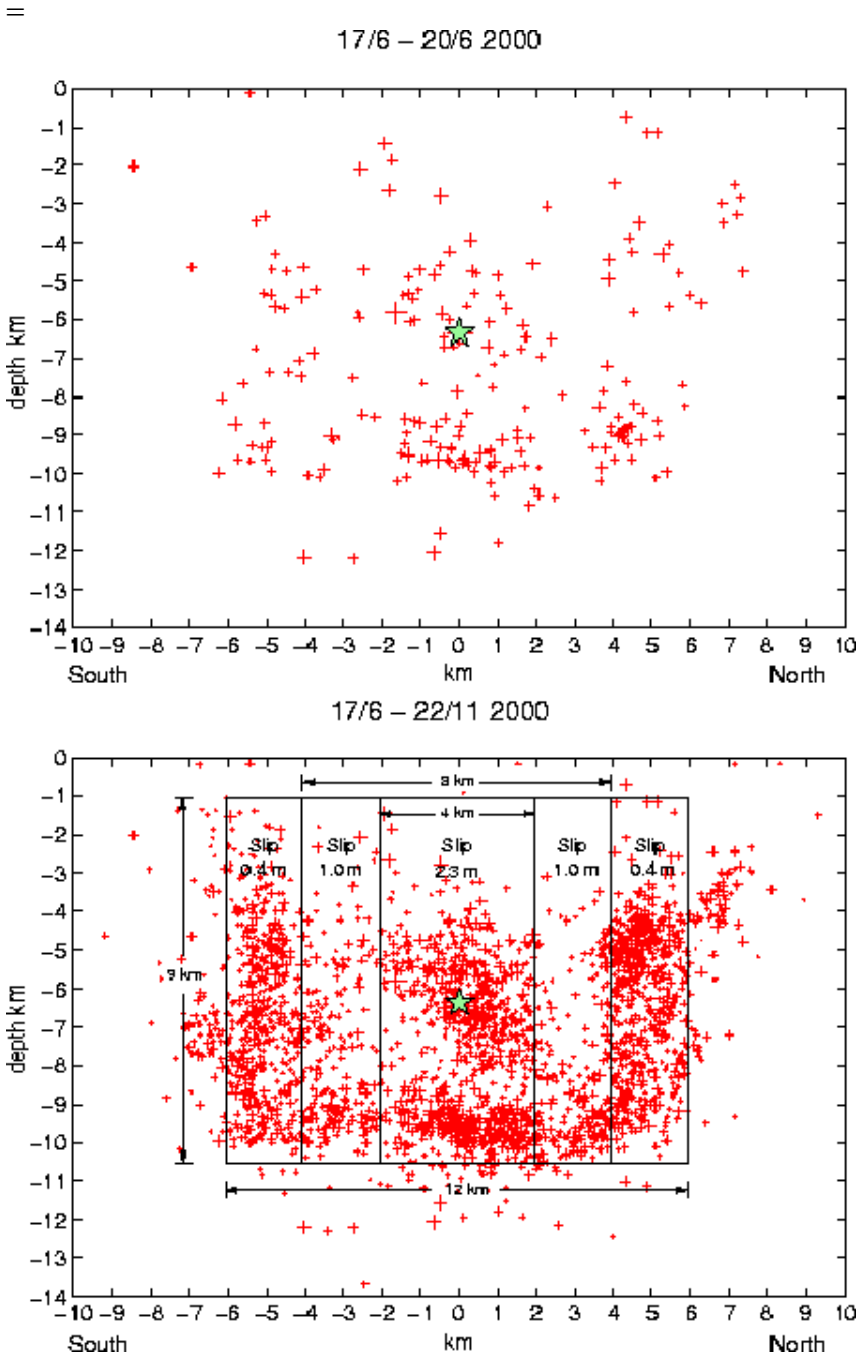

Figure 2. *Aftershocks of the June 17 earthquake within 3 km of the fault plane are shown along with a tentative slip model. The frame at the top shows aftershocks during the first 32 hours. The second frame shows the aftershocks until November 22, 2000, and a rupture model to fit observations from local volumetric strainmeters, with variable right-lateral slip on a 12 km long fault (Alan Linde and Kristján Ágústsson, personal communication).*

As seen from the figure the fault dimension is determined from the assumed high seismicity end effects of the fault, to the south and north as well as to the bottom of the fault. Defining the fault plane as a dislocation plane it may even be correct to conclude that the dimensions would even be smaller, i.e. the microearthquake end effects would express high stresses near the end of the fault rather that the end itself.

Preliminary modelling of local measurements by volumetric strainmeters, assuming rigidity 36 N/m^2, indicates variable slip as shown in Figure 2, and a moment of $4.8 * 10^{18}$ Nm (Alan Linde and Kristján Ágústsson, personal communication; Stefánsson et al. 2003). Assuming uniform slip along the fault the rupture dimension suggested by aftershocks, and the moment estimated by USGS, an average right-lateral displacement of 1.5 m is inferred. Studying the spatial distribution of the aftershocks (i.e. aftershocks within a couple of kilometers from the fault) the following observations are noticable (Figure 2). The observations suggest that the earthquake initiated in the center of the rupture which appears to have extended down to 10 km. This is slightly deeper, but comparable to the depth of the brittle/ductile boundary inferred from earlier microearthquake studies: around 8 km in this part of the SISZ (Stefánsson et al. 1993; Tryggvason et al. 2002). A few early aftershocks occurred at 12 km depth, well into what usually is considered the ductile zone. This suggests that ductility depends on strain rate which of course is expected to be high immediately after and near a large earthquake. A concentration of aftershocks close to the hypocenter of the main shock is suggesting a asperity there, a few kilometers in diameter (from Stefánsson et al. 2003).

The June 21 earthquake

The IMO determined origin time of the June 21 earthquake was 00:51:46.95 GMT, the hypocenter was at 63.98°N, 20.71°W, and a hypocentral depth of 5.1 km. The aftershocks indicate a vertical fault, 15 km long, striking N2°W extending from the surface to 8 km depth (Figure 3).

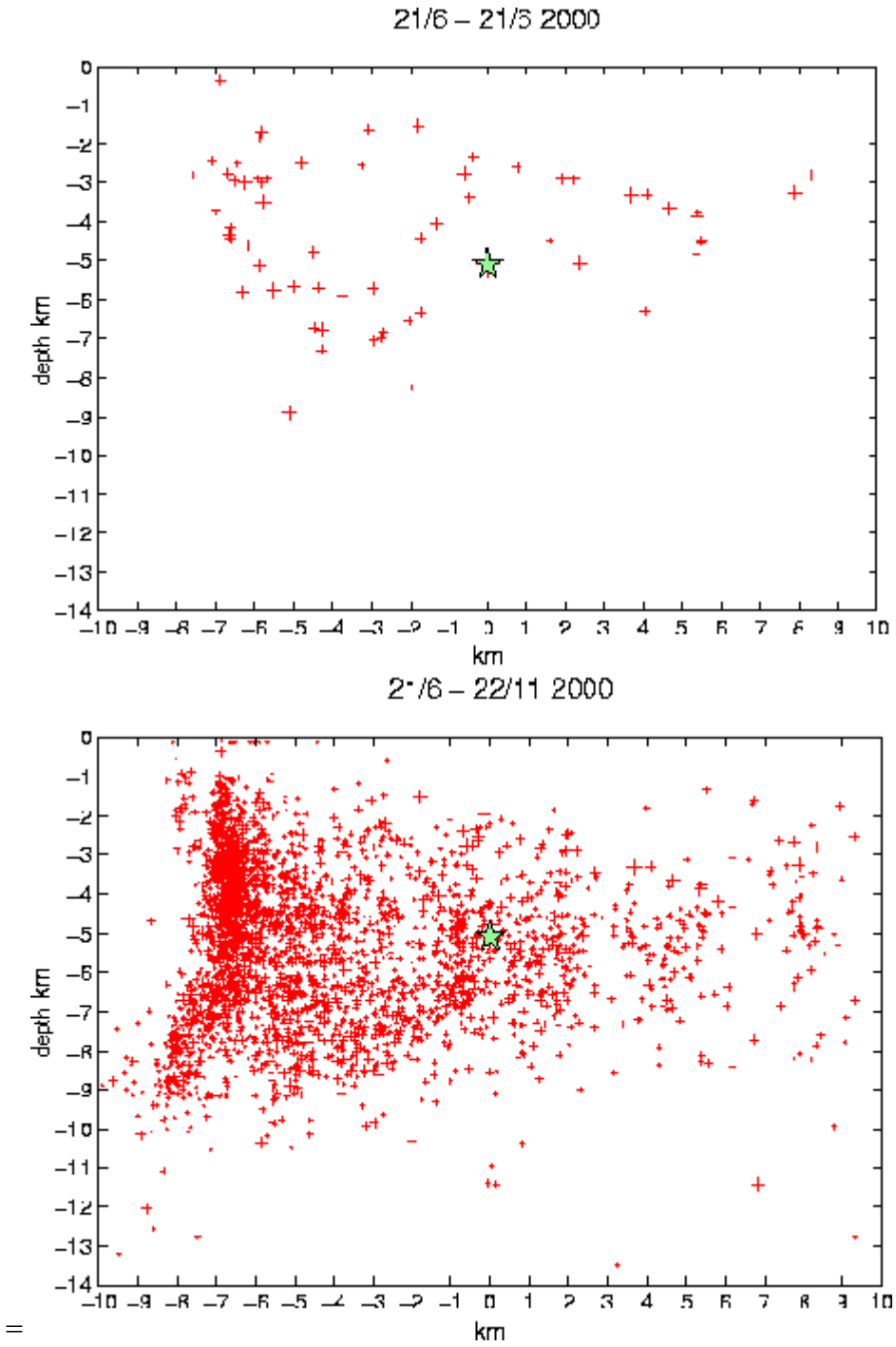

Figure 3. *The figure shows the aftershocks of the June 21 earthquake, within 3 km of the fault plane. The frame at the top shows aftershocks during the first 32 hours. The second frame shows the aftershocks until November 22, 2000.*

Surface fissures indicating general right-lateral motion coincide with and are found all along the main fault as it is reflected in the aftershocks. Related ENE-WSW fault with left-lateral motion was also observed near the southern end of the main fault. The USGS Rapid Moment Tensor Solution gives a moment of $5.2 * 10^{18}$Nm, assuming a best fitting double-couple solution. Preliminary magnitudes by NEIC were mb=6.1 and Ms=6.6. The strainmeter observations were not good enough to provide an independent estimate of the moment. Assuming uniform right-lateral slip as indicated by the surface fissures, fault size indicated by the aftershocks and the moment of USGS, a 1.2 meter right-lateral coverage slip of the main fault is implied (from Stefánsson et al. 2003).

The estimated length of the two faults by microearthquake aftershock is 11-12 km and 15 km respectively. In fact the real dislocation along the fault may have even smaller dimension. There is no contradiction with the slightly larger dimension of the fault planes modelled on basis of deformation observations, reflecting aseismic deformation at the ends, i.e. deformation without earthquakes, to bothe ends of the fault dislocation.

Other observations relevant for modelling the source process
Above we have only considered time independent models, neither taken into account information about the source time function of the earthquakes nor the time functions of the build-up and the afterworking of them.

In the following I indicate some sources of further information that will extend our sphere.

There are indications that the waveform of the first earthquake involved a nucleation process that was seen by the local seismic network as well as by volumetric strainmeters (Ragnar Slunga, personal communication; Alan Linde and Kristján Ágústsson, personal communication). The waveform indicates that this results from a 3 km diameter asperity in the center of the fault plane of the June 17 earthquake.

Studies of the long-term microseismic preparatory process (WP2 of this report; Stefánsson et al. 2005) indicate stationary patterns surrounding the source indicating high pore fluid pressures and fluid movements in a large area around the becoming fault.

Studies of b-values, WP2.2, show low b-values near the nucleation point of the earthquakes, but high b-values in other areas often at greater depth, indicating high pore fluid pressures at depth.

The modelling work in WP6.2 allows for much more complex models than assumed in the modelling above, taking in various ways into account lithosphere/asthenosphere relationships and possible intrusive events related to earthquake release.

These are just exapmples of other information from various workpackages. All information gained in the project can be utilized in modelling the overall source process.

Socio-economic relevance and policy implication

It is significant to understand the overall mechanism of earthquake processes in the SISZ. Earthquakes reaching magnitude 7 are expected there and have through historical times caused huge destruction. After the M=6.6 (Ms) earthquakes of the year 2000 a challenging question is if the sequence is over, or more could be expected and where. A sequence of 5 large earthquakes (Ms>6) broke through the central and the western part of the SISZ in the year 1896. 16 years later, in the year 1912, a magnitude 7 earthquake broke through the easternmost part of the zone. West of what usually is called the SISZ on the Reykjanes peninsula there is a region where an earthquake of magnitude 6.3 occurred in 1929, only 15-20 km from the city of Reykjavík. What can be expected in that area is of enormous interest to know.

It can be expected that the project will render innovative results concerning earthquake nucleation and release process in general. It will help in developing earthquake warnings, and thus can be of social and economic benefit for earthquake-prone areas in general.

Discussion and conclusions

There are no conclusions except that the multidisciplinary observations and evaluation in many WP´s of the first-term of PREPARED provide information that will render a well constrained and innovative model of the earthquake processes in the SISZ.

Plan and objectives for the next period

The last 6 months of the project involve the merging together of significant results in various workpackages of the project A special PREPARED session (NH4.04) will be held at the EGU General Assembly in Vienna on April 29, as well as a PREPARED partner meeting a day later. Other meetings of a few partners are expected during the summer for the same purpose.

References

Árnadóttir, Þ., S. Hreinsdóttir, G.B. Guðmundsson, P. Einarsson, M. Heinert & C. Völksen 2001. Crustal deformation measured by GPS in the South Iceland Seismic Zone due to two large earthquakes in June 2000, *Geophys. Res. Lett*. 28, 4031-4033.

Dziewonski, A.M., G. Engström & N.N.Maternovskaya 2001. Centroid –moment tensor solutions for April –June 2000. *Phys. Earth Planet. Inter.* 123, 1-14.

Pedersen, R., F. Sigmundsson, K.L. Feigl, & Þ. Árnadóttir 2001. Coseismic interferograms of two Ms=6.6 earthquakes in the SISZ, June 2000. *Geophys. Res. Lett.* 28, 3341-3344.

Pedersen, R., S. Jónsson, Þ. Árnadóttir, F. Sigmundsson & K.L. Feigl 2003. Fault slip distribution of two Mw=6.5 earthquakes in South Iceland estimated from joint inversion of InSAR and GPS measurements, *Earth and Planetary Science Letters* 213, 487-502.

Stefánsson, R. R. Böðvarsson, R. Slunga, P. Einarsson, S.S. Jakobsdóttir, H. Bungum, S. Gregersen, J. Havskov, J. Hjelme & H. Korhonen 1993. Earthquake prediction research in the South Iceland seismic zone and the SIL project. *Bull. Seism. Soc. Am*. 83(3), 696-716.

Stefánsson, R., G.B. Guðmundsson & P. Halldórsson 2003. The South Iceland earthquakes 2000 - a challenge for earthquake prediction research. *Icelandic Meterorological Office - Report* 03017, 21 pp.

Stefánsson, R. & G.B. Guðmundsson 2005. About the state-of-the-art in providing earthquake warnings in Iceland. *Icelandic Meteorological Office - Report.* In press.

U.S.G.S. National Earthquake Information Center. Previous Fast Moments. http:/wwwneic.cr.usgs.gov/neis/FM/previous/0006.html.

Tryggvason, A., S.Th. Rögnvaldsson & Ó. Flóvenz 2002. Three-dimensional imaging of the P- and S-wave velocity structure and earthquake locations beneath Southwest Iceland. *Geophys. J. Int. 151*, 848-866.

WP 4.1 Source mechanism and fault dimensions of the June 17 and June 21 earthquakes determined from mapping of aftershocks

Objectives

To determine the source mechanisms and fault dimensions of the two large earthquakes on June 17 and June 21, using local events. That is:

Define the locations, dimensions and possible sub-fault details in the fault planes of the J17 and J21 earthquakes, by relatively locating the thousands of aftershocks on each of the two faults.

- Map the post-seismic slip as a function of location and time on the two large faults in order to understand the evolution of the post-seismic stress.

In addition:

- Determine the magnitude and mechanism of the two M~5, dynamically triggered events on Reykjanes Peninsula on June 17.

Methodology and scientific achievements

Interactively analyzed events are fed into the multievent relative location algorithm described in the M12 report, in order to map the fault dimensions and finer details of J17 and J21.
Joint interpretation of the improved hypocenter distribution and the possible fault-plane solutions of individual microearthquakes is performed, in order to study the finer details of post-seismic slip on the two large faults as a function of time and space.

Two M~5 events on Reykjanes Peninsula were dynamically triggered by the shear waves from the J17 event. Their wave forms, which were riding on top of the surface waves from the main event, were therefore clipped and obscure at many of the recording stations, making determination of their mechanism problematic. By using the wave forms from an August 2003, M5 event on Reykjanes Peninsula, the magnitudes of the two triggered events are derived. Together with the constraints on fault sizes and orientations obtained from the relatively located aftershocks, the mechanisms are estimated.

Socio-economic relevance and policy implication

Large historic earthquakes in the South Iceland Seismic Zone (SISZ), like the June 2000 earthquakes, have caused devastation on farms and small towns in southern Iceland. As was borne out by the J17 event, they can also remotely trigger other large events in the SISZ and on Reykjanes Peninsula (RP); either dynamically, like the two M~5 events on RP, or statically, like the J21 earthquake. Increased knowledge about the location of major faults, the character of faulting in the SISZ, and the possibility of remote triggering of earthquakes, can lead to clearer regulations on building standards and building sites in southwest Iceland. This knowledge may also increase awareness in local communities and help inhabitants to prepare for and cope with the effects of future destructive earthquakes.

Discussion and conclusion

A bulletin of all the relocated earthquakes on the J17 and J21 faults has already been delivered in D79 (WP5.1), and the delivery report can be found in the appendix to WP 5.1. Some of the finer structure on the two faults has already been displayed in the M12 report, but further detailed analysis of their subfaults and conjugate faults is still under way.

Magnitude and mechanism determination of the two M~5, dynamically triggered events on Reykjanes peninsula is near completion and an article is in preparation.

Plan and objectives for the final period

In the remaining period the fault mapping will be finalized, with a closer look taken at the finer details of subfaults. A joint interpretation with focal mechanisms of individual events will be performed to analyze the slip of the fault patches in space and time. An article will be written, summarizing the results of the fault mapping in this work package and WP5.1. An article on the source mechanism of the dynamically triggered earthquakes on June 17 will also be completed.

Abstracts

Hjaltadóttir, S. and K. S. Vogfjörð, 2004. Relative event locations and mapping of faults in southwest Iceland (in Icelandic). Geoscience Society of Iceland, Spring meeting 2004. p. 54-55.

Hjaltadottir, S., K. S. Vogfjord, R. Slunga, 2005. Mapping subsurface faults in southwest Iceland using relatively located microearthquakes. *Geophysical Research Abstracts*, Vol. 7, 06664, EGU General assembly, Vienna, Austria, 24-29 April, 2005.

Vogfjörð, K. S., 2003. Triggered seismicity in SW Iceland after the June 17, Mw=6.5 earthquake in the South Iceland Seismic Zone: The first five minutes. *Geophysical Research Abstracts*, Vol, 5 11251, EGS-AGU-EGU Joint Assembly, Nice, France, 6-11 April, 2003.

Vogfjörð, K. S., S. Hjaltadóttir and R. Slunga, 2005. The M~5 triggered events in the South Iceland Seismic Zone on June 17, 2000: Determination of fault plane magnitude and mechanism. *Geophysical Research Abstracts*, Vol 7, 10274, EGU General assembly, Vienna, Austria, 24-29 April, 2005.

WP 4.2 Waveform inversions for moment distribution on the fault

1 Objectives of the reporting period

Report on the inversions of observed data related to both June 2000 Iceland events for the moment distribution on the fault.

2 Scientific/technical progress made in different WP´s according to the planned time schedule

We study the two Mw 6.5 earthquakes occurred in the Southern Iceland Seismic Zone on June 17 and 21, 2000 by inverting strong motion records.The two events occurred on two parallel N-S striking, right-lateral strike-slip faults, separated by about 17 km. The used fault model for both events is a two 20 km long and near-vertical fault extending from the surface to approximately 15 km depth. To solve the inverse problem, we use the method of linear programming and we stabilize the solution by using physical constraints.

The inversions are performed for different grid sizes and different nucleation points. The constraints of the positivity of the slip rates on the fault is used in all cases in this study. We use only data from a set of rock-stations distributed uniformly around the fault. The accelerograms are filtered at 1Hz and we model about 15 sec of the signals.

2.1 Waveform Inversion for the 17 and 21 June 2000 earthquake in Iceland. Summary of the cases treated.

The statistical parameters considered and reported are:

$$l2-error=\sqrt{\frac{\sum(s_i-r_i)^2}{\sum(r_i)^2}}$$

$$l1-error=\frac{1}{n_u}\sum\frac{|s_i-r_i|}{|r_i|}$$

$$fit=\sum|x_i colj_i-coli_i|$$

x_i = inverted slip rates
colj = synth. from contributing grids
coli = column data

si are the values of the synthetic calculated seismograms and *ri* those of the real ones.

nx is the number of cells along strike,

nh is the number of cells along dip,

x-step is the cell's dimension,

NP is the nucleation point.

Idt is the source time function time step (an integer # of deltim(time sampling interval of the seismogram)).

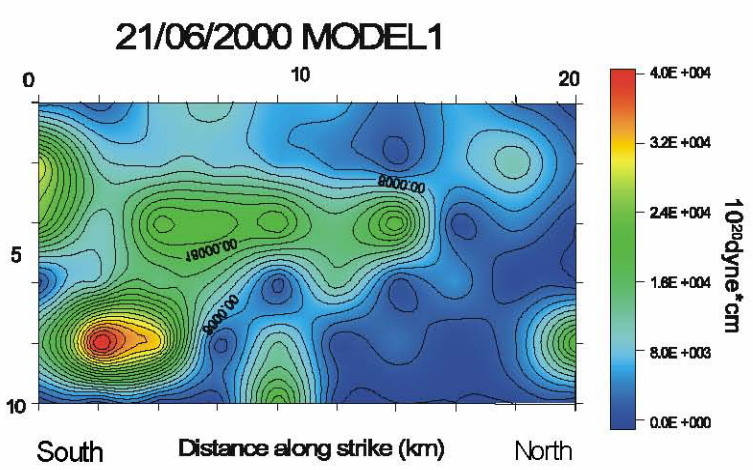

	model1
nx	10
nh	6
x-step	2
dip	90
strike	358
rake	172
NP	5,3
idt	3
momflag	yes
EPS	1.00E-05
delta	0.1
nu(eq.)	1008
nv (unk.)	827
l1-err	0.6
l2-err	0.77
fit	ok 1.48

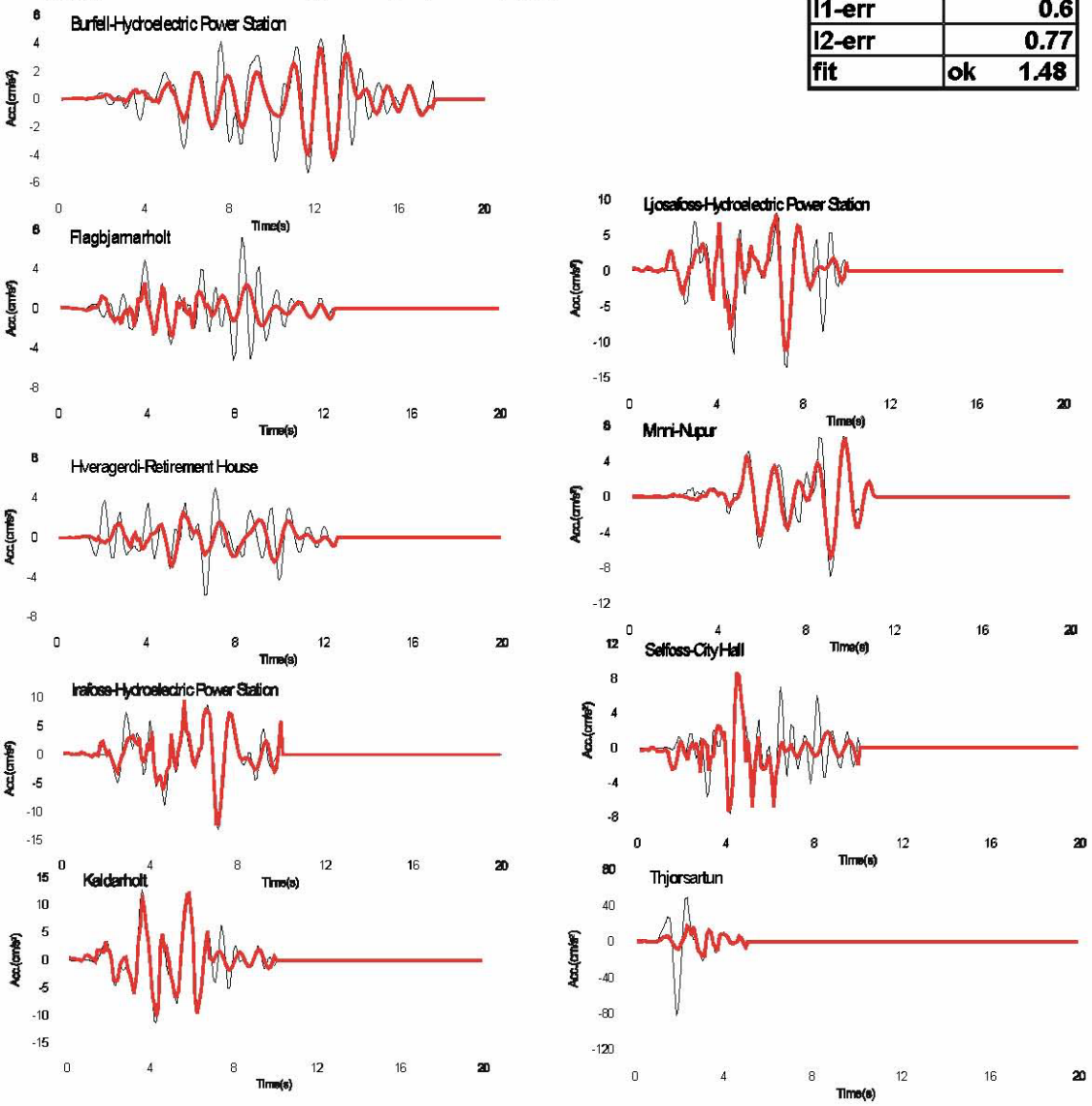

2

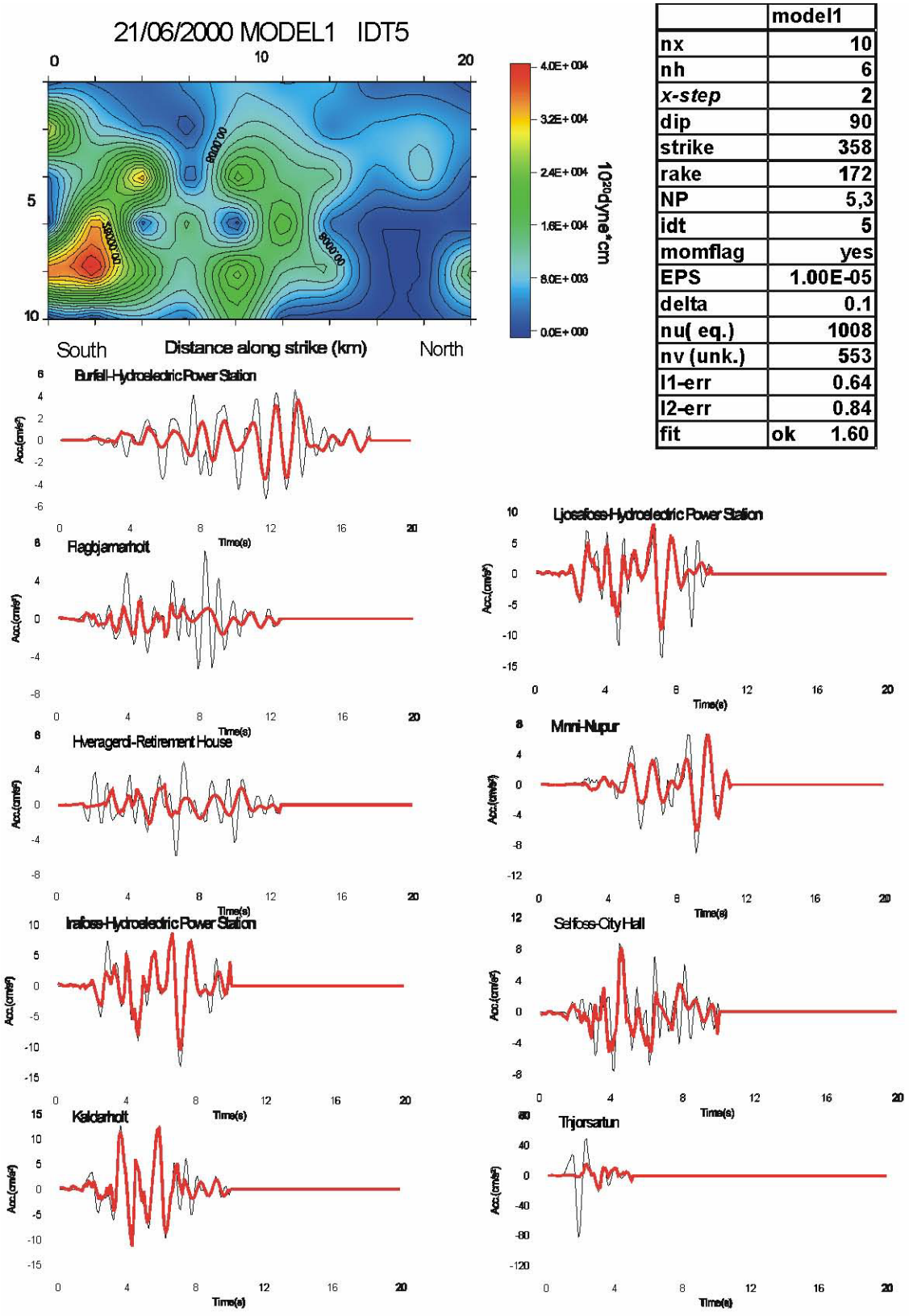

	model1
nx	10
nh	6
x-step	2
dip	90
strike	358
rake	172
NP	5,3
idt	5
momflag	yes
EPS	1.00E-05
delta	0.1
nu(eq.)	1008
nv (unk.)	553
l1-err	0.64
l2-err	0.84
fit	ok 1.60

3

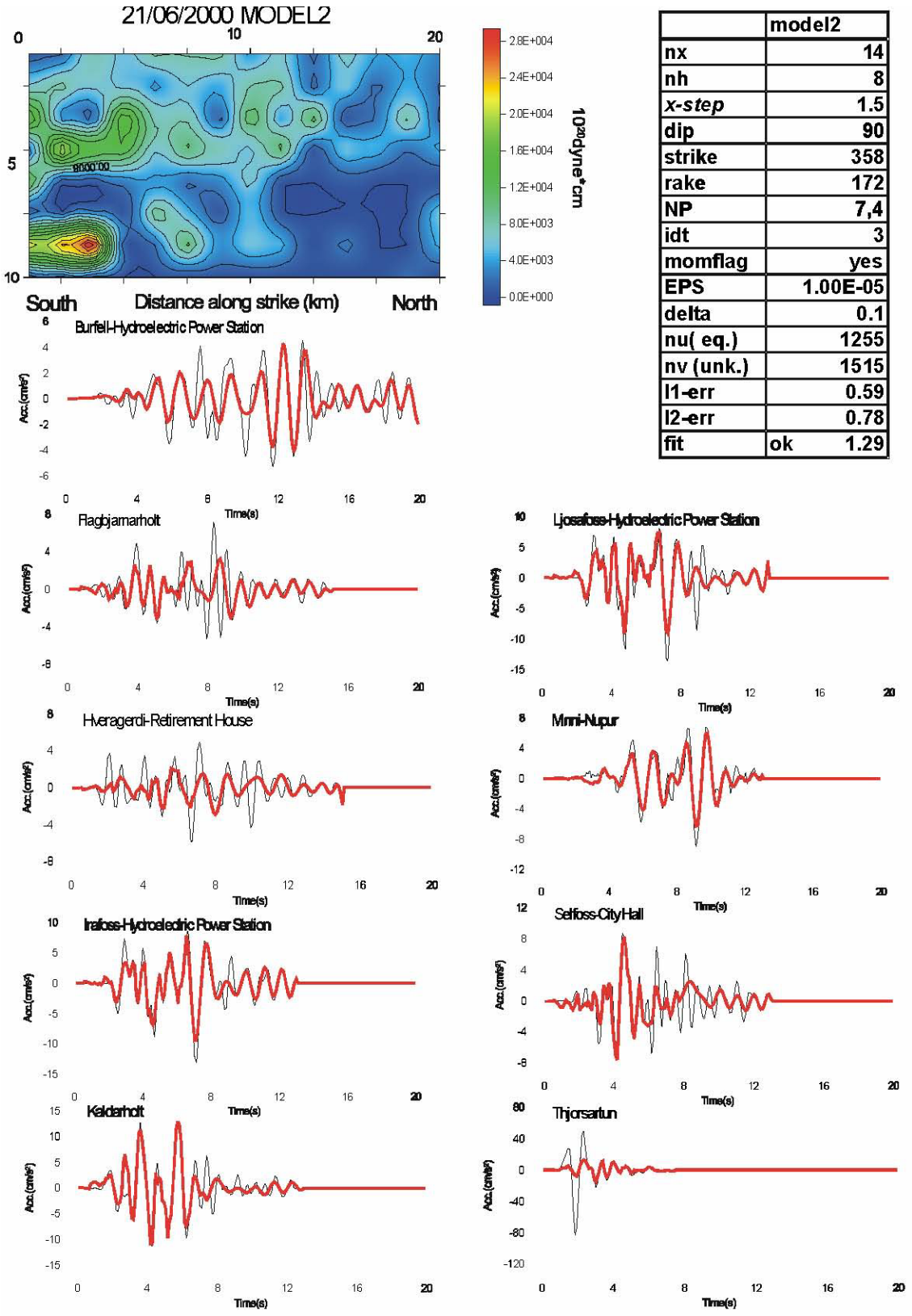

	model2
nx	14
nh	8
x-step	1.5
dip	90
strike	358
rake	172
NP	7,4
idt	3
momflag	yes
EPS	1.00E-05
delta	0.1
nu(eq.)	1255
nv (unk.)	1515
l1-err	0.59
l2-err	0.78
fit	ok 1.29

4

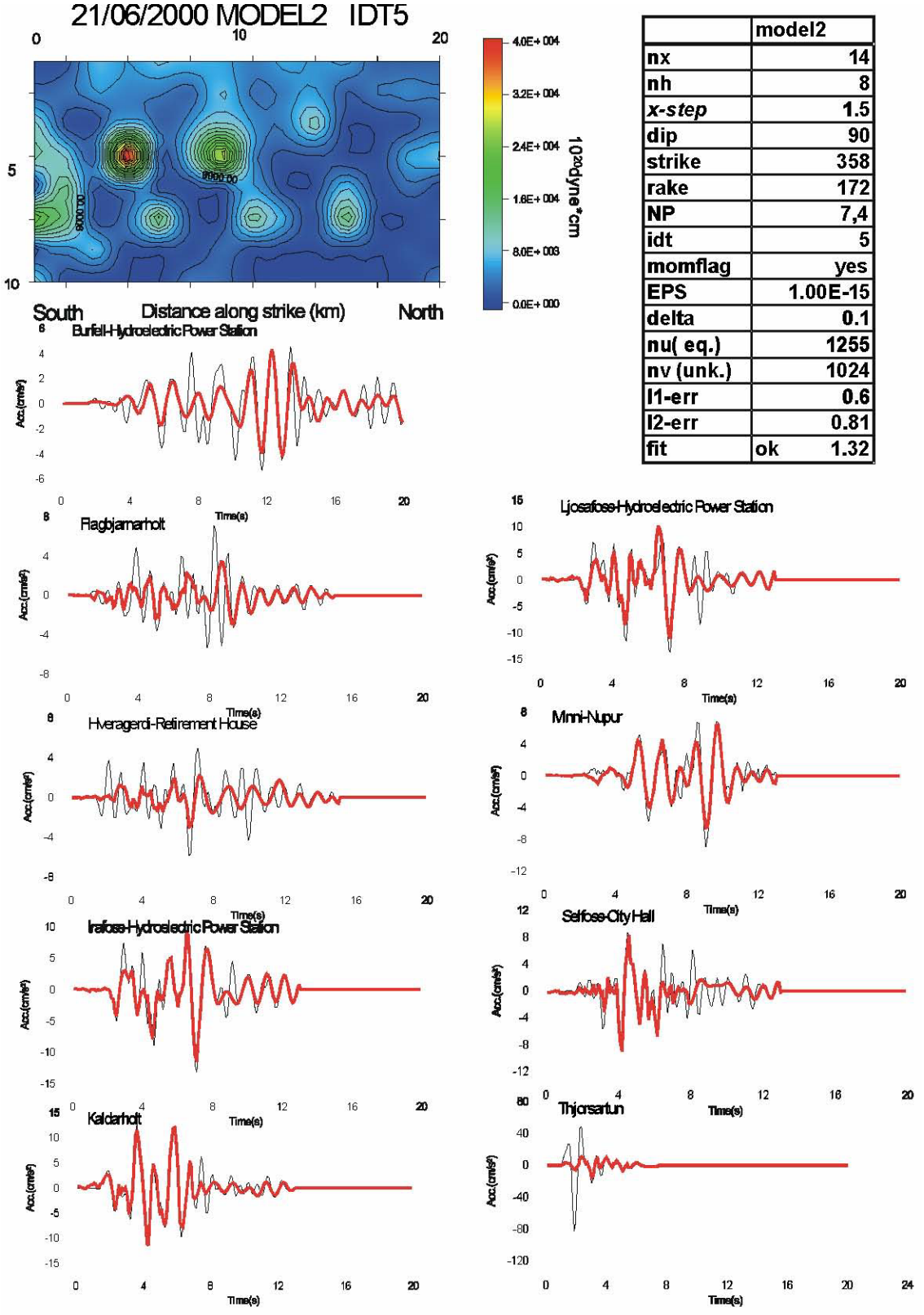

	model2
nx	14
nh	8
x-step	1.5
dip	90
strike	358
rake	172
NP	7,4
idt	5
momflag	yes
EPS	1.00E-15
delta	0.1
nu(eq.)	1255
nv (unk.)	1024
l1-err	0.6
l2-err	0.81
fit	ok 1.32

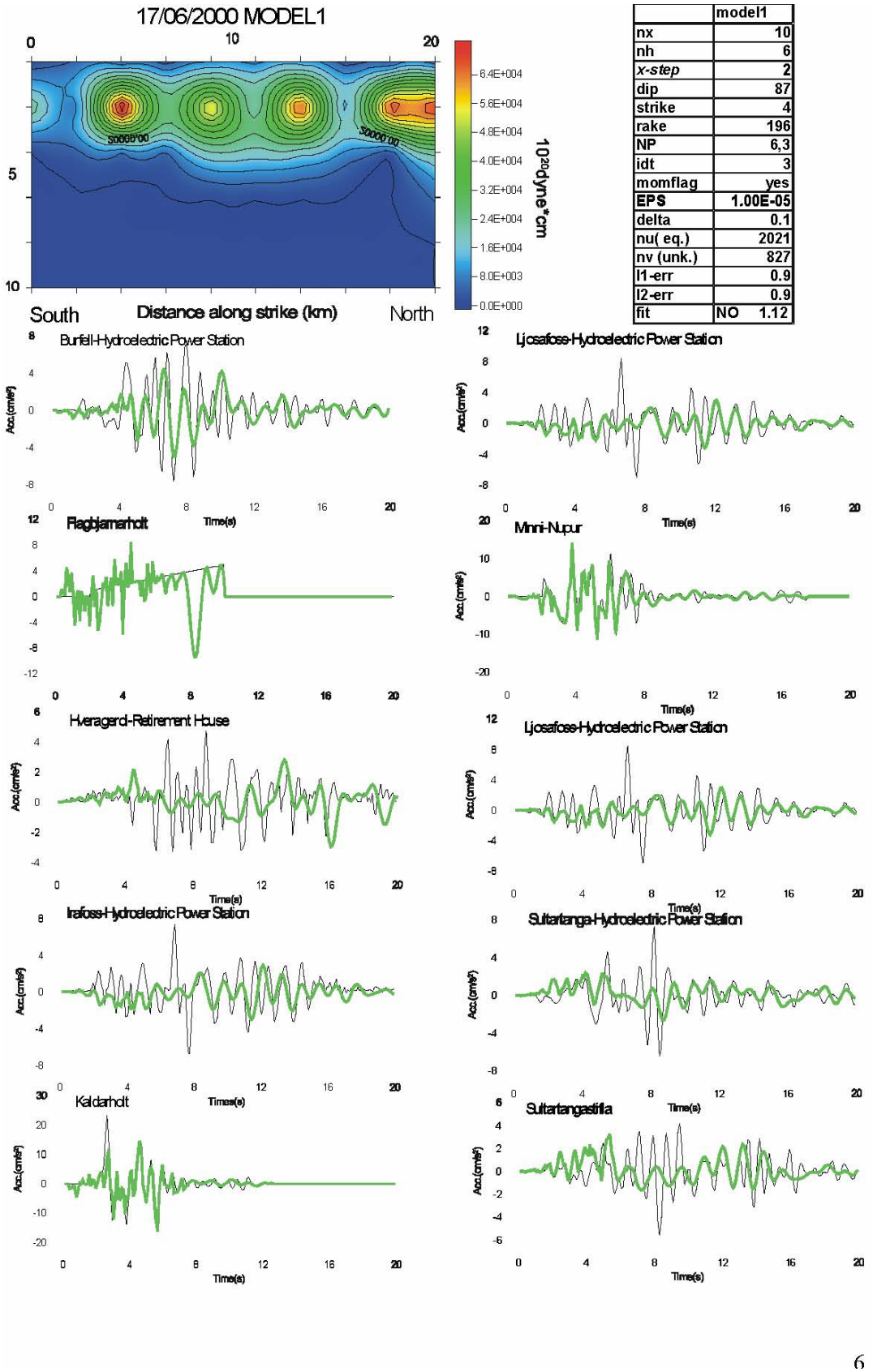

	model1
nx	10
nh	6
x-step	2
dip	87
strike	4
rake	196
NP	6,3
idt	3
momflag	yes
EPS	1.00E-05
delta	0.1
nu(eq.)	2021
nv (unk.)	827
l1-err	0.9
l2-err	0.9
fit	NO 1.12

6

These results indicate that for the June 21 earthquake most of the moment release is concentrated at the southern bottom end of the fault (about 8-9 km depth), while for the June 17 event, the moment is essentially concentrated near the surface (upper 5 km).

2.2 Problems encountered

Probably the poor results related to the inversions of the June 17, 2000 event are due to the strong assumption on the absolute timing of the strong motion records related to this event.

WP 4.3 Surface fractures in the source region of the June 2000 events

a) Objectives

1. Cast light on the relationship between surface faulting and faulting at depth during the June 2000 events.
2. Map the surface fractures in the area surrounding the two main faults active in the earthquakes.

Deliverables

1. A map of surface fractures in the central part of the South Iceland Seismic Zone was proposed. An overview map of the whole zone has been prepared, and detailed maps are available as well.
2. Map of faulting during the June 2000 events is available.
3. Presentations at two international meetings.
4. Paper on surface fracturing during the June 2000 events was published in 2005 (Clifton and Einarsson, 2005)
5. Input into the general modelling of the June 2000 events.

b) Methodology and scientific achievements

The epicentral zone of the SISZ shows widespread evidence of recent faulting (Einarsson et al., 1981). Historical documents mention surface faulting during some of the earthquakes, and in the case of the events of 1630, 1784, 1896 and 1912 the fractures have been located and mapped in detail (e.g. Einarsson and Eiríksson, 1982, Bjarnason et al., 1993). The fractures of 2000 have been mapped as well (Clifton and Einarsson, 2005). Structures resembling those of the 1912, 1896 and 1630 ruptures are found throughout the seismic zone. They can be grouped into systems interpreted to represent faults, more than 25 of which have been identified so far. The faults are transverse to the seismic zone and are arranged side-by-side with spacing of about 1 km between them.

In WP 4.3 we use differential GPS instruments to map in detail the remaining fractures of 2000 as well as all older fractures in the surrounding areas.

This work package consisted mainly of fieldwork in the source areas of the South Iceland Seismic Zone. During this reporting period emphasis was put on following areas: The Flói district west of the town Selfoss, the Holt area in the centre of the zone, and the Land-Rangárvellir district near the eastern end of the zone. Finally, fractures were mapped in the Grímsnes district, thought to be associated with the Grímsnes volcanic system near the northern border of the zone. A field assistant, Benedikt Ófeigsson, was hired for the summer and fall months of 2004 to assist PE in the field and analyse the data. A summer student from France, Guillaume Biessy, also participated in the fieldwork. Student groups from the University of Iceland contributed significantly to the mapping effort on field trips in October 2004. Teaching assistants were Dr. Maryam Khodayar and Ásta Rut Hjartardóttir. The work was mainly mapping previously known fractures, tracing them in the field with the GPS-mapping tools. With the experience and confidence gained during the 2000 earthquakes it was possible to identify considerably more fault structures than before. The fracture systems thus turned out to be more continuous than previously thought. Several fault segments were found that had not been identified before. These include segments belonging to the 1630 fault in Land district, fractures in Skeið district, thought to belong to the event of 1784, and one segment

active in the 1912 earthquake in Rangárvellir. The high rate of new discoveries suggests that further fieldwork may still be productive.

Work delivered so far

1. All major, known surface fault segments of the South Iceland Seismic Zone have been field checked and mapped by differential GPS instruments.
2. Surface faulting of the 2000 earthquakes was more extensive than previously thought. Additional faults have been mapped and a paper published in Tectonophysics (Clifton and Einarsson, 2005).
3. A simplified map of all known surface faults of the SISZ has been prepared for general use. This map is already in use on the earthquakes information website of the Iceland Meteorological Office (vedur.is) as a background to the real-time earthquakes locations of the South Iceland Seismic Zone. The map is also to be seen on a public information sign of the Icelandic Road Department at the epicentre of the June 21 earthquake of 2000 (see Fig. 1).
4. The general map base of the Icelandic Geodetic Survey has been incorporated into the mapping software. Detailed maps of faults can now be produced on that base for any sub-area. A sample of such a map is seen in Fig. 2.
5. Results of work under this work package have been presented at several meetings, including the Spring Meeting of the Icelandic Geoscience Society 2004 (Einarsson et al., 2004). A poster will be presented at the EGU meeting in Vienna in April 2005 (Einarsson et al., 2005).

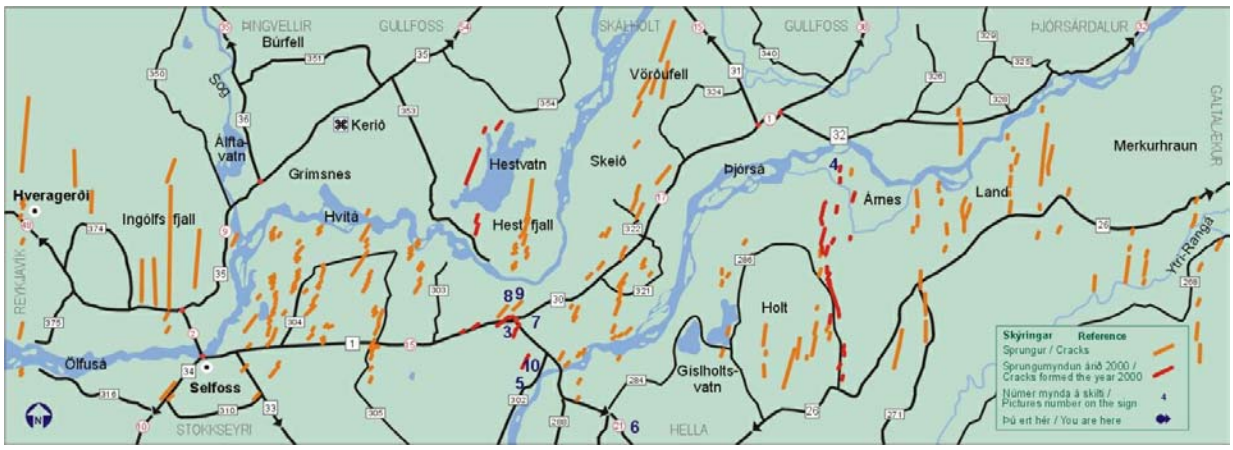

Fig. 1. *The main fracture systems of the South Iceland Seismic Zone. Fractures that are either known or suspected to be of Holocene age are orange. Red lines show fractures active in the 2000 earthquakes.*

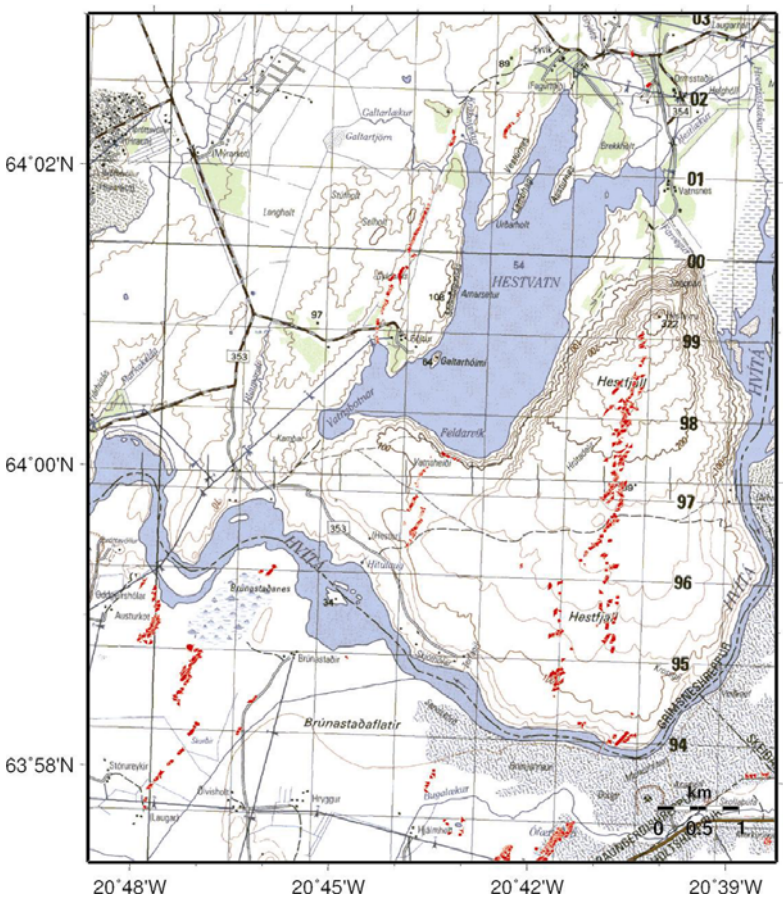

Fig. 2. *Fracture map of the Hestfjall area in the central part of the South Iceland Seismic Zone showing all identified Holocene fault structures. The squares form a 1 km x 1 km grid. The map base is from the Iceland Geodetic Survey.*

c) Socio-economic relevance and policy implication

The earthquakes of June 2000 had many socio-economic implications. One of them was that structures in a seismically active region can be built to withstand earthquakes as long as reasonable building practices are used and the structures are not built directly across faults. A reliable fault map, one of our deliverables, is clearly of high importance here. An effort has been made to provide easy access to the fault data so that a fault map can be produced on the conventional map base for any area of the seismic zone. Recent examples show, however, that the construction community is still not ready to make use of this new knowledge. It should be one of the priority issues to publicise the new fault map and educate the construction sector about its use. It should also be mentioned that the National Energy Company (Landsvirkjun), who is planning two hydropower projects within the seismic zone, is making every effort to circumvent fractured bedrock as foundation for their structures. Furthermore, the Road Department is using the fault map in their planning work for a new bridge on the river Ölfusá.

d) Discussion and conclusions

The mapping effort under this work package has filled in the previously known picture of the South Iceland Seismic Zone. A more complete picture has been gained of the previously known faults and new fault segments have been discovered. With the new fault map in hand it is interesting to compare it to the distribution of hypocenters in the zone. This comparison has led to new insights into the connection between faults at depth and surface fractures.

e) Plan and objectives for the next period

Although significant progress has been made in the reconnaissance of the seismic zone, many aspects are still unclear and need attention.

1. *Mapping.* We recognise that not all faults have been found so far in spite of considerable effort. We therefore plan further fieldwork in the summer of 2005 in order to trace faults into difficult terrain. This is particularly in the Grímsnes area.

2. *Faults at depth.* We will work with other researchers of the PREPARED-project to correlate faults on the surface with faults at depth as shown by hypocenters.

3. *Reconstruction of historic earthquakes.* Assuming that the present background activity is a combination of late aftershocks of previous earthquakes and events due to stress accumulation in the interseismic period, one can make inferences about the source faults of the latest historic earthquakes. We have started work on the 1912 earthquake along these lines (Einarsson et al., 2004) and plan to continue with the 1896 and 1784 sequences.

References

Bjarnason, I. Þ., P. Cowie, M. H. Anders, L. Seeber and C. H. Scholz. The 1912 Iceland earthquake rupture: Growth and development of a nascent transform system. Bull. Seism. Soc. Am., 83, 416 - 435, 1993.

Clifton, A., P. Einarsson. Styles of surface rupture accompanying the June 17 and 21, 2000 earthquakes in the South Iceland Seismic Zone. Tectonophysics, 396, 141-159, 2005.

Einarsson, P., and Jón Eiríksson. Earthquake fractures in the districts Land and Rangárvellir in the South Iceland Seismic Zone. Jökull, 32, 113-120, 1982.

Einarsson, P., S. Björnsson, G. Foulger, R. Stefánsson and Þ. Skaftadóttir. Seismicity pattern in the South Iceland seismic zone. Í: Earthquake Prediction - An International Review (Ed. D. Simpson and P. Richards). American Geophys. Union, Maurice Ewing Series 4, 141-151, 1981.

Einarsson, Páll, Maryam Khodayar, and Steingrímur Þorbjarnarson, and students of the courses Tectonics and Current Crustal Movements in the Faculty of Science of University of Iceland in 2003.. Surface ruptures in the South Iceland earthquake of 1912. Icelandic Geoscience Soc. Spring Meeting 2004. Abstracts of papers and posters, p. 47.

Einarsson, P.; Khodayar, M.; Clifton, A. ; Ofeigsson, B.; Thorbjarnarson, S.; Einarsson, B.; Hjartardottir, A. R. A map of Holocene fault structures in the South Iceland Seismic Zone. Paper at the General Assembly of the European Geosciences Union, Vienna, April, 2005. Abstract EGU05-A-08858, 2005.

WP 4.4 Deformation model for the June 2000 earthquakes from joint interpretation of GPS, InSAR and borehole strain data

a) Objectives

The objectives of the work package are to evaluate the 3D co-seismic deformation associated with the June 2000 earthquakes and derive a deformation model for the earthquakes based on joint interpretation of all the available geodetic data.

b) Methodology and scientific achievements related to workpackages

We have completed the analysis of InSAR and GPS data to derive the co-seismic displacement field for the June 17 and June 21, 2000, main shocks and three triggered earthquakes on the Reykjanes Peninsula (e.g. *Pagli et al.,* 2003). The data for the June 2000 main shocks have been analysed and a joint inversion of the InSAR and GPS data for fault geometry and slip distribution has been completed (*Pedersen et al.*, 2003), assuming rectangular dislocations in an elastic half-space. In the inversion procedure the InSAR data is first unwrapped, and then the number of InSAR data is reduced by quadtree partitioning algorithm to speed up model computations. We have used this same method of analysis and inversion to obtain best fit source parameters and locations for the three M~5 triggered earthquakes on Reykjanes Peninsula (*Clifton et al.*, 2003). The study has been completed and published in the Journal of Geophysical Research (*Árnadóttir et al.*, 2004). Figure 1 shows the dataset used in the joint inversion for the events on the Reykjanes Peninsula.

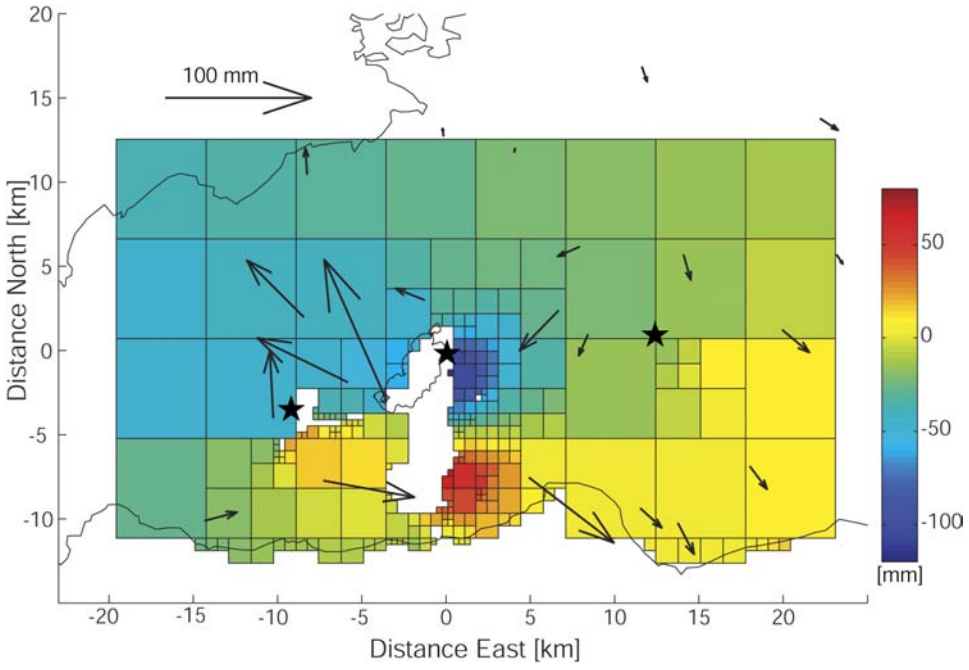

Figure 1. *Quadtree partitioned, unwrapped InSAR data from Track 367 covering the June 17, 2000 triggered earthquakes on Reykjanes Peninsula. The colour scale shows slant range displacements (~23 degrees from vertical), in the direction toward the satellite in mm. Blue is range increase, and red is range decrease, signifying subsidence and uplift respectively. The co-seismic GPS displacements are shown with black arrows. Black stars show epicentre locations determined from seismic data.*

We use a non-linear inversion algorithm to estimate the fault geometries and locations for the three triggered events on June 17, assuming uniform slip on three rectangular faults. The preferred model indicates three near vertical faults with primarily right-lateral strike slip (Figure 2). The largest observed co seismic deformation signal is near lake Kleifarvatn. Our study suggest that the event near Kleifarvatn (second triggered event) had significantly larger moment (Mw=5.9) than seismic estimates (Mw~5-5.5), indicating a component of aseismic slip on the fault.

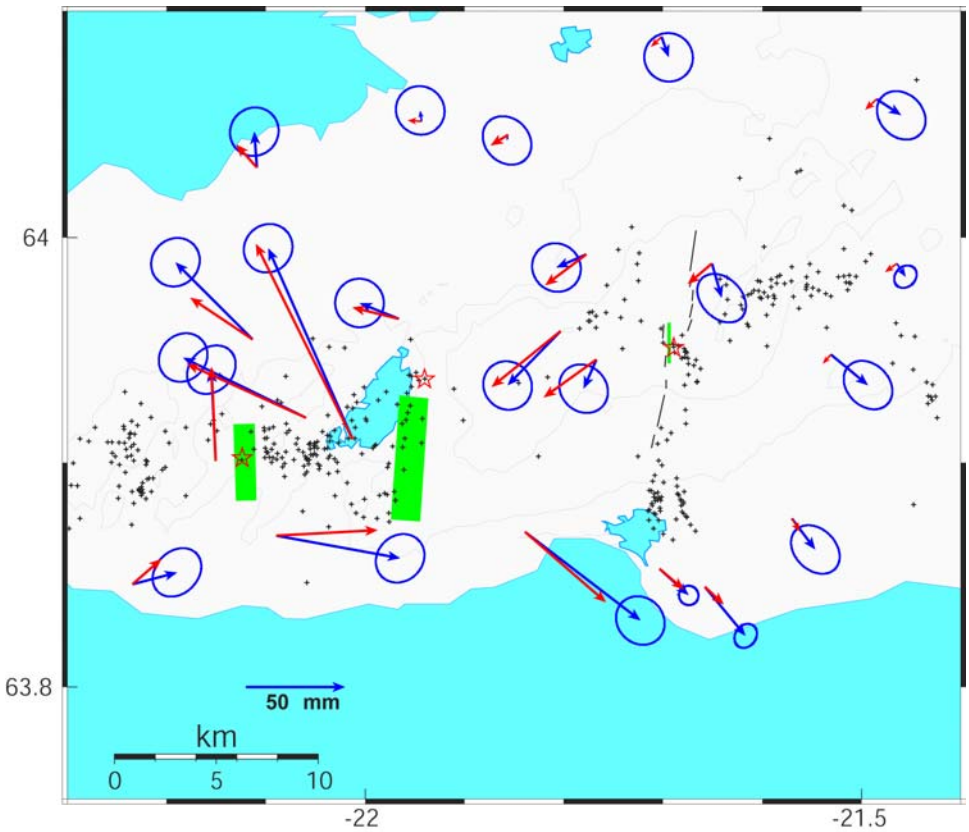

Figure 2. *Horizontal coseismic displacements (blue arrows with 95% confidence ellipses) and model prediction (red arrows) for the three June 17 earthquakes on Reykjanes Peninsula. The surface projection of the three fault models is shown with green. Black crosses indicate M>1 earthquakes located with the SIL seismic network from June 17 to December 31, 2000. The red stars show the locations of the the June 17 earthquakes.*

We want to examine the role of static Coulomb failure stress changes in triggering of the events on Reykjanes Peninsula. For this, we use the distributed slip models for the June 17 main shock (Pedersen et al., 2003) and fault models from this study to estimate the change in Coulomb failure stress (CFS) following *Árnadóttir et al.* (2003). The static stress calculations indicate a very small increase (0.02 MPa) in the static Coulomb failure stress due to the June 17 main shock and first triggered event on Reykjanes Peninsula at the hypocenter of the second triggered event (*Árnadóttir et al.*, 2004). The event at Kleifarvatn, however, increased the Coulomb stress at the hypocenter of the third event by 0.1-0.2 MPa (see Figure 3). This and the timing of the first two events (26 s and 30 s following the main shock, respectively) supports the view that the first two events were dynamically triggered by surface waves from the June 17 main shock (K. Vogfjörd, personal communication, 2004). The third triggered event occurred almost 5 minutes after the June 17 main shock, and could therefore be triggered by the static stress changes caused by the second event (at Kleifarvatn). The second event also appears to have loaded the fault that ruptured in the first triggered event. This fault is capable of M~6 events, and probably last ruptured in such a large

event in 1968. This study has implications for future seismic hazard assessment on Reykjanes Peninsula.

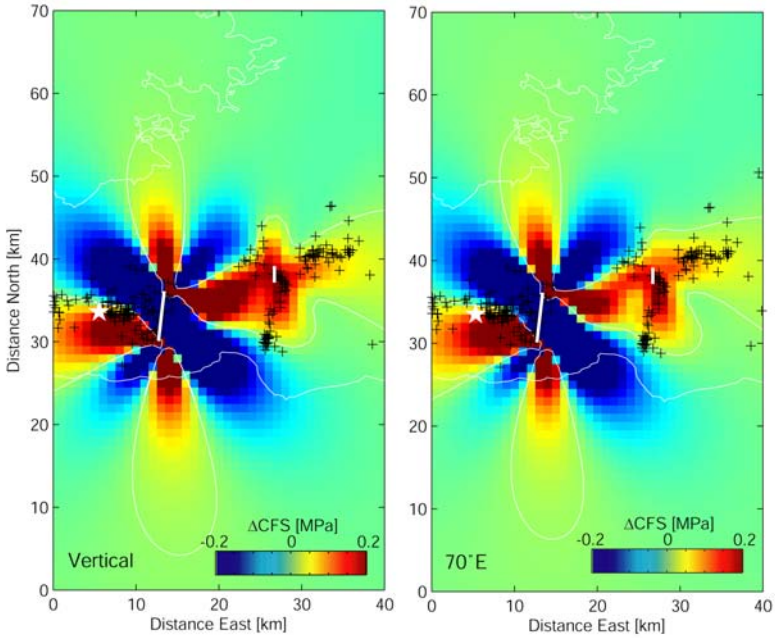

Figure 3. *Static coseismic Coulomb failure stress (CFS) changes due to the June 17 main shock in the SISZ and first two triggered earthquakes on the Reykjanes Peninsula, at 3 km depth for N-S, right lateral strike slip faults. (a) Vertical receiver faults (b) receiver faults dipping 70° east. Warm colour indicates stress increase, and contours surround areas where the CFS increased by more than 0.01MPa. The white star shows the epientral location of the third event. Black crosses mark the same earthquake locations as shown in Figure 1 and 2. The surface projections of the fault models are shown with white lines.*

We participated with P1 and P6 in the study of the Reykjanes Peninsula events.

c) Socio-economic relevance and policy implication

The deliverables of this workpackage are the first detailed estimates of co-seismic slip distribution on faults in the South Iceland seismic zone and a detailed study of three triggered events on the Reykjanes Peninsula. They provide important information that can be used in estimation of seismic hazard in the area. The algorithm we have developed can be adapted for use for similar scenarios of events, in other hazardous areas in Europe.

d) Discussion and conclusions

We have modeled the co-seismic surface displacements due to the June 17 and June 21, 2000, main shocks and three triggered events on the Reykjanes Peninsula. We have used the fault models to calculate static Coulomb failure stress changes for the whole area. The models obtained from geodetic data can be compared with similar models obtained in other workpackages (e.g. WP4.2), and are already implemented in the dynamic stress calculations in WP6.2.

e) Plan and objective for the next period

We are collaborating with P10 (Kurt Feigl) to refine the model of the June 2000 SISZ earthquakes, using finite element modelling techniques. We are also collaborating with P10 in re-processing the GPS data using the GAMIT/GLOBK software to estimate pre- co- and post-seismic deformation in the SISZ. We plan to use the relative relocations of the aftershocks (results from WP5.1) to refine the fault geometries. We will also examine relationships between areas of surface rupture (WP5.2), refined aftershock locations and high fault slip.

References

Árnadóttir,Th., H. Geirsson and P. Einarsson, Coseismic stress changes and crustal deformation on the Reykjanes Peninsula due to triggered earthquakes on 17 June 2000, *J. Geophys. Res.* 109, B09307, doi:10.1029/2004JB003130.

Árnadóttir,Th., S. Jónsson, R. Pedersen and G. Gudmundsson, Coulomb stress changes in the South Iceland Seismic Zone due to two large earthquakes in June 2000, *Geophys. Res. Lett.*, vol. 30, doi:10.1029/2002GL016495, no. 5, 2003.

Clifton, A.E., C. Pagli, J.F. Jónsdóttir, K. Eythórsdóttir, and K. Vogfjörd, Surface effects of triggered fault slip on Reykjanes Peninsula, SW Iceland, *Tectonophysics 369*, 145-154, 2003.

Pagli et al., Triggered fault slip on June 17, 2000 on the Reykjanes Peninsula, SW Iceland captured by radar interferometry, *Geophys. Res. Lett., 30(6),* 1273, doi:10.1029/2002GL015310, 2003.

Pedersen, R., S. Jónsson, Th. Árnadóttir, F. Sigmundsson, and K.L. Feigl, Fault slip distribution of two Mw=6.5 earthquakes in South Iceland estimated from joint inversion of InSAR and GPS measurements, *Earth and Planetary Science Letters, 213*, 487-502, 2003.

WP 5 New hazard assessment/New methods for improving assessment of probable earthquake effects

Objectives

On basis of the unique observations made in relation to the June 2000 earthquakes in the SISZ as well as on basis of results of modelling the earthquake sources in time and space we aim towards a more detailed hazard assessment both as concerns the location and severity of probable earthquake hazard. This improvement is very significant basis for a general risk assessment.

Methodology and scientific achievements related to workpackages including contribution from partners

Faults and fractures in the area have been mapped in detail. This has been done by mapping fault and fractures at depth by microearthquake studies described in WP5.1 and also by surface observations (WP5.2). The mapped area takes to the whole of what is usually named the South Iceland seismic zone (SISZ) as well as to its prolongation towards west on the Reykjanes peninsula. In this area fault traces at depth were "illuminated" by aftershocks, that can be used to map fault segments at depth along the entire 100 km long EW trending plate boundary.

Fault that opened to the surface at several places along this line have been mapped as well as older faults and fissures (WP5.2, WP4.3, WP5.6).

Digital fracture maps of the Reykjanes peninsula have been made using GIS. These maps also include rock falls and mountain slopes (WP 5.2)

These observations will now be compared to find the faults that can be expected to be the location of large future earthquakes, as well as detecting the sites for other potential geohazards.

All this mapping will be integrated into a new hazard map of SW Iceland.

This mapping is also a significant input into modelling stresses and tectonic interaction of the plate boundary in general (WP6).

Evaluation of data from digital strong motion records near the origin (WP5.3), complemented with information on surface effects as mapped by geologists (WP4.3 and 5.2), complemented with faults seismically mapped at depth (WP4.1 and 5.1), complemented with intensities based on questionnaires, will improve the basis for mapping of earthquake hazard probability. Historical earthquakes are being reevaluated (WP5.4) in the light of these recent findings to enhance our observational basis.

Paleostress fields and traces of prehistorical earthquakes have been studied inWP5.6, adding to documentation of our earthquake history.

Coupling between events are a strong concept in developing time dependent hazard assessments and warnings. Here coupling based on Coulomb stress changes is significant and applied for modelling in WP4.4 for short-term changes and in WP6.1 for modelling of historical data. Dynamic coupling was also experienced during the 2000 earthquakes and has been modelled in WP6.2.

Drastic changes in groundwater and geothermal water systems in the area were observed, especially following the June 2000 earthquakes. These have been analyzed and compared to the detailed models of the earthquakes to understand better the relation between such earthquakes and hydrological changes (WP5.5, WP2.3, WP4.4).

WP5 operates like a forum consisting of representatives from especially WP5.1-5.6 and WP4.2 for integrating the results from the multidisciplinary work. Most of the other workpackages of the project have also produced results which can be applied here, not least the modelling packages WP6.1 and WP6.2.

Up to the last part of the project period the work in WP5 has been limited to discussion with individual contributors but will gradually be extended throughout the project.

Socio-economic relevance and policy implication

Information of what ground motions can be expected at various places in populated areas is socially and economically significant. Where will the faults rupture the surface and when is of huge significance in any earthquake-prone country.

Social and economic impacts of a destructive earthquake or the knowledge that a destructive earthquake is to be expected is enormous and can be of such an effect to break up communities.

Knowledge of what can be expected leads to direct precautions in where and how man made structures are built, or leads to strengthening or removal of existing vulnerable buildings. It implies various technical and social precautions and preparedness that can mitigate the impact of earthquake hazards in various ways, on people and on society. Methods for spacially detailed time dependendent hazard assessment which are emerging in this project will be significant to realize such precautions

Discussion and conclusion

The multidisciplinary fault mapping together with progress in modelling the earthquake processes in the SISZ will help to make a more detailed and secure hazard assessment for the whole region. A special application will be a real-time hazard assessment, for nowcasting and short-term warnings, when the probable location is detected of a probably impending earthquake.

Plan and objectives for the next period

The objective of WP5 for the this last period is to merge together the results of the various WP´s into a common new detailed hazard map as well as into producing other tools for fast evaluations and visualization of hazard conditions, and a WP5 report near the end of the period.

WP 5.1 Mapping subsurface faults in southwestern Iceland with the microearthquakes induced by the June 17th and June 21st earthquakes

a) Objectives

To map sub-surface fault planes and slip directions on faults in south-west Iceland that were illuminated by the microseismicity induced by the June 17th (J17) and June 21st (J21) earthquakes. This includes faults within and around the South Iceland seismic zone (SISZ), as well as within the rift zone on Reykjanes peninsula. Thousands of smaller earthquakes followed J17 and J21, induced either by seismic waves propagating from the two, or by the slower propagating change in stress field, resulting from the large (roughly 1m) slips on their several kilometer long faults. The resulting map is a significant input to the detailed hazard map, which will be prepared in the project, as closeness to active faults is critical for the ground motion of shallow earthquakes in South Iceland. The map is also a necessary input for models of stress field changes in time and space.

b) Methodology and scientific achievements related to workpackages including contributions from partners

Roughly nineteen thousand microearthquakes recorded by the SIL seismic network between June and December 2000 and interactively analyzed, have been relatively relocated using the multi-event relocation method described in the M12 report. Approximately half of them occured outside the two main faults. This analysis increases the location accuracy to such a degree that individual fault patterns become resolvable.

The study area, southwest Iceland, was divided into 13 partly overlapping boxes for analysis. Faults and clusters have already been identified in eleven boxes. Most faults strike close to north and show a dominant right-lateral slip direction, often with a small normal component, as commonly observed in the SISZ. In the Western Volcanic Zone (WVZ), north-east fault directions are more common, but right-lateral motion is still the dominant slip direction. In many areas, fault strikes occationally deviate from the normal trend of the area and more easterly directions can be observed. These are predominantly left-lateral strike-slip faults with a small normal component.

c) Socio-economic relavance and policy implication

A detailed map of subsurface faults and slip directions, along with surface features mapped in the Reykjanes Peninsula (WP5.2) and the SISZ (WP4.3), will be an important contribution to the refinement of a tectonic map and for the mapping of the stress field in southwest Iceland. The fault map may also have great value for geothermal power companies and water suppliers in southwest Iceland, as it reveals subsurface faults, not seen before and possibly the plumbing system delivering fluid into the geothermal systems in the Hengill-Hellisheiði area and Geysir, as well as water wells.

d) Discussion and conclusion

Delivery 79, a catalogue of relocated earthquakes from June-December 2000, is already completed and the delivery report is attached in Appendix 2. Delivery 80 comprises a map of subsurface faults and corresponding slip directions and it is close to completion.

The fault mapping with the aftershocks has proven invaluable in determining the fault dimensions of the two dynamically triggered M~5 events on June 17th, although the aftershock distribution is not contiguous. Their waveforms are clipped and ride on top of the J17 shear waves, and thus their exact location and mechanism determination has proven problematic. Two other earthquakes of similar size occured within minutes of the J17 event. The plane of the most eastern event is well defined by the aftershock activity, but hardly any aftershocks have been mapped on the fault of the most western event. Further analysis of these triggered events can be found in report WP4.1.

e) Plan and objectives for the next period

In the next few weeks, identification of faults in the remaining boxes will be completed. Additionally, an overall slip direction will be calculated for each fault/cluster. Following this work, the primary aim is to write an article about the correlation between subsurface faults and mapped surface faults (see WP5.2 and WP4.3).

Abstracts

Hjaltadóttir, S., Vogfjörð, K. and Slunga, R., Relative locations of earthquakes in SW-Iceland, Summer school on Tectonic-Magmatic Interaction, 31 August - 8 September, 2003, Geysir, South Iceland, p. 18, Nordic Volconological Institute report 0303, Reykjavik, Iceland, 2003.

Hjaltadóttir, S., Vogfjörð, K. and Slunga, R, Einarsson, P., Stefánsson, R., Relative locations of microearthquakes and mapping subsurface faults in southwest Iceland (in Icelandic). Science Symposium (Raunvísindaþing), Askja, University of Iceland, 16-17 April, 2004. p. 75.

Hjaltadóttir, S., Vogfjörð, K. S. 2004: Relative event locations and mapping of faults in southwest Iceland (in Icelandic). Geoscience Society of Iceland, Spring meeting 2004. p. 54-55.

Hjaltadóttir, S., K. S. Vogfjord, R. Slunga, 2005: Mapping Subsurface Faults in Southwest Iceland Using Relatively Located Microearthquakes. Geophysical Research Abstracts, Vol. 7, 06664, 2005.

WP 5.2 Mapping and interpretation of earthquake rupture in the Reykjanes peninsula and other surface effects there and in the SISZ

Deliverable D82: Hazard map(s) of Reykjanes Peninsula and accompanying report

A series of thematic maps were made to illustrate areas on Reykjanes Peninsula which may experience hazards related to seismicity; i.e. rupture, rockfall, damage from shaking. A digital fracture map was produced containing over 6600 individual faults and open fractures, each feature possessing attributes which may be easily accessed within a GIS environment. The fracture map was made using digital 3-band (real color), orthorectified aerial photographs and a digital elevation model (DEM) purchased from Loftmyndir hf. in Reykjavík. Resolution of the photos is 0.5 meters per pixel. The DEM has a grid spacing of 20 meters and vertical accuracy of 5 meters. A considerable amount of field-checking and ground-truthing was conducted during the course of mapping. Real-time differential GPS data was collected along a number of faults in order to check the spatial accuracy of the air photos and to check some assumptions made during the mapping process, such as fault dip and vertical offset. However, most mapping of fractures was acheived by tracing vector line coverages over 0.5 meter per pixel images using Erdas Imagine software (V.8.6). In order to facilitate interpretation, photos were also draped over the DEM and viewed in a 3-d environment (VirtualGIS) within the Imagine software package. Attached to each line is a set of attributes, including line length and strike, which can be accesssed within a GIS by clicking on the line. The files created are seamlessly interoperable with ArcGIS and have been imported into an ArcGIS environment for some of the analyses described in this report. Maps shown in this report were made using ArcMap.

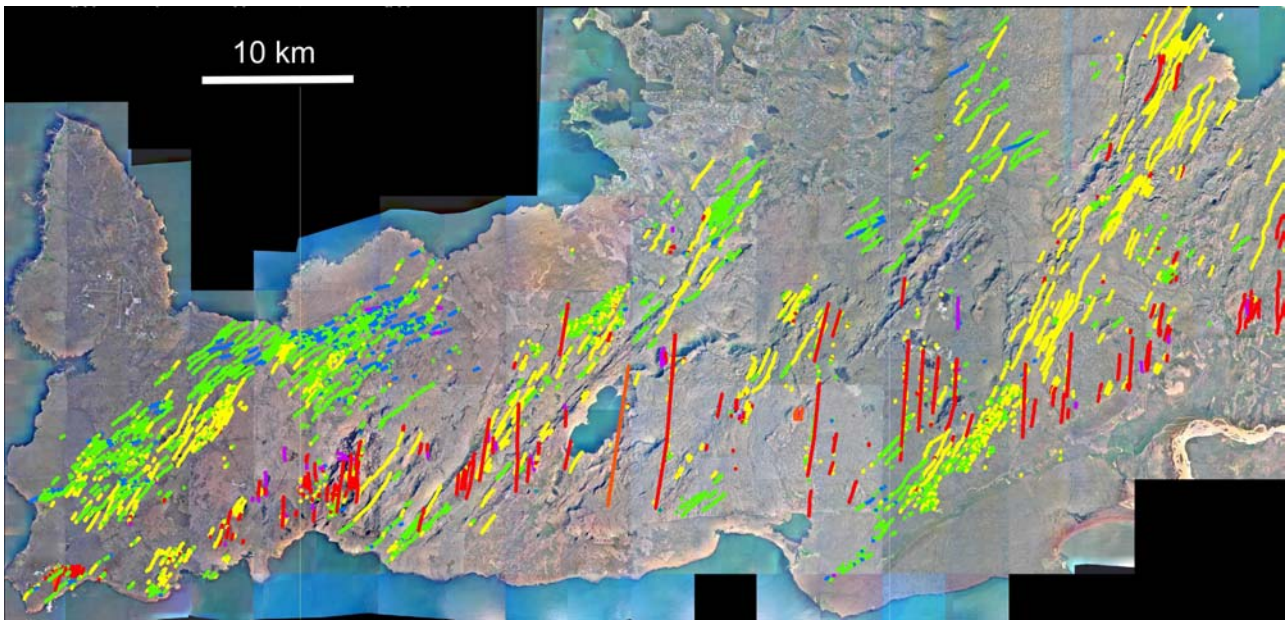

Fig. 1. *Map of fractures on the Reykjanes Peninsula. Fractures are shown with a symbology based on strike direction. Red = 000° to 020°; Yellow = 020° to 040°; Green = 040° to 060°; Blue = 060° to 080°; Purple = 080° to 180°. Map overlain on photomosaic with 2 meters per pixel resolution.*

The map in Figure 1 shows fractures superimposed on a 2 meter per pixel resolution photomosaic of the Reykjanes Peninsula. Fractures are shown with a color symbology representing strike

direction. Fractures striking between 000° and 020° are shown in red, between 020° and 040° in yellow, between 040° and 060° in green, between 060° and 080° in blue, and between 080° and 180° in purple. Prominant on this map, represented primarily in red, is a system of closely spaced, N- to NNE-striking faults similar in geometry and spacing to the system of strike-slip faults mapped in the South Iceland Seismic Zone (see Clifton and Einarsson, 2005; fig.2). Data suggests that these faults are accomodating left-lateral strain through book-shelf style faulting on right-lateral strike-slip faults in a manner similar to that identified in the South Iceland transform zone further to the east (e.g. Einarsson and Eiriksson, 1982). However, field data indicates that there is considerably more vertical offset along some of these faults than is observed in the South Iceland Seismic Zone. It is these faults which have generated several large ($M \geq 5$) earthquakes on the peninsula during the past 100 years. Records or accounts from the period before the late nineteenth century are sparse. Three N-striking faults within this zone slipped in a right-lateral sense during the large earthquakes ($M \geq 5$) that were triggered on 17 June 2000 (Clifton et al., 2003a; Pagli et al., 2003; Árnadóttir et al., 2004).

Faults shown in yellow, green and blue in Figure 1 are mainly normal faults, but many are open fissures without visible vertical offset. Some open fissures are believed to represent the damage zone of faults at depth propagating upwards and form due to flexure of lava layers during fault propagation. Other open fissures may form due to extension during dike injection events. Further study is required to better constrain these two types of open fissures. Leveling studies conducted during the past 40 years (Tryggvason, 1970; Anell, 2004) show that subsidence is ongoing along at least some of these faults, though it is not clear whether their motion is seismic or aseismic in nature. Much remains to be learned about the behavior of these large normal faults. It has been assumed that they move primarily during so-called magmatic episodes along the plate boundary and are often referred to as "rift-related" structures, but it is not known whether they also move during amagmatic periods. Nor is it known how large an earthquake may occur during a slip event along one of these normal faults. The geometry of many of these "rift-related" structures suggests that they have experienced oblique-slip, and a few are favorably oriented to accomodate strike-slip motion. They are highly segmented and possess an en-echelon geometry, some with a left-stepping sense suggestive of right-lateral strike-slip and some with a right-stepping sense suggesting left-lateral strike-slip. A synoptic diagram (fig. 2) shows the predominant fault strikes and their geometric relationships with respect to the trend of the plate boundary (rift trend) and that of the direction of plate spreading. These geometries are expected in a highly oblique rift zone such as the Reykjanes Penisula (see Clifton et al., 2003b).

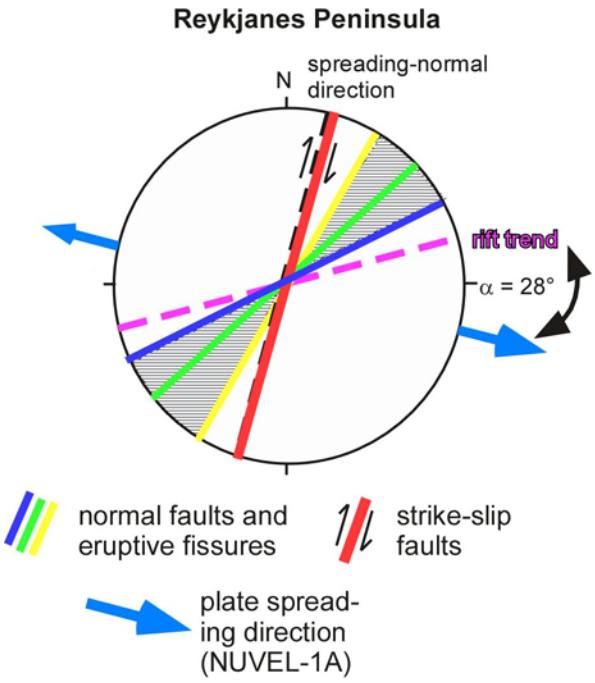

Fig. 2. *Synoptic diagram of structures on the Reykjanes Peninsula showing their geometric relationship to the NUVEL-1A spreading direction and the trend of the rift zone.*

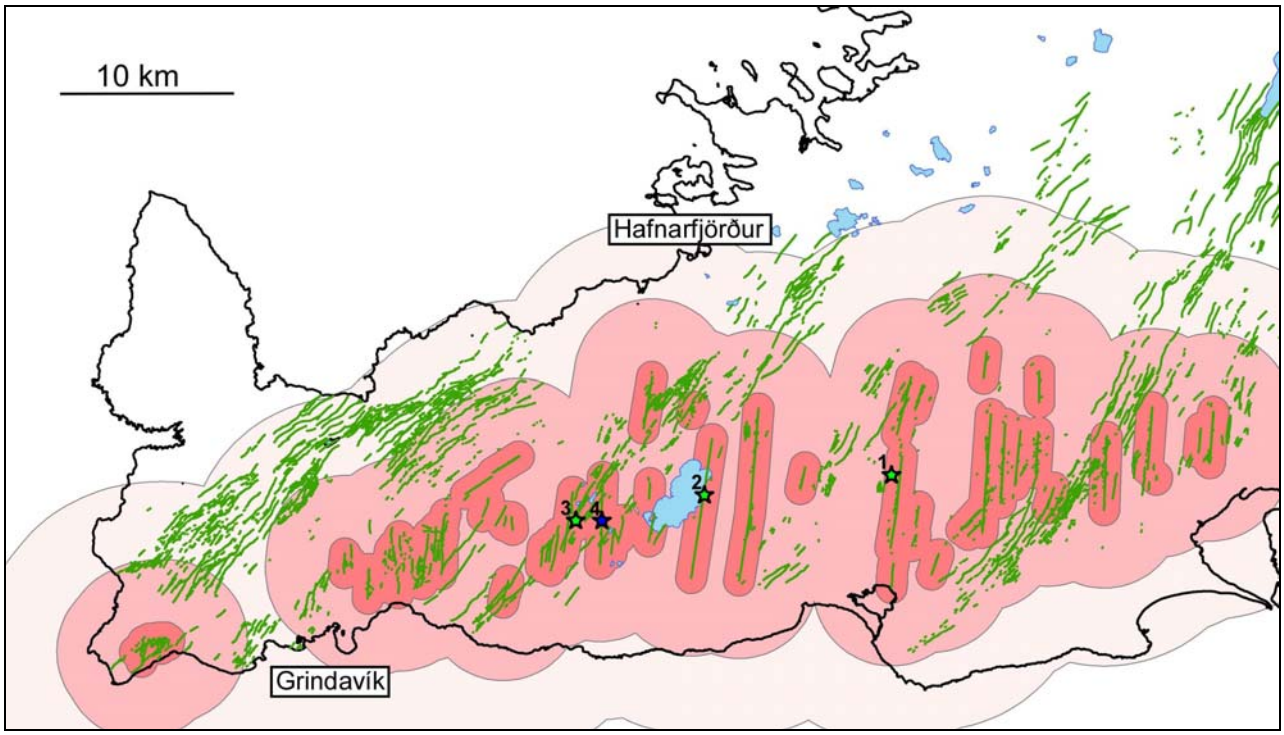

Fig. 3. *Map showing 1 km, 5 km and 10 km buffer zones around strike-slip faults on Reykjanes Peninsula. Green stars represent the epicenters of earthquakes that occurred on 17 June 2000. 1) Hvalhnúkur fault; 2) Kleifarvatn fault; and 3) Núpshlíðarháls fault. Blue star shows the epicenter of the M5 earthquake that occurred on 23 August 2003.*

The map in Figure 3 shows the same faults, this time without color coding. Faults which have been identified as strike-slip are surrounded by three buffer zones. The inner zone is 1 km wide around each fault, a central buffer zone 5 km wide and an outer zone 10 km wide. Although the amount of damage that can be expected in this zone has not been quantified, estimates can be made based on the events of 17 June 2000 (epicenters represented by green stars) and a more recent event on 23 August 2003 (epicenter represented by blue star) in the same general area. The area within the 1 km buffer zone is likely to experience damaging surface effects if an earthquake of magnitude 5 or greater were to occur along a specific fault. This is likely to include primary surface rupture, fissuring due to shaking and/or subsidence of the soil layer, rock slides, block slides and slumps and rockfall. All of these occurred along the Kleifarvatn fault, and all but primary surface rupture occurred along the Núpshlíðarháls fault on 17 June 2000 and the fault responsible for the 23 August 2003 earthquake. People who were within the 1 km buffer area for the Kleifarvatn fault describe effects equivalent to MM VIII. The area within the 5 km and 10 km buffers would feel the effects to a lesser degree. Primary surface rupture would not be expected at these distances from the epicenter. On 17 June 2000, the town of Hafnarfjörður, more than 10 km from the epicenter of all three earthquakes, experienced effects comparable to MM IV or V. Due to the short time span in which they occurred, it cannot be determined with certainty which of the three earthquakes caused these effects.

Many large normal faults are in close proximity to known strike-slip faults and it is possible that they could experience triggered slip during a strike-slip event if they are geometrically compatible. Such a scenario may be exemplified by the fault geometry shown in Figure 4. An earthquake along the largest of the strike-slip faults shown in red could very possibly induce slip on the left-stepping set of faults (shown in yellow) directly to the north. Field evidence shows that these faults have accumulated significant vertical displacement (on the order of meters) in the past 5000 years, but

preliminary examination of kinematic indicators such as opening vectors and secondary fracturing suggest that they have experienced oblique slip. These faults are less than 10 km from densely populated areas and movement along them could at the very least cause damage due to shaking. The map in Figure 5 shows a 1 km buffer zone around all normal faults and open fissures.

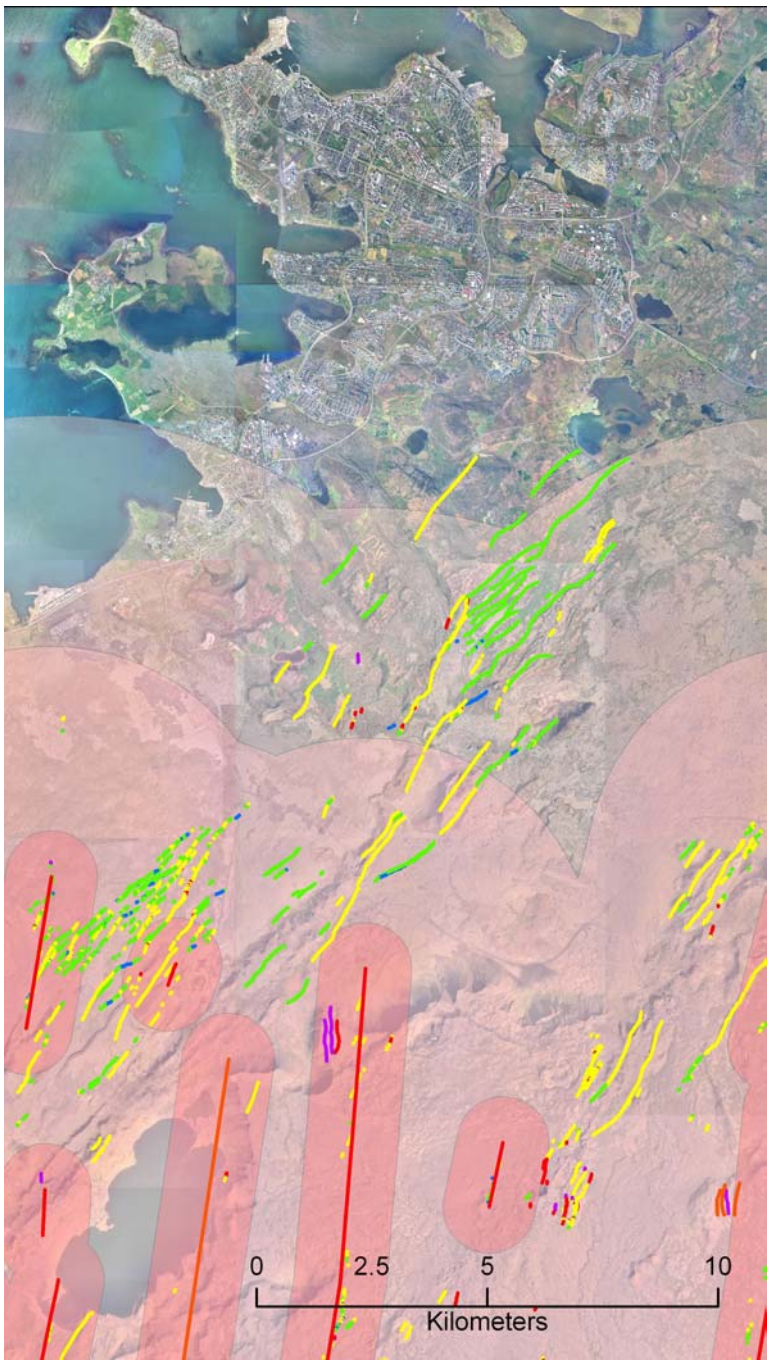

Fig. 4. *Blowup of a portion of the photomosaic showing the greater Reykjavík area. Overlain of the photo are the fracture map from Fig. 1 and the buffer zones from Fig. 3.*

It is clear from the maps in fig.5 and 3 that most areas on the Reykjanes Peninsula are less than a few kilometers from a potentially active fault. However, some areas are clearly more vulnerable to hazards than others. The most common surface effect from the 17 June 2000 earthquakes was rockfall from steep slopes. The thematic map shown in Figure 6 shows the results of a slope analysis (in terms of percent slope) for the entire peninsula, which was calculated from the DEM using Erdas Imagine software. Surface effects from two of the three 17 June 2000 earthquakes (Figure 7) are plotted on the air photo over which the slope map has been overlain. The great majority of points represent locations of rock fall, and all of these occurred on slopes greater than 30 percent (magenta and purple). These slopes were mainly comprised of highly jointed hyaloclastite, some with lava caps. Boulders which fell varied greatly in size, from several meters in diameter to less than a meter. Rock and block slides occurred within the 1 km buffer area around the Kleifarvatn and Núpshlíðarháls faults, but rockfall was much more wide-spread. No rockfall occurred in the immediate vicinity of the Hvalhnúkur fault because local relief there is very small. However, many occurrences of rockfall were reported from cliffs along the south coast road which may have been triggered by the Hvalhnúkur earthquake (see below). Specific instances of rockfalls and slides are described more thoroughly in Clifton et al. 2003a.

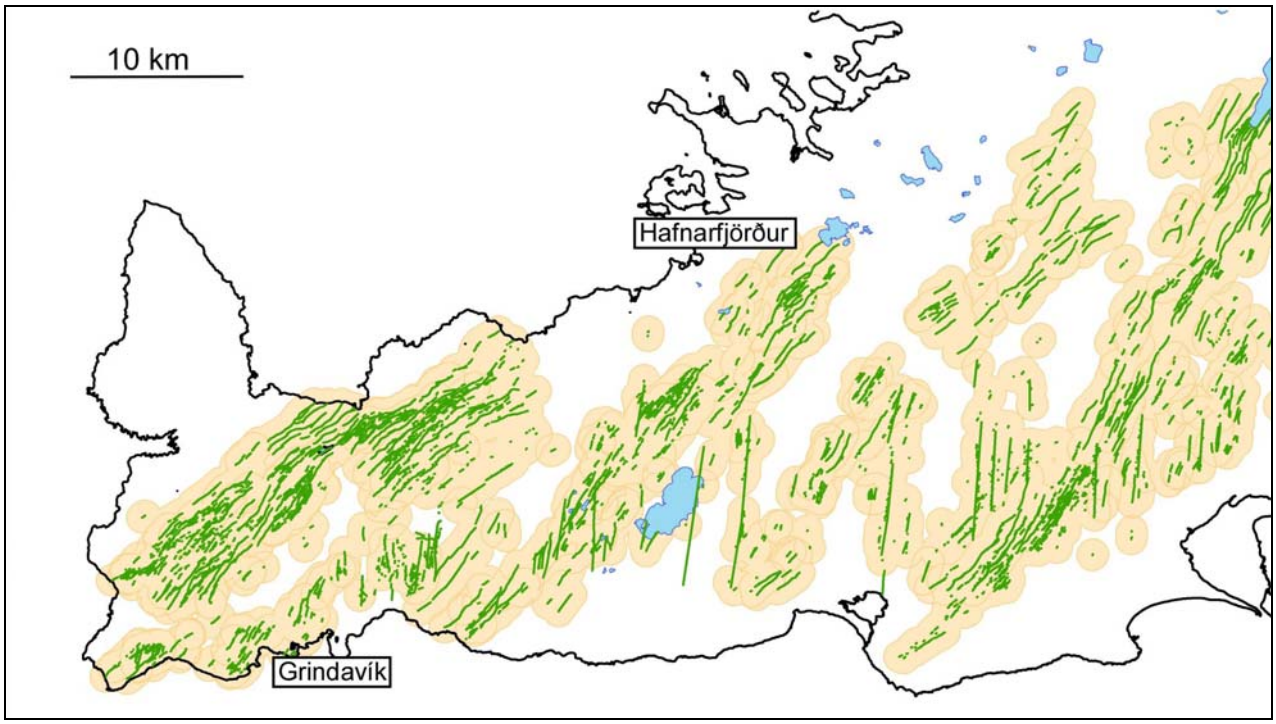

Fig. 5. *Map showing 1 km buffer zones for all normal faults and open fractures on the Reykjanes Peninsula.*

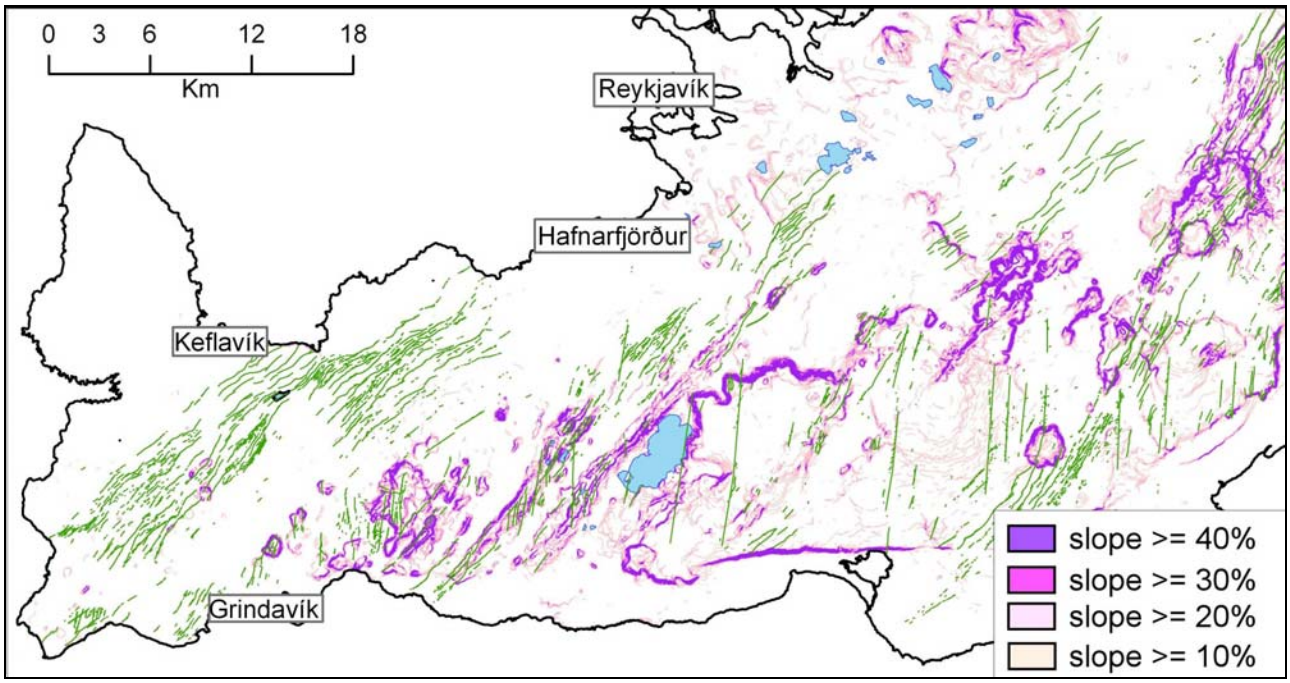

Fig. 6. *Map showing percent slope on the Reykjanes Peninsula. Fracture map is superimposed.*

Fortunately, the main population centers on Reykjanes Peninsula have little topographic relief (see Figure 6) and do not have to be concerned about rockfall hazard. There are two areas however which bear concern. One is the south coast between Krísuvík and Selvogur (Figure 8). Although this area is essentially unpopulated, a new main road is to be constructed here in the next few years. Not only is traffic expected to increase, but easy access to this part of the peninsula could lead to increased construction of summer houses. Rockfall could present a serious hazard along this road when an earthquake occurs, as these cliffs are the steepest on the peninsula and in some locations

the road will by necessity pass directly in the shadow of the cliffs. There are currently several summer houses built on the north shore of Hlíðarvatn opposite some of the steepest cliffs which could be damaged by falling rocks during an earthquake. Recently a young boy was killed by a falling boulder along the shores of this lake. It is believed that the boulder was set in motion by a small seismic event.

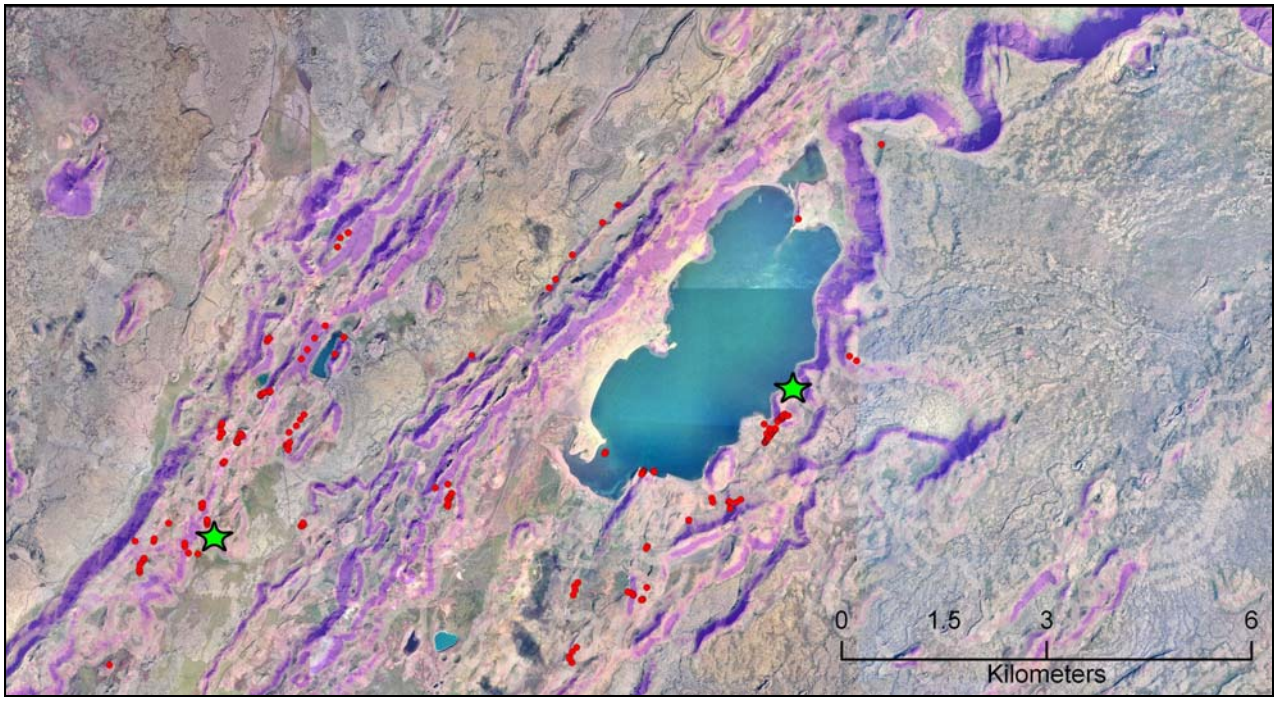

Fig. 7. *Blowup of a portion of the photomosaic showing the area around the Kleifarvatn and Núpshlíðarháls faults. Superimposed are the slope map and locations of mapped surface effects (in red) for the 17 June 2000 earthquakes. Green stars show epicenters of those earthquakes.*

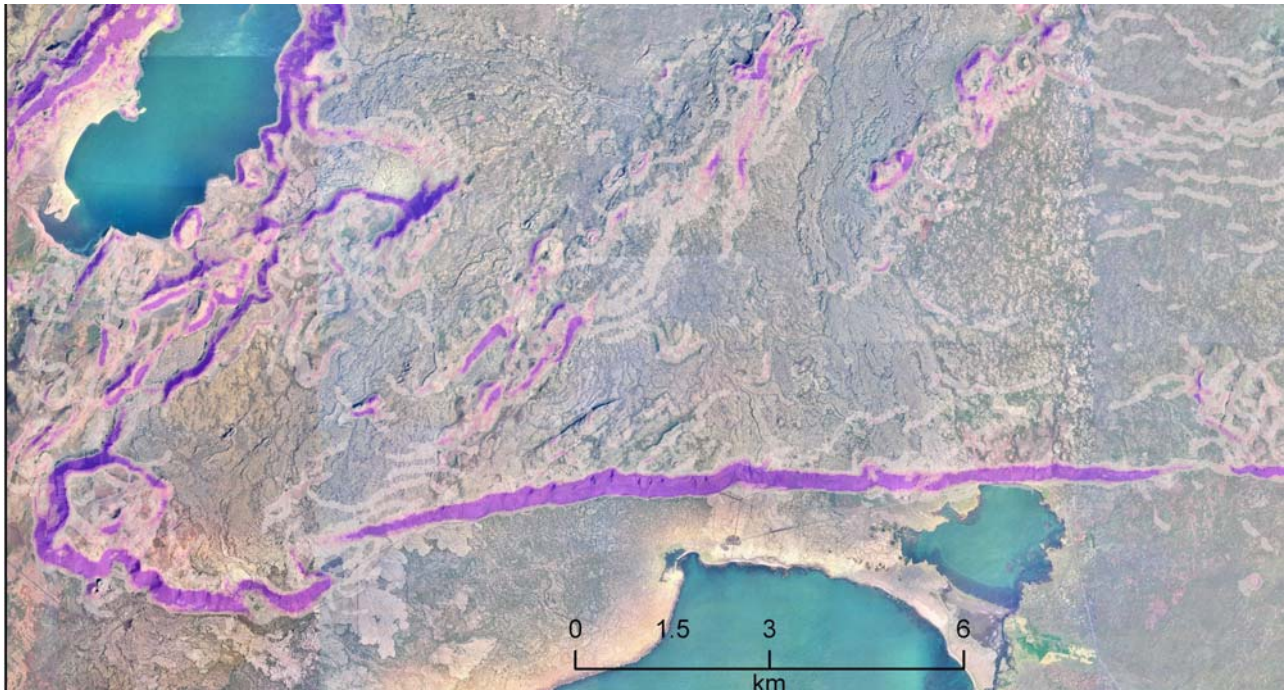

Fig. 8. *Blowup of a portion of the photomosaic showing the southeast coast of the Reykjanes Peninsula. Superimposed is the slope map*

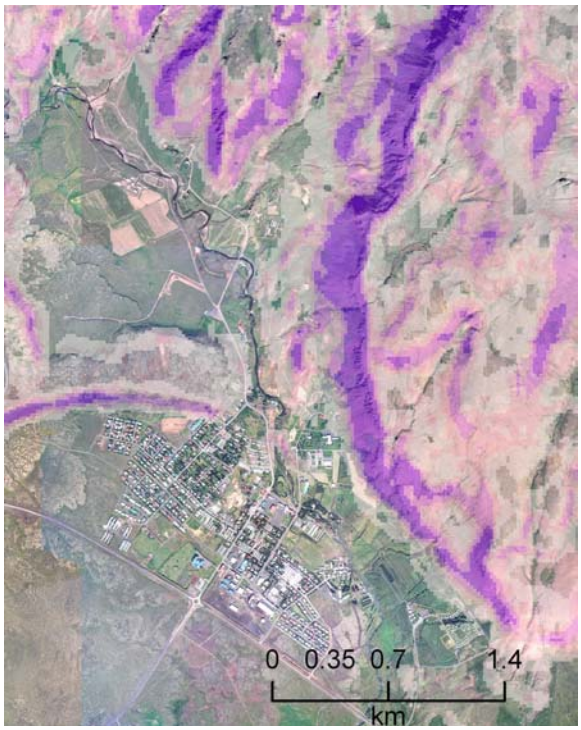

Fig. 9. *Blowup of a portion of the photomosaic showing the area around Hveragerði. Superimposed is the slope map.*

The other area of concern is the town of Hveragerði (Figure 9). The town is surrounded by steep hyaloclastite slopes and many right-lateral strike-slip faults have been mapped within a 10 km radius. The area has experienced many M5 earthquakes in historic times and was most recently the site of 2 M5 earthquakes in 1998. The first of those earthquakes set off two landslides and generated considerable rockfall in the immediate vicinity (see Clifton et al. 2002). The epicenter of that earthquake was approximately 5 km west of Hveragerði, and no reports of rockfall were made in the town. However, it is likely that M≥5 earthquake closer to the town could cause rockfall or landslides from the steepest slopes.

References

Anell, I., 2004, Subsidence in rift zones, analyzing results from repeated precision leveling of the Vogar profile on the Reykjanes Peninsula, Southwest Iceland, Masters thesis, Lunds Universitet, Sweden.

Árnadóttir, Th., H. Geirsson and P. Einarsson, 2004, Coseismic stress changes and crustal deformation on the Reykjanes Peninsula due to triggered earthquakes on 17 June 2000, Journal of Geophysical Research, 109, B09307, doi:10.1029/2004JB003130

Clifton, A. and Einarsson, P., 2005, Styles of surface rupture accompanying the June 17 and 21, 2000 earthquakes in the South Iceland Seismic Zone. Tectonophysics 396, p.141-159.

Clifton, A.E., C. Pagli, J.F. Jónsdóttir, K. Eythorsdóttir, K. Vogfjörð, 2003a, Surface Effects of Triggered Fault Slip on Reykjanes Peninsula, SW Iceland. Tectonophysics 369, 145-154.

Clifton, Amy E. and Schlische, R.W., 2003b, Fracture populations on the Reykjanes Peninsula, Iceland: Comparison with experimental clay models of oblique rifting. Journal of Geophysical Research, 108(B2), 2074, doi:10.1029/2001JB000635

Clifton, Amy E., Freysteinn Sigmundsson, Kurt L. Feigl, Gunnar Guðmundsson,and Thóra Árnadóttir, 2002, Surface effects of faulting and deformation resulting from magma accumulation at the Hengill triple junction, SW Iceland, 1994 - 1998. Journal of Volcanology and Geothermal Research (JVGR), 115, 233-255.
Einarsson, P. and Eiríksson, J., 1982, Earthquake fractures in the districts Land and Rangárvellir in the South Iceland Seismic Zone. Jökull 32, 113-120.

Pagli, C., R. Pedersen, F. Sigmundsson, and K.L. Feigl, 2003, Triggered fault slip on June 17, 2000 on the Reykjanes Peninsula, SW-Iceland captured by radar interferometry, Geophysical Research Letters, 30(6), 1273, doi:10.1029/2002GL015310.

Tryggvason, E., 1970, Surface deformation and fault displacement associated with an earthquake swarm in Iceland. Journal of Geophysical Research, 75, 4407-4422.

WP 5.3 Study of the strong ground motion, acceleration and intensities of the two large earthquakes

a) Objectives

The main objective of this work package is to study the characteristics of ground acceleration in earthquakes in Iceland. To obtain a better estimate of the earthquake hazard it is important to develop mathematical models for the ground acceleration and study the identified earthquake parameters that describe the attenuation of the seismic waves, the duration of the shaking and local site effects.

The strong ground acceleration measurements have been acquired by the Icelandic Strong Motion Network that is run by the Earthquake Engineering Research Centre of the University of Iceland and has been operated for close to 20 years. The most important measurement were obtained in South-Iceland $M_w = 6.5$ earthquakes in South-Iceland in June 2000.

b) Methodology and scientific achievements

The methodology applied here is to model the ground acceleration with Brune's extended source model. Using Parseval's theorem a theoretical ground motion model has been derived that describes the attenuation of rms-acceleration with respect to epicentral distance and seismic moment. The conventional approach to describe attenuation is empirical and uses relations with parameters that are identified using regression analysis and do not have any direct physical link with the earthquake process. The parameters of the theoretical equation have parameters that have direct physical meaning and are estimated from the acceleration measurements by fitting the model and minimising the error. The theoretical model is shown here below:

c) Theoretical attenuation model

Far-field approximation

$$\log_{10}(a_{peak}) = \log_{10}\left(\left(\frac{7}{16}\right)^{1/3}\frac{2pC_P R_{\theta\phi}\Delta\sigma^{2/3}}{\beta\rho\sqrt{\kappa}}\right)+\frac{1}{2}\log_{10}\left(\frac{\Psi}{T_d}\right)+\frac{1}{3}\log_{10}(M_o)-\log_{10}(R)$$

Near-field approximation

$$\log_{10}(a_{peak}) = \log_{10}\left(\frac{1}{\sqrt{\pi}}\frac{7}{8}\frac{pC_p}{\rho\beta r^3\sqrt{\kappa_o}}\right)+\frac{1}{2}\log_{10}\left(\frac{\Psi_o}{T_o}\right)+\log_{10}(M_o)$$

Here, a_{peak} is the peak value of acceleration (PGA), p is a so-called peak-factor, $R_{\theta\phi}$ denotes the average radiation pattern, C_P is the partitioning factor, ρ is the material density of the crust, ω denotes frequency in rad/s, β is the shear wave velocity, R is the distance from source to site, ω_c is the corner frequency of the displacement spectra, $\Delta\sigma$ denotes the stress drop, M_o is the seismic moment, μ is the shear modulus, r is the radius of the circular fault. κ_o and κ are the so-called spectral decay

parameters, T_o and T_d are duration, Ψ_o and Ψ are dispersion functions in the near- and far-field respectively. The dispersion functions Ψ_o and Ψ are evaluated in terms of the parameters $\lambda = \kappa_o / \tau$ and $\lambda = \kappa\omega_c$ respectively and have closed form solutions.

The theoretical model is applied to PGA data from the two earthquakes in South-Iceland in the year 2000. Attenuation of peak ground acceleration as a function of epicentral distance is presented for horizontal components and is shown in the figure. The parameters from the model were estimated from the acceleration data. The fit was found to be better than for the empirical models found in the literature. The results of the study were presented in the paper: *Attenuation of strong ground motion in shallow earthquakes*, paper 1616 presented at the 13th World Conference on Earthquake Engineering in Vancouver, Canada, August 1-6, 2004.

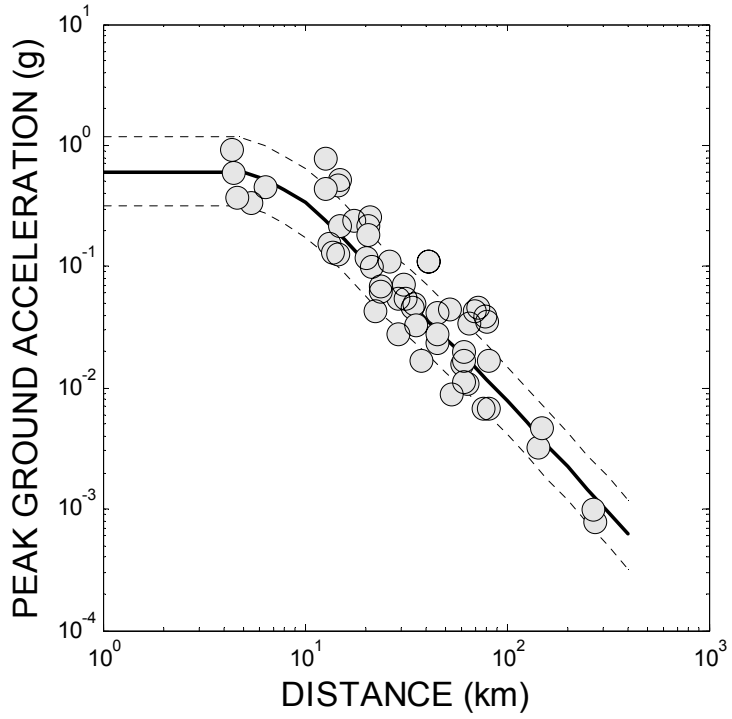

PGA values from 98 components of data from the June 2000 earthquakes in Iceland. The solid black curve represent the mean value of the theoretical attenuation model. The dashed lines represent +/- one standard deviation.

d) Socio-economic relevance

Realistic estimates of the ground accelerations in earthquakes is important for determining the seismic loading structures must withstand to be considered safe. The ground motion is greatly affected by the geological conditions in each region. It is therefore necessary to study the ground motion locally and develop ground motion models that take into account the amplitude, frequency content, duration and site effects. It is important to develop mathematical models that make it possible to provide realistic estimates of the seismic loading that the structures must withstand.

In this work package the acceleration measurements in Iceland are studied and ground estimation models developed that have socio-economic benefits. The ground motion is greatly affected by the geological conditions in each region. Reliable estimates of the ground motion in each region with respect to amplitude, frequency content and duration are very important for the safe design of structures. Good estimates of the ground acceleration or the loading that the structures experience

during earthquakes are vital in this context. This makes it possible to design structures strong enough to withstand the earthquakes without wasting resources.

e) Discussion and conclusion

The approach applied here for the modelling of ground motion in Icelandic earthquakes is a theoretical one and assumes that the earthquake occurs on a near vertical fault with a strike-slip mechanism and that the length and width of the fault plane are of similar size. We have developed an attenuation equation that is based on source models and has been found to give a good fit to the Icelandic data.

The shortcomings of the conventionally used empirical attenuation equations have been recognised by many researchers. There is a multitude of various empirical attenuation relations that have been developed and the variability in the ground motion they estimate is great. The parameters of these equations are determined from data that comes from earthquakes a wide range of magnitudes and different source mechanism. It should be noted that the values of the source parameters are dependent on the type of model that is applied. This should be considered when comparing source parameters from different modelling approaches.

The source models can be converted into digital filters and used for simulation of ground acceleration time series. These time series reflect the mean trends represented bye the models and can not be expected to produce identical results as seismological models obtained by inversion. We believe however that the applied approach provides a good approximation for engineering purposes.

f) Plan and objectives for the next period

In the next period of the project we will continue studying site effect and use an inversion process to separate source, path and site. A comparison will be made of the site effects obtained using the H/V method. We will also incorporate the site effect into the simulation process by means of a digital filter.

WP 5.4 Reevaluation of the historical earthquakes in light of the new observations

Objectives

The aim of the project is to reevaluate magnitudes, locations and possible fault sizes for historical events in the South Iceland seismic zone back to year 1700.

Methodology and scientific achievements related to the work packages including contributions from partners

According to the description of WP5.4 the start month is M12 and the only milestone is the final deliverable of the package: A new catalogue of historical earthquakes in South Iceland Lowland.

Former estimates of magnitudes and locations of historical events in the area have been based on: 1) the area of damage zone (defined where at least half of all houses collapsed); 2) the Icelandic formula for attenuation of intensities and finally; 3) the instrumentally observed magnitude (Ms=7.0) of an earthquake in the SISZ in 1912.

Now we can add the experience from the events in June 2000. For this we have detailed information about the earthquakes, exact locations, fault geometry and slip. The effects of the earthquakes (surface faulting and intensities) are also far better known than for the historical events.

A comparison of detailed information from the year 2000 earthquakes with incomplete data from the historical events gives the possibility to reevaluate magnitudes, locations and fault sizes of historical events.

It is also necessary to reevaluate the historical sources we have used to estimate intensities and damages caused by earthquakes.

At the beginning of the work a new attenuation formula for Iceland was developed and some historical documents have been reanalyzed and reinterpreted for estimating intensities. The new attenuation formula is on the form

$$MMI = a + bM - c*\Delta - d*\log(\Delta)$$

as explained by Bakun et al. 2003.

We often have only a few intensity estimates for our calculations. Therefore the method described in the abovementioned paper suits for many historical earthquakes. In other cases we have to use the felt area or the area where at least half of all houses collapsed.

Reference

Bakun, W.H, A.C. Johnston & M.G. Hopper 2003. Estimating locations and magnitudes of earthquakes in Eastern North America from modified Mercalli intensity. *Bull Seism. Soc. Am* 93, 190-202.

WP 5.5 Hydrogeological changes associated with the June 2000 earthquakes

a) Objectives

The main objectives in this period were as follows: (a) analyse the data sets (fractures, push-ups, etc.) generated during the June 2000 earthquakes, (b) to develop general models of the South Iceland Seismic Zone (SISZ), (c) to study well-exposed analogies to the SISZ at deep crustal levels, so as to be able to put the results from the geothermal changes and related aspects of the 2000 earthquakes into a general tectonic and hydrogeological framework, and (c) make numerical models of hydrogeological effects of strike-slip faulting in general, and those associated with the June 2000 earthquakes in particular.

The general main aims of the studies related to this project can be summarised as follows: (1) To understand the mechanics of the June 2000 earthquakes and the associated hydrological changes. (2) To explore the possibilities of using deformation of the volcanoes in the vicinity of the SISZ as precursors to large earthquakes in the SISZ; in particular, how crustal deformation, seismicity and changes in geothermal fields in Hengill and Eyjafjallajokull, and abrupt changes in the eruption frequency of Hekla, can be related to the loading to failure of the SISZ. (3) How stress transfer from the nearby volcanoes and volcanic zones may trigger, or suppress, seismogenic activity in the SISZ.

b) Methodology and scientific achievements

1. A comparison has been made, mostly in 2003, between the surface features, faults and visible crustal structure of the SISZ and its adjacent parts (the West Volcanic Zone and the East Volcanic Zone) and the deeply eroded features observed in the nearby Pleistocene and Tertiary lava piles in Southwest and Southeast Iceland. The SISZ is underlain by a layered crust, and the dips and mechanical properties of these layers have effects on the faults that developed during the June 2000 earthquakes as well as the associated changes in the geothermal fields during the earthquakes. Furthermore, in Southwest Iceland, and particularly in Southeast and East Iceland, extinct magma chambers that are presumably similar to those that currently exist (or have existed) in the central volcanoes adjacent to the SISZ, such as Hengill, Hekla and Eyjafjallajokull, can be observed and used as a basis for numerical models similar to those presented in Gudmundsson and Brenner (2003 Terra Nova; 2005 submitted to GJI).

When these extinct magma chambers were active, they gave rise to geothermal fields similar to those that are currently active in the Hengill Volcano. It is believed that the intense seismic activity in the Hengill Volcano and its surroundings that was a precursor to the June 2000 earthquakes (Gudmundsson and Brenner 2003) is largely related to fluid-pressure changes in the associated geothermal field during loading of that field by the SISZ. It is also observed that most of the inactive faults in the Pleistocene and Tertiary lava pile have mineral veins (extinct hydrofractures) along the fault cores and in the damage zones, suggesting a close correlation between fluid-driven fractures and seismogenic faulting in the SISZ as well as in Hengill.

The field studies in 2003 were carried out in collaboration with two assistant scientists, Sonja L. Brenner (Germany) and Ines Galindo (Spain). Both are experts on fractures, in particular faults and associated geothermal fluid transport, and one (SLB) has already worked on numerical models of the SISZ (cf. Gudmundsson and Brenner 2003; 2005).

All these field observations, together with studies of the active geothermal fields in South and Southwest Iceland, are being used for making numerical models to explain the hydrological changes associated with the June 2000 earthquakes, as well as to extend and develop further the model of the SISZ and its adjacent volcanoes, presented in Gudmundsson and Brenner (2003).

To complement the field studies, aerial photographs and satellite images have been obtained of selected areas within, and adjacent to, the SISZ, in particular areas in Southwest Iceland (Hengill, Reykjanes Peninsula), and in South Iceland (Hekla, Eyjafjallajokull). Faults and other date from these areas provide further constraints on the numerical models.

2. In South Iceland, there are no deeply eroded sections where the hydromechanical infrastructure of strike-slip faults similar to those of June 2000 can be studied. In the deeply eroded Tertiary and Pleistocene parts of Iceland, strike-slip faults with displacements similar to those in the June earthquakes are rare (except in the Husavik-Flatey Fault, which is a very different tectonic environment from that of SISZ). To provide analogies for the strike-slip faults of the SISZ, deeply eroded strike-slip faults in a layered crust with clear evidence of fluid transport have been studied in the Bristol Channel, in South Wales and on the Somerset Coast (SW England).

These faults dissect layers, mainly limestone and shale, which have properties not so dissimilar from those of young lava flows and scoria or soil layers. The limestone layers, however, are normally 0.5 m thick or less, compared with lava flows in Iceland being 5-10 m thick. It follows that mechanical effects on fault structure and fluid transport are easier to study in the Bristol channel than in Iceland.

Abrupt changes in fault attitude are common at contacts between layers. Also, all the faults have clear damage zones and cores, and nearly all the mineral veins are confined to these rock units. That is to say, fluid transport at the time of fault and geothermal activity was almost entirely confined to the faults and the surrounding damage zones. This indicates a clear analogy with the present-day strike-slip faults in the South Iceland Seismic Zone and the associated geothermal fields and fluid transport. Of particular interest are pull-apart structures along the strike-slip faults in UK: these have commonly acted as major conductors for geothermal water. Similar structures, but larger, occur along some of the strike-slip faults of the SISZ. In the numerical models of the faults of the SISZ, an account is taken of the similar structures observed in the layered rocks in UK.

3. Studies at the National Energy Authority (Grimur Björnsson, subcontractor), including a televiewer measurements and analysis of the geothermal boreholes in the SISZ, are progressing. The new data gathered from the subcontractor will be used to test the models discussed above.

4. The main achievements during the reporting period are the many new numerical models of strike-slip faults with varying core and damage-zone properties. These new models complement the earlier general models of the SISZ (Gudmundsson and Brenner, Terra Nova; GJI submitted). As is indicated above, the main results of these new numerical models may be summarised as follows:

- When the fault tip is nearby, or inside, a hyaloclastite mountain, the slip, for a given loading conditions and fault geometry, is much larger than when the tip is far away from the mountain.
- In models where hyaloclastic mountains are absent but the damage-zone thickness around the fault increases with time, the maximum displacement (u) on a fault of a given length and with a constant loading condition, gradually increases. Thus, for rupture (trace) length (L), the ratio u/L gradually decreases with time, so that the slip in individual earthquakes in relation to the rupture length increases with time.

- Even as the fault slip in individual earthquakes increases, the displacement (slip) profile remains similar as regards shape. Thus, for this type of loading and with gradually increasing damage-zone thickness, the displacement profile remains a smooth, convex curve with a maximum slip at the fault centre.

c) Socio-economic relevance

The work made in this package has great socio-economic relevance, in particular in the following fields (both as regards South Iceland and in general):

- Earthquake hazard analysis
- Earthquake risk analysis
- Fracture-generated and maintained permeability and transport of crustal fluids (gas, oil, groundwater, geothermal water)
- Understanding and using geothermal reservoirs
- Interaction between volcanic and seismogenic zones
- Understanding volcanic unrest and hazards
- Volcanic risk analysis.

d) Discussion and conclusion

The work in this package is progressing as planned, despite the fact that all the work had to be concentrated on one year (extended to one and a half) instead of two years. The work has already lead to many new ideas and models concerning the mechanics of seismogenic faulting in the SISZ and the related fluid transport. In particular, the effects of mechanical heterogeneities and layering on faulting and fluid transport appear to be of fundamental importance for understanding the mechanics of earthquakes, and associated changes in geothermal fields and permeability, in the SISZ. The implications of these findings will be explored in the final half year of the Prepared project.

e) Plan and objectives for the next period

These may be briefly summarised as follows:

- Fracture and fluid transport studies in the SISZ and the surrounding areas in the spring and summer of 2005. Analysis will be made of the fault systems of the Hengill Volcano, fractures of the SISZ, and analogous geothermal fields in the lava pile of SE Iceland. A group of 5 people (at least) from Gottingen will be in Iceland in early June and, as planned, again later in the summer for field studies, testing of model implications, and gathering data for model refinement. These include Gudmundsson and Brenner, and at least 3 students working on this project.

- Refinement and publishing of the new numerical models of the effects of (1) soft inclusions such as hyaloclastite mountains on strike-slip fault displacement in the SISZ, and (2) properties of the damage zone and fault core on fault displacement during loading to failure.

- Further testing of some of the models results on fracture and fluid data from the June 2000 earthquakes.

- Presentation of the results at conferences and meetings, and publication of the main results in international scientific journals. The planned conferences include the AGU spring meeting in New Orleans in May and the EGU Meeting in Vienna in April.

WP 5.6 Paleo-stress fields and mechanics of faulting

1. Objectives

The main purpose of the WP 5.6 is the description of the stress field and understanding of the mechanical behaviour of an active seismogenic zone, the South Iceland Seismic Zone (SISZ). In that way, our first aim was to determine how the stresses are distributed along the active faults and their evolution, using the earthquake data base of IMO. In a second time, to recognise the parameters which could control the nature and the distribution of the surface rupture traces induced by major earthquakes, we carried out field measurements of recent (plio-quaternary) faults and a detailed GPS mapping along selected parts major historical active faults. All these works deal with analysis of faulting in terms of geometry and mechanics, based on both the inversion of focal mechanisms of earthquakes and of fault slip data analysis, and the analysis of surface deformations associated to major earthquakes.

2. Methodology and scientific achievements

The main methodologies used in WP 5.6 are:

- Inversion of fault slip and of double-couple earthquake focal mechanisms (from the SIL network) data to obtain the recent (Plio-Quaternary) and the present-day stress tensors.
- Analysis of surface features of faults (mapping and geometrical analysis)
- Numerical modelling (distinct-element, finite-element)

A second field work has been carried out in the South Iceland Seismic Zone, 17th May – 3rd May, 2004 (F. Bergerat, J. Angelier and M. Bellou) for (1) fault slip data collection in the easternmost part of the SISZ, (2) accurate GPS mapping with a kinematic GPS equipment and (3) measurements of push-up structures along some historical faults near Leirubakki.

2.1 Fault slip data measurements

The collection of data has been carried out in 6 sites. The analysis in terms of stress tensors indicate a main tectonic regime characterised by NW-SE extension. Stress permutations allow the occurrence of strike-slip faulting characterising the same direction of extension (permutation $\sigma1/\sigma2$), and of perpendicular normal faulting characterising an opposite direction of extension (permutation $\sigma2/\sigma3$) (Fig. 2).

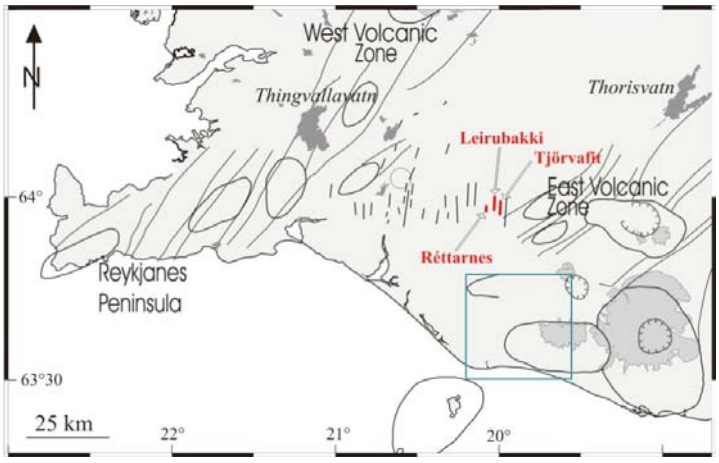

Figure 1 *– Location of the studied historical seismic faults (red lines) and area investigated for fault slip data analysis (blue square) in the South Iceland Seismic Zone*

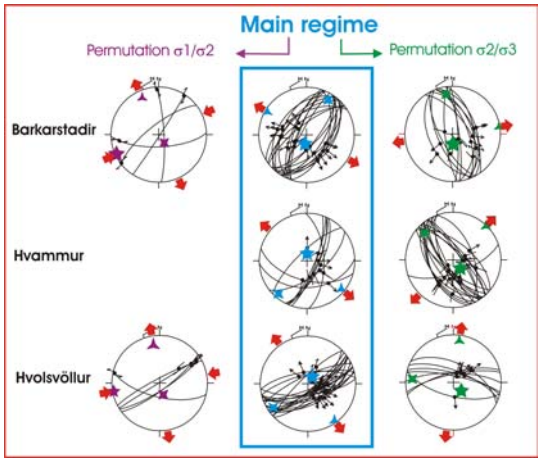

Figure 2 *– Examples of selected sites illustrating the main tectonic regime and the two minor regimes due to stress permutations*

Contrary to the central part of the SISZ (see 2004 report), the easternmost part (close to the junction with the Eastern volcanic zone) is dominated by extension tectonics and normal faulting.

2.2 Surface features of historical seismic faults

We focused our field work on two historical seismic faults located in the eastern part of the SISZ: the Réttarnes and the Tjörvafit Faults (Fig.1) on both sides of the Leirubakki Fault. These faults (Fig.3) are N-S trending right-lateral strike-slip faults. The magnitudes of these earthquakes are unknown and the surface traces that we have found are not precisely dated. A preliminary work has been carried out in order to locate the major structures along these faults thanks to the aerial photographs.

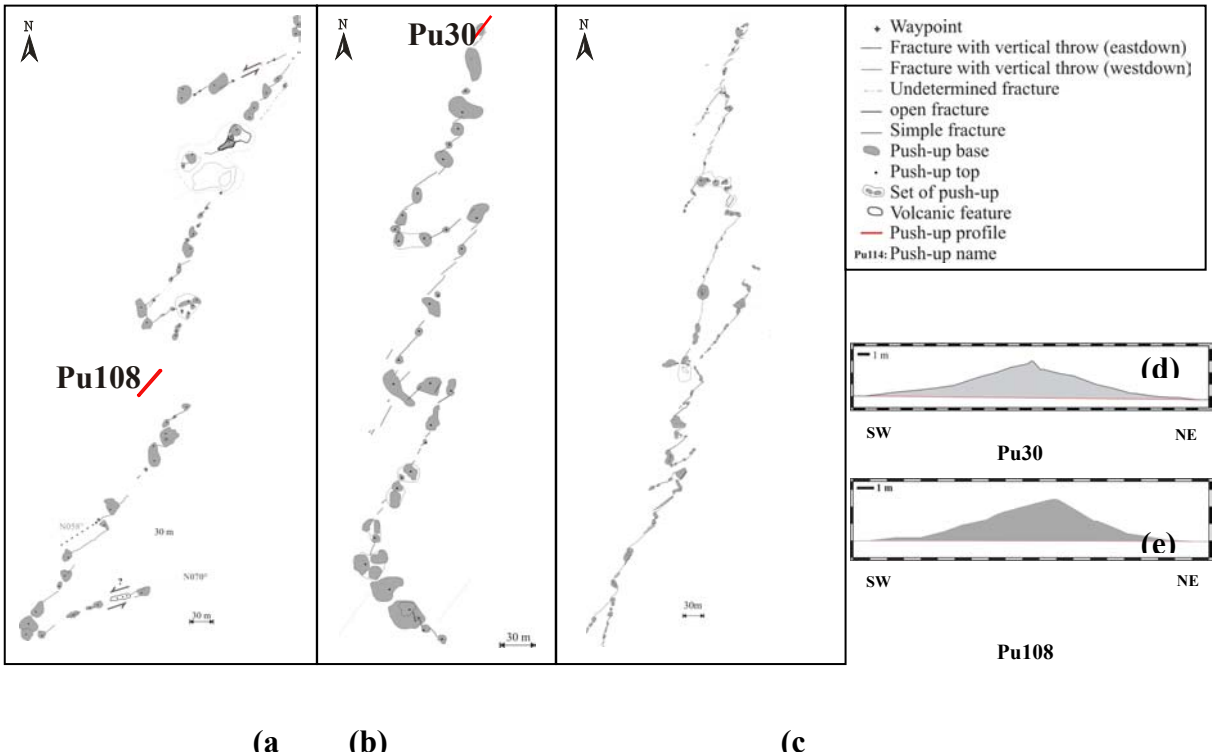

Figure 3 *– Mapped faults: (a) the Tjörvafit Fault, (b) the Réttarnes Fault and (c) the Leirubakki Fault (after Bergerat et al., 2003).*
(d) Push-up profile made along the Réttarnes Fault according to the N038° direction
(e) Push-up profile made along the Tjörvafit Fault according to the N042° direction

The Réttarnes Fault

Field measurements and GPS mapping were conducted along the "Réttarnes" Fault, a 010°-trending right lateral strike-slip fault. Because of poor exposures north of the "aa" lava flow dissected by the fault and because of the presence of the Ytri-Rangá river in the South, its surface length can only be traced for 614 m. The fault trace is composed by three right-lateral segments, which are ranging between 173 and 223 m long and trending between 020° and 030°.

Along this fault, 38 individual fractures were mapped. We classified these fractures into three categories, "simple" fractures (i.e., no visible opening or shear), fractures with a vertical throw (east or west side down) and open fractures. The table summarise the trends and the lengths of the fractures:

Type of fracture	Percent of the total data set	Strike range	Length range
Open Fracture	19%	Dispersion	< 10m (71%)
Simple Fracture	23%	040°-060° (67%)	10-15m (67%)
Fracture with a vertical offset	58%	030°-050° (55%)	10-20m (40%)

Because of a few number of fractures, we noticed a dispersion of the values, especially in terms of length.

The Tjörvafit Fault

The "Tjörvafit" Fault is a 010°-trending right lateral strike-slip fault located near the "Réttarnes" Fault (about 2,5km to the east). Because of poor exposures north and south of the "aa" lava flow dissected by this fault, we only mapped a 987m long trace. This trace is composed of four segments. Two of these segments are right-lateral and are ranging between 415-478m long and trending between 030° and 040°. The other segments are left-lateral and are ranging between 189-198m long and trending between 067° and 070°

Along this fault, 42 individual fractures were mapped. The table presents the trends and the lengths of the fractures:

Type of fracture	Percent of the total data set	Strike range	Length range
Open Fracture	7%	Dispersion	5-15m (82%)
Simple Fracture	74%	50°-70° (70%)	10-20m (51.5%)
Fracture with a vertical offset	19%	50°-70° (50%)	10-15m (50%)

Along the Réttarnes, the Tjörvafit and the Leirubakki Faults we also mapped and studied 39 push-ups (see for example (d) and (e) on Fig.2), in order to define the displacement (i.e. the shortening) along these faults. For this study we realised 44 profiles of push-ups, the results are presented in the following sub-section.

2.3 Analyse of push-up structures

Evaluating the largest magnitude that can reasonably be expected in a seismically active zone is a crucial issue for earthquake hazard mitigation. This is the case in the SISZ, where destructive earthquakes have occurred. By determining earthquake displacements on active faults, one may evaluate the magnitude of historical earthquakes through empirical relationships between co-seismic displacement and earthquake magnitude. However, because active strike-slip faults affect

tabular series of Quaternary lava flows, the determination of their lateral offset is difficult. To determine such offsets, the most useful features are the push-up structures.

The push-up structures develop as folds across rock bridges, as a result of the segmentation of strike-slip faults. These features consequently record the amount of shortening, and hence reveal the lateral offset of the fault. The structural analysis of push-ups is however made complex by the volume change induced by co-seismic deformation, and also by the post seismic collapse of hillocks. Their behaviour is influenced by both the fault segmentation and the décollement depth. The Selsund case study suggested that some earlier analyses, in which volume changes had been neglected, may have resulted in slightly underestimated offsets, and hence magnitudes.

An important target was the Leirubakki Fault, where the largest earthquake in South Iceland could well have occurred. We consequently undertook analyses along this major post-glacial rupture trace, and also along two faults East and West of the Leirubakki Fault. The results confirm that volume changes at the time of push-up formation and syn-tectonic collapse of deformed rocks during the earthquake, in many cases followed by post-seismic gravitational sagging, cannot be neglected. They indicate that the magnitude of the earthquake was significantly larger than 7, assuming that the structures developed during a single major earthquake, which is likely.

In agreement with studies of damage zones of historical earthquakes, our structural analysis of push-ups suggests that earthquakes with magnitudes around, or larger than, 7 have been common in the South Iceland Seismic Zone. A geometrical method is developed for analysing push-up structures bringing contribution to the evaluation of magnitudes of ancient earthquakes along strike-slip faults, and hence to earthquake risk assessment.

3. Socio-economic relevance

This study contributes to a better understanding of earthquake processes and mechanisms in the SISZ. Associated with the other studies carried out with the other WP of the PREPARED project, the WP 5.6 is socially and economically important for Iceland and other seismic areas.

4. Discussion and conclusion

The study of recent and present day brittle deformations (fault slip data and focal mechanisms of earthquakes), as well as the analysis of surface traces of historical major faults, allow a better understanding of the mechanics of earthquakes. Combining these different elements highlights the crustal process leading to large earthquakes.

5. Plan and objectives for the next period

In agreement with the project, the last six months will include:

- Numerical modelling in France (UPMC) and in Italy (UNIBO) in cooperation with the Bonafede group WP 6.2
- Presentation of the results in the EGU General Assembly in Vienna, April 2005
- Participation to the PREPARED Final Meeting in Vienna, April 2005
- Preparation of papers to be published in international journals

WP 6 Modelling and parameterizing the SW Iceland earthquake release and deformation processes

Objectives

Modelling and parameterizing the strain build-up and strain release in the SW Iceland earthquake zones on basis of all available relevant multidisciplinary data.

Methodology and scientific achievements related to workpackages including contribution from partners

WP 6 is based on inputs from progress and results of WP6.1 and WP6.2, as well as results of other workpackages parameterizing or modelling on basis of various observations. Several models have been created to describe faulting in the SISZ models which explain significant observations of geophysics and geology. The June 2000 earthquakes yield new information which constrain such a model.

WP6.1 and WP6.2 have continued modelling work carried out within the PRENLAB projects, fulfilling more multidisciplinary information, and especially observations of the June 2000 earthquakes.

The lead cotractors of WP6.1 and WP6.2 will create a forum with other partners of the consortium to discuss and to merge a general model of the area. It will inform the participants about emerging results regarding the general characteristics of the SISZ and the linked Reykjanes peninsula, so they can be applied directly in the various WP´s. The WP6 is a forum for communication of results and discussion between the lead contractors in WP6.1 and WP6.2, GFZ Potsdam and DF.UNIBO, as well as IMOR, SIUI and CNRS-UMR 5562.

Based on historical seismicity since 1700 and an elastic/viscoelastic layered model, GFZ Potsdam has in WP6.1 estimated elastic, viscoelastic shear stresses as well as Coulomb stress modelling the seismic history. The option is to approach time dependent earthquake hazard assessment for the area as a whole, i.e. where along the zone is most probable that the next earthquake will strike. These models do not show so far to be able to predict where the next earthquake will occur in the region, except possibly in the short-term (within a year or less). It appears that local sources for fracturing stress is needed to explain the seismic history in time and space. Such a source may be upwelling of fluids from below into the brittle crust increasing the pore pressure suggested earlier (see WP2 of this report; Stefánsson and Guðmundsson 2005). Crack models in poroelastic media have been developed which indicate that episodes of fluid migration can increase the pore pressure and thus decrease the threshold of instability of a fault region. Long-term (may be hundreds of years) build-up of pore pressures may locally explain both the spacial distribution and direction of the faults and be a key to long-term prediction of place and time for the next large earthquakes, i.e. time dependent hazard assessment.

In WP6 the triggering of early aftershocks up to 100 km after the June 17 earthquake, has been modelled as dynamic stress transfer (triggering) at sites close to fracture criticality.

All these results as well as information from most other WP´s of the project add up to making a general model possible to explain the overall behaviour of the region.

But how to model the multidisciplinary information from the plate boundary as a whole or from the SISZ only, taking into account its heteorogeneous rheology and the structural complexity? A method is being tested to apply three-dimensional finitie element modelling for this purose (Appendix 1 of this report).

Socio-economic relevance and policy implication

The objective of this WP is significant for all other efforts for risk mitigation in the area, the general hazard assessment, the time dependent hazard assessment, for the warning algorithms and for nowcasting for risk mitigation purposes.

Discussion and conclusions

For a general modelling and parameterizing of the SW Iceland earthquake release and deformation processes results from most other WP´s are needed. New knowledge and understanding is emerging in the various WP´s that may lead to new understanding of the South Iceland seismic zone earthquake processes.

Plan and objectives for the next period

Intensive work for merging together the outcome of the various WP´s rending information, significant for the WP6 objectives. A very significant occasion for this is the PREPARED session and the PREPARED final meeting and other meetings and discussions during the EGU General Assembly in Vienna in April 2005.

Reference

Stefánsson, R. & G.B. Guðmundsson 2005. About the state-of-the-art in providing earthquake warnings in Iceland. *Icelandic Meteorological Office - Report.* In press.

WP 6.1 Earthquake probability changes due to stress transfer

a) Objectives

The probabilistic approach to determine seismic hazard assumes that earthquakes occur randomly in space and time. Contrary to this, evidence was found that an event triggers the following one by changing the shear or Coulomb stress at the site of the second event. It also means that the likelihood of the next event is conditionally increased or decreased.

In the South Iceland Seismic Zone (SISZ), this was found for the two large earthquakes in June 2000 (cf. Árnadóttir et al. 2003, 2004 for co-seismic and Jónsson et al. 2003 for poro-elastic post-seismic triggering).

Encouraged by this and by the findings of Roth (2004) that earthquakes in the SISZ usually occurred at high shear stress areas, we modelled the stress field to find evidence for shear and Coulomb stress (CFS) triggering among the 13 strong events ($M \geq 6$) since 1706.

b) Methodology and scientific achievements related to workpackages including contributions from partners

We considered the following contributions: stress increase by plate motion, co- and post-seismic seismic stress changes due to earthquakes, assuming a layered visco-elastic half-space with Maxwell rheology. The calculations were done with out own software (Wang et al., 2005). The source parameters of the earthquakes were taken from the Icelandic Meteorological Office (espec. Páll Halldórsson) and from WP 5.4. The crustal structure given by Stefánsson et al. (1993) and Menke (1999) was used.

Since the last report, we have recalculated the stress fields taking the revised locations of historical events into account that were provided by sub-project 5.4.

However, computing shear stress and Coulomb stress changes in the SISZ again did not lead to definite conclusions regarding the time and location of the next event. Figure 1 shows the results for shear stresses before each event in the series. The conclusions are summarized in Table 1. Figure 1 shows that the average shear stress along the rupture is generally higher for the visco-elastic models. With exception of the two events in 2000, the stress increase and decrease during time is very similar for the elastic and the visco-elastic modelling results. Even though the shear stress component along the slip direction of the earthquakes is high before most of the events, it reaches its maximum only in 6 out of the 12 cases (earthquakes of 1732, 1734, 1784a, 1896a, 1896c and 1986e) before the subsequent event in case of elastic models. For inelastic models the ratio is 7 out of 12 (1732, 1734, 1784a, 1896a, 1896c, 1986e and 2000b). Both results mean that triggering should have occurred already earlier, i.e. by the time of the first shear stress maximum.

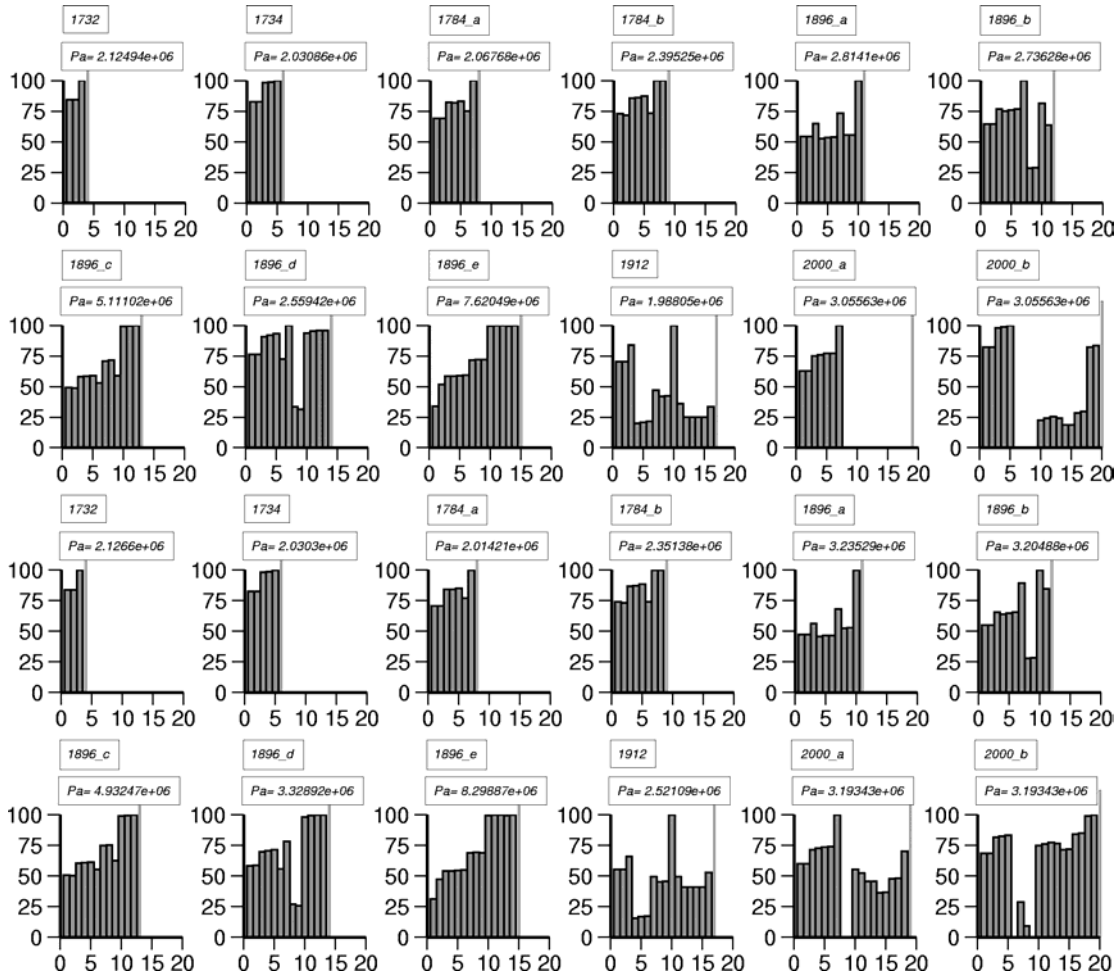

Figure 1: Comparison between elastic (upper two rows) and visco-elastic (lower two rows) modelling results for shear stress evolution, centring the background field at 64.0° N. The stress field was evaluated before and after each event (for events occurring within one year the inter-seismic time was assumed to be zero and post- and pre-event stress levels can be assumed to be equal, e.g. post 1784_a and pre 1784_b; this results in 19 different values). The maximum average shear stress (in Pa) indicated on top of each individual figure corresponds to 100%. Note that in 1986d the maximum is reached already after the event 1896c whereas the pre-seismic stress is lower in both models.

	Elastic model		Visco-elastic model	
Criterion	Success ratio	Events meeting the Criterion	Success ratio	Events meeting the criterion
High, i.e. ≥50% of the maximum for that rupture	10 / 12	1732, 1734, 1784a, b, 1896a, b, c, d, e, 2000b	12 / 12	1732, 1734, 1784a, b, 1896a, b, c, d, e, 1912, 2000a, b
Maximum since 1706	6 / 12	1732, 1734, 1784a, 1896a, c, e	7 / 12	1732, 1734, 1784a, 1896a, c, e, 2000b
Maximum for 1st events only*	3 / 5	1732, 1784a, 1896a	3 / 5	1732, 1784a, 1896a

Table 1. *Stress level at the rupture plane of the triggered event.*

* This refers to single events (1912) and 1st events of sub-series (1732, 1784a, 1896a, 2000a).

	ΔCFS > 0 MPa		ΔCFS ≥ 0.01 MPa	
	Success ratio	Events meeting the criterion	Success ratio	Events meeting the criterion
At ≥50 % of the rupture plane	9 / 12	1732, 1734, 1784b, 1896a, c, d, e, 1912, 2000b	6 / 12	1734, 1784b, 1896a, c, e, 2000b
Maximum since 1706	2 / 12	1732†, 1734	2 / 12	1734, 1784 a ???
At ≥50 % of the rupture plane of 1st events** only	3 / 5	1732, 1896a, 1912	1 / 5	1896a
At ≥50 % of the rupture plane inside clusters only	6 / 7	1734, 1784b, 1896c, d, e, 2000b	5 / 7	1734, 1784b, 1896c, e, 2000b

Table 2. *Coulomb stress changes (for both the co-seismic and co- + post-seismic stress changes*) at the rupture plane of the triggered event. Here, only pairs of triggering and triggered events are considered.*

* The results of the elastic and the inelastic model differ but not essentially with respect to the criteria applied here.

** This refers to single events (1912) and 1st events of the clusters (or sub-series) namely 1732 & 1734, 1784a & b, 1896a, …, e, 2000a & b.

† This is trivial as it is the first triggered event in the whole series.

When examining the Coulomb stresses before the events, the results are not more convincing than for shear stresses, as can bee seen in Table2. Only when we consider event clusters, the earthquakes that occurred after the 1st event seem to be triggered by the preceding one(s) (cf. last row of Tab. 2).

c) Socio-economic relevance and policy implications

Our work is intended to aid in the long-term earthquake warnings through time-dependent hazard assessments. It might allow for directing risk mitigating efforts, research, and monitoring towards areas with increased hazard. But presently, we are lacking a clear trigger criterion for the following events. Nevertheless, in case of future events, the modelling of Coulomb stress changes (triggering of subsequent events) allows at least to indicate areas where one would expect increased aftershock activity.

d) Discussion and conclusions

Uncertainties in the model parameters (e.g. location of the historical events, rupture history, viscosity, knowledge about events prior to 1706, i.e. background stress field) as well as the simple approach used (e.g. 1D crustal structure, disregard of stress transfer due to volcanic activity) complicate the evaluation of the results. Generally, the modelling showed that it is impossible to constrain the stress field such that the impending event can only occur at its known location. There are always large areas in which stress levels seem to be high enough to trigger an event.

We can state that strong events in the SISZ are presumably not triggered by preceding events but could rather occur randomly with the stress provided by plate tectonics. Therefore, calculating conditional probabilities makes no sense when the long-term probabilities are unchanged, unless we detect triggering mechanisms that we have overlooked so far.

Concerning the clustering of strong events (in 1732 / 1734, 1784, 1896, and 2000), we may surely assume that another strong event is probably ahead (4 in 6 cases) during the next months. And it makes sense to calculate the spatial distribution of the shear stress changes and of the CFS to estimate the most likely focal area.

e) Plan and objectives for the next period

During the last months, we will consider other stress transfer mechanisms than we did so far. Events in the SISZ appear parallel to each other perpendicular to the strike of the SISZ. Successful Coulomb stress change reports come mainly from areas, where there is one mature main through going fault (e.g. The North-Anatolian Fault Zone or the San Andreas fault zone), while secondary faults branch off or run only partly in parallel. The immaturity of the fault zone could lead to high sensitivity of the frictional properties of the fault gouge for dynamic passage of waves, therefore to changes in rock physical properties which influence future ruptures. In this case, it is an open question if the stress changes can influence a future event across several decades.

References

Þóra Árnadóttir, Sigurjón Jónsson, Rikke Pedersen, Gunnar B. Guðmundsson, Coulomb stress changes in the South Iceland Seismic Zone due to two large earthquakes in June 2000, Geophys. Res. Lett., 30 (5), 9-1 to 9-4, 1205, doi: 10.1029/2002GL016495, 2003.

Þóra Árnadóttir, Halldór Geirsson, Páll Einarsson, Coseismic stress changes and crustal deformation on the Reykjanes Peninsula due to triggered earthquakes on 17 June 2000, J. Geophys. Res., 109 (B9), B09307, doi: 10.1029/2004JB003130, 2004.

G. Guðmundsson and K. Sæmundsson, Statistical analysis of damaging earthquakes and volcanic eruptions in Iceland from 1550-1978. J. Geoph., 47, 99-109, 1980.

Sigurjón Jónsson, Paul Segall, Rikke Pedersen, Grímur Björnsson, Post-earthquake ground movements correlated to pore-pressure transients, Nature, 424 (6945), 179-183, doi: 10.1038/nature01776, 2003.

W. Menke, Crustal isostasy indicates anomalous densities beneath Iceland, Geophys. Res. Lett., 26 (9), 1215-1218, 1999.

Frank Roth, Stress changes modelled for the sequence of strong earthquakes in the South Iceland seismic zone since 1706, Pageoph, 161 (7), 1305-1327, doi: 10.1007/s00024-004-2506-5, 2004.

R. Stefánsson, R. Böðvarsson, R. Slunga, P. Einarsson, S. Jakobsdóttir, H. Bungum, S. Gregersen, J. Havskov, J. Hjelme, H. Korhonen, Earthquake prediction research in the South Iceland seismic zone and the SIL project, Bull. Seism. Soc. Am., 696-716, 1993.

Rongjiang Wang, Francisco Lorenzo Martín, and Frank Roth, A semi-analytical software PSGRN/PSCMP for calculating co- and post-seismic deformation in a layered viscoelastic-gravitational half-space, Computers and Geosciences (submitted Feb. 2005)

WP 6.2 Model stress in the solid matrix and pressures in fluids permeating the crust

a) Objectives

WP 6.2 addresses three major objectives through theoretical modelling: (1) Modelling of fault complexities in the SISZ employing crack models in layered elastic media (D98); (2)Lithosphere-asthenosphere interaction under the SISZ, taking into account viscoelastic constitutive relationships and intrusive events across rheological discontinuities (D99); (3) Fault instability in the SISZ, taking into account poro-elastic constitutive relationships (D100); (4) triggered seismicity and the interaction between the two large earthquakes of year 2000 in the SISZ (D101). These objectives include interaction with WP 5.1, WP 5.2, WP 5.5, WP 5.6, WP 6, WP 6.1.

b) Methodology and scientific achievements related to workpackages including contributions from partners

D98 – Original mathematical solutions for crack models in trans-tensional environment

The double en-echelon pattern of surface fractures observed in connection with most large earthquakes in the SISZ cannot be explained by the stress created by the seismic fault alone. In Belardinelli et al. (2002), secondary earthquake fractures were interpreted as frictionally controlled shear faultlets opening near the surface where the tensile induced by the main fault (MF) is greater than the overburden load. In order to understand why the MF does not break to the surface as a single plane surface, it may be conceived that a plastic layer intervenes between the brittle crust at depth and a brittle lava layer at the surface. Within the plastic layer shear stresses greater than a given threshold cannot be attained, thus stress concentration at the tip of the MF must be redistributed all over a wider region undergoing plastic deformation. An elastic layer with thickness H is in slippery contact with a plastic layer thick d on top of an elastic half-space. A right-lateral strike slip fault slips at depth and the plastic deformation is modelled in terms of aseismic slip over an unwelded interface at depth H. The problem is solved in terms of 3 interacting cracks (the MF and the two unwelded surfaces) employing the boundary element method with non-uniform discretization. Results are shown in Figure 1 for the most interesting case, in which the MF meets the unwelded interface.

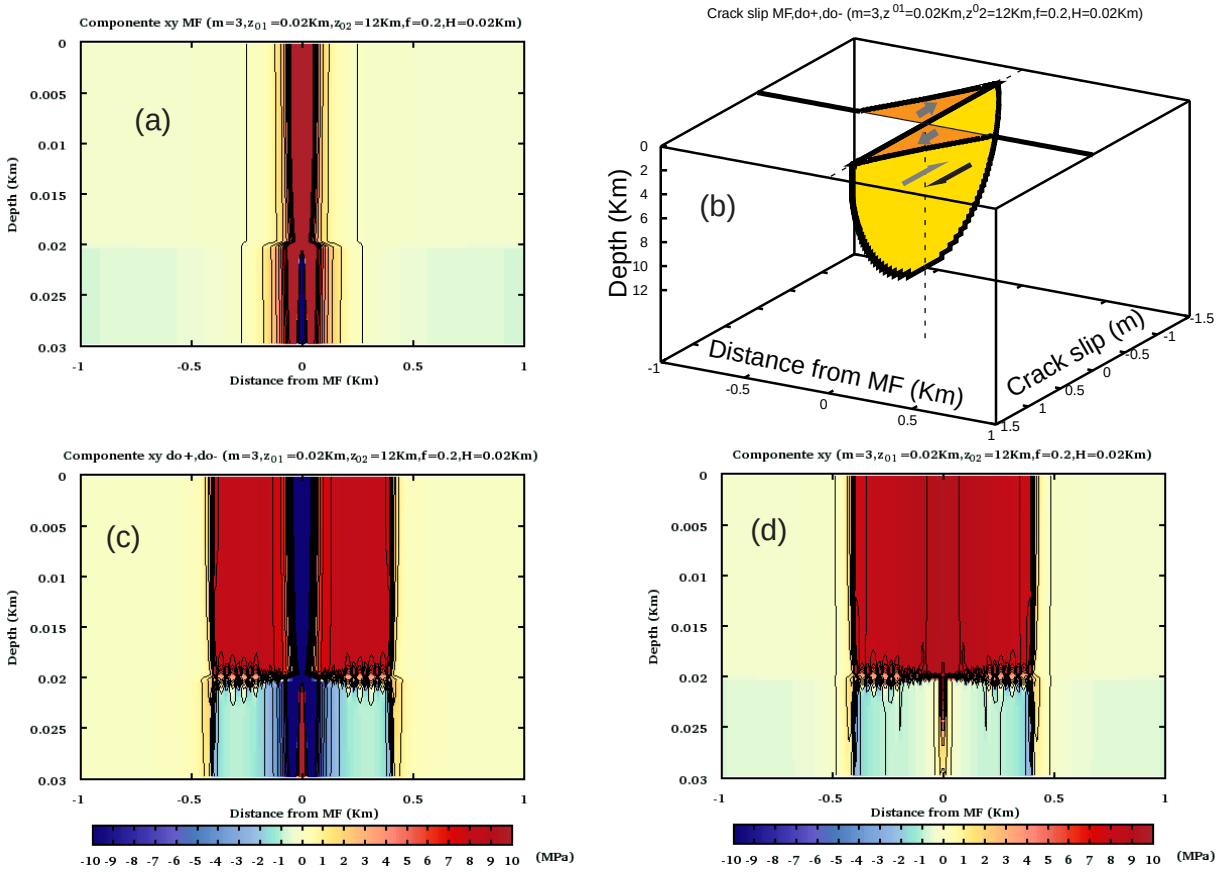

Fig. 1. *Shear stress produced by the MF (a) terminating at the interface with a thin (20 m) layer of lower rigidity. If the interface becomes unwelded (b), two symmetric horizontal cracks develop in opposite direction, which release most of the shear stress produced by the MF (c) and the overall effect (d) is that stress spreads out horizontally and decreases at depth. Note that the vertical scale is 30 m in the stress plots (a), (c), (d) while the horizontal scale is ±1km.*

The MF is open at the interface where its slip equals the width of unwelding. The result is that the lateral extent of the high deviatoric stress induced by faulting is much wider than it was in absence of unwelding and stress values are lower and nearly uniform. Another interesting feature of the solution is that negative shear stress are induced below the interface. Accordingly, secondary shear fractures may only open above the interface, within horizontal distances of a few hundred meters from the fault strike. Similarly, absolute tensile stress are confined within this region and may cause secondary fractures opening up in mixed mode or "tertiary" fractures in pure tensile mode.

D99 – Crack models in viscoelastic media

Previously obtained solutions (PRENLAB project) for elementary dislocations in layered media have been generalized to the viscoelastic case. For tensile (mode I) and edge (mode II) dislocations, a medium composed by two welded half-spaces with different viscosity and elastic parameters was considered. For screw dislocation (mode III) it was possible to derive solutions relative to an elementary dislocation in an elastic layer bounded by an upper free surface and welded to a viscoelastic half-space. All the viscoelastic models employ Maxwell rheology. These solutions are original ones and allow to obtain analytically the time-evolution of the interaction between layering and faults or fluid intrusion in viscoelastic media. The analytic elementary

solutions have been then applied to crack models, in order to analyze the displacement and stress field produced by more realistic structures.

Strike-slip faults. We considered the case of a mode III dislocation embedded in a layered medium made up of a layer with rigidity μ_1 welded to a half-space with rigidity μ_2 and viscosity η. At *t=0* the crack problem is solved, in order to obtain the solution for an elastic medium. For $t > 0$ stress components start to relax. Stress and displacement maps can be plotted for different times, showing the onset of stress discontinuities. Aftershocks distribution is predicted to be time-dependent.

Fluid-filled cracks. Here we consider a fluid intrusion across a layer interface. The two media have the same rigidity μ but the lower medium is viscoelastic. The maps of the horizontal stress for *t = 1* day and *t= 4* months show that the compressive stress produced by the fluid intrusion gradually increases at the interface, on the side of the less viscous medium. This is due to the increasing asymmetry of the effective elastic parameters. Fluid intrusions in viscoelastic media are predicted to cause time-dependent influences on local stress field.

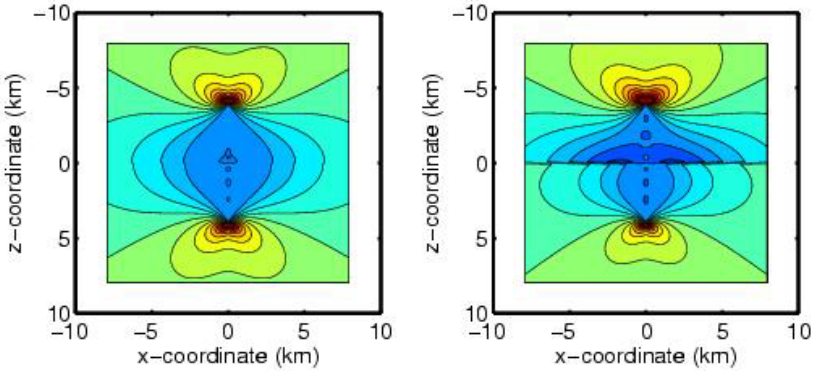

Fig. 2. *Horizontal stress for t = 1 day and t= 4 months.*

D100 - Crack model in poroelastic media

We analyze the effects of fluids trapped within deep rocks, which come suddenly into contact with shallower fractured regions, modifying their temperature, pressure, permeability and stress conditions. In particular we examine the solutions of a set of two coupled equations for heat and pressure transfer in compressible thermo-poro-elastic fluid-saturated media, which become suddenly connected with an hot and pressurized fluid reservoir.

The model employed is 1D and it is constituted by a layer $0<z<b$, which, before the connection, is at reference pressure (hydrostatic value) P_{ref} and temperature T_{ref} and by a reservoir, which occupies the half space $z<0$, characterized by a pressure P_0 and a temperature T_0 higher than the reference values. At the time t=0 the reservoir is connected with the medium and the fluid migrates upward in response to the overpressure and temperature excess at the boundary.

We have considered different rocks, but we have concentrated our attention on basaltic rocks. The fluid and materials parameters are considered to be constant, except the viscosity, which has been assumed temperature dependent, and the permeability, which has been considered pressure dependent.

The viscosity dependence on temperature has been obtained starting from experimental data for water at high temperature and pressure. Our attention is however concentrated on the permeability

dependence on pressure: it has been obtained starting from a model constituted by layers of intact porous rock with a constant intrinsic permeability K_r, alternated with layers characterized by a periodic distribution of interacting fractures represented by Volterra dislocations, whose opening depends linearly on the pressure within. The effective permeability of the whole system results to depend on the pressure and on three geometrical parameters of the model: the horizontal and vertical distances between the centers of two near dislocations D, and d and their length h.

The solutions have been calculated through a numerical procedure for different values of the boundary conditions and a comparison has been done between the solutions calculated taking into account the permeability dependence on pressure and a constant permeability.

The first solutions show often marked differences with respect to those for a constant permeability, especially for the pressure field in rocks with low intrinsic permeability. In the region where the permeability increases with respect to its initial value, the pressure gradient decreases and the layer is characterized by higher pressure values with respect to those seen for a constant permeability (fig. 2).

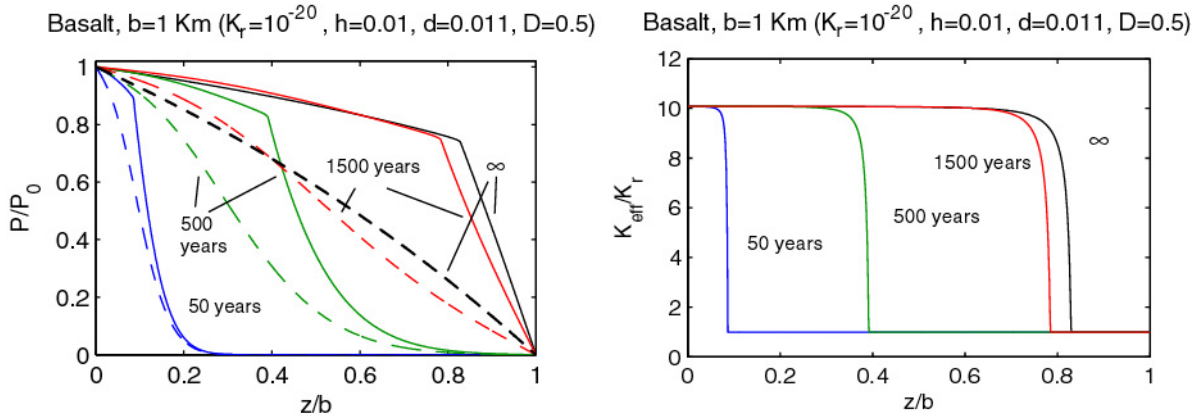

Figure 3. *a) Comparison between solutions calculated for a pressure dependent permeability (solid lines) and for a constant permeability (dashed lines). The intrinsic permeability for the Basalt is here equal to 10^{-20} m^2, and the layer length (b) is equal to 1 Km. b) Trend of the effective permeability within the layer.*

So these results involve that the permeability dependence on pressure can influence significantly the trend of the pressure field. If the layer 0<z<b is identified as the brittle-ductile transition layer, these solutions show that episodes of fluid migration can increase the pore pressure up to lithostatic values and then decrease substantially the instability threshold of a fault region, with obvious seismogenic implications.

D101 - Article and report on triggered seismicity in terms of dynamic fault interaction

A fault could behave differently if or if not a perturbing earthquake on another fault occurs: this is the principle underlying fault interaction studies. This principle in particular implies that earthquakes could be triggered by other earthquakes. The validity of the latter implication can be tested by means of seismicity rate change observations usually made after an earthquake in a time window of years suitable to represent aftershock sequences in the near field. Even at large distance from the epicenter compared to the fault dimension, earthquakes can perturb transiently the state of stress of other seismogenic faults. In far-field conditions, the assumption of a time window of years could be incorrect, since the stress perturbation created by the first event tends to be negligible and

other processes can be more effective in causing subsequent events. At large distance compared to the fault dimension, the causative link between an earthquake and a subsequent event is more convincing if the temporal separation between the two is of the order of the arrival time of the seismic wave generated by the first earthquake in the locations of subsequent events (instantaneous dynamic triggering). Observations of this kind are sporadic, also due to technical difficulties in performing them. However fault rheology studies based on rate and state dependent friction support the instantaneous triggering effect. An evidence of this kind is the case of the early events observed in the Reykjanes Peninsula after the June 17-th 2000 earthquake in the South Iceland Seismic Zone. We completed our study of fault interaction due to dynamic stress changes in the case of these early events. We verified that they could have been dynamically triggered in the framework of rate and state dependent fault rheology if the effective normal stress in the triggered fault was relatively low before the events. This suggests a peculiar condition for regions located west of seismic ruptures in the South Iceland Zone. (Paper submitted for publication on Journal of Geophysical Research).

c) Socio-economic relevance and policy implication

D98 and D99 – Understanding the detailed processes in which surface fractures develop, in connection with seismic faulting at depth, has important implications for seismic risk analyses in the fault region SISZ. Similarly, the role played by viscoelastic relaxation at depth may help understanding the post-seismic evolution of seismicity, particularly in regions with high geothermal gradient, like the SISZ.

D100 – The role played by fluids in the preparatory stage of an earthquake, as described by this modelling, has important implications in understanding the overall seismicity pattern in the SISZ, both in the long term and in the short term, and also provides a conceptual scheme within which precursory Rn anomalies can be interpreted and other hydro-geochemical parameters may be devised to monitor a fault region approaching to seismic failure.

D101 - Seismicity rate change estimates are the basic ingredient of studies of time-dependent probability of future earthquakes. It is then relevant to have verified that the SISZ earthquakes can affect the probability of other earthquakes even at a distance of several tens of kilometres. In this region, at least, seismic risk study cannot be based on conventional attenuation laws only.

d) Plan and objectives for the next period

Ongoing Interaction on D87 with UGOE.GZ.SG, on D89 with UPMC and on D99 with IMOR. Presentation of results at EGU 2005 General Assembly in Vienna 24-29 april 2005. Submission of papers to peer-reviewed journals.

Appendix 1

CNRS.DTP, Toulouse, France

Finite-element modeling of co-seismic and post-seismic crustal deformation: simple tests to study the convergence and the capabilities of the TECTON software package

Since our previous report, we have extended our modeling approach to handle a visco-elastic rheology during the post-seismic interval. We have performed tests to demonstrate the temporal convergence using different time steps (Figure 1, Figure 2). We obtain good results using step sizes that are smaller than the characteristic Maxwell time.

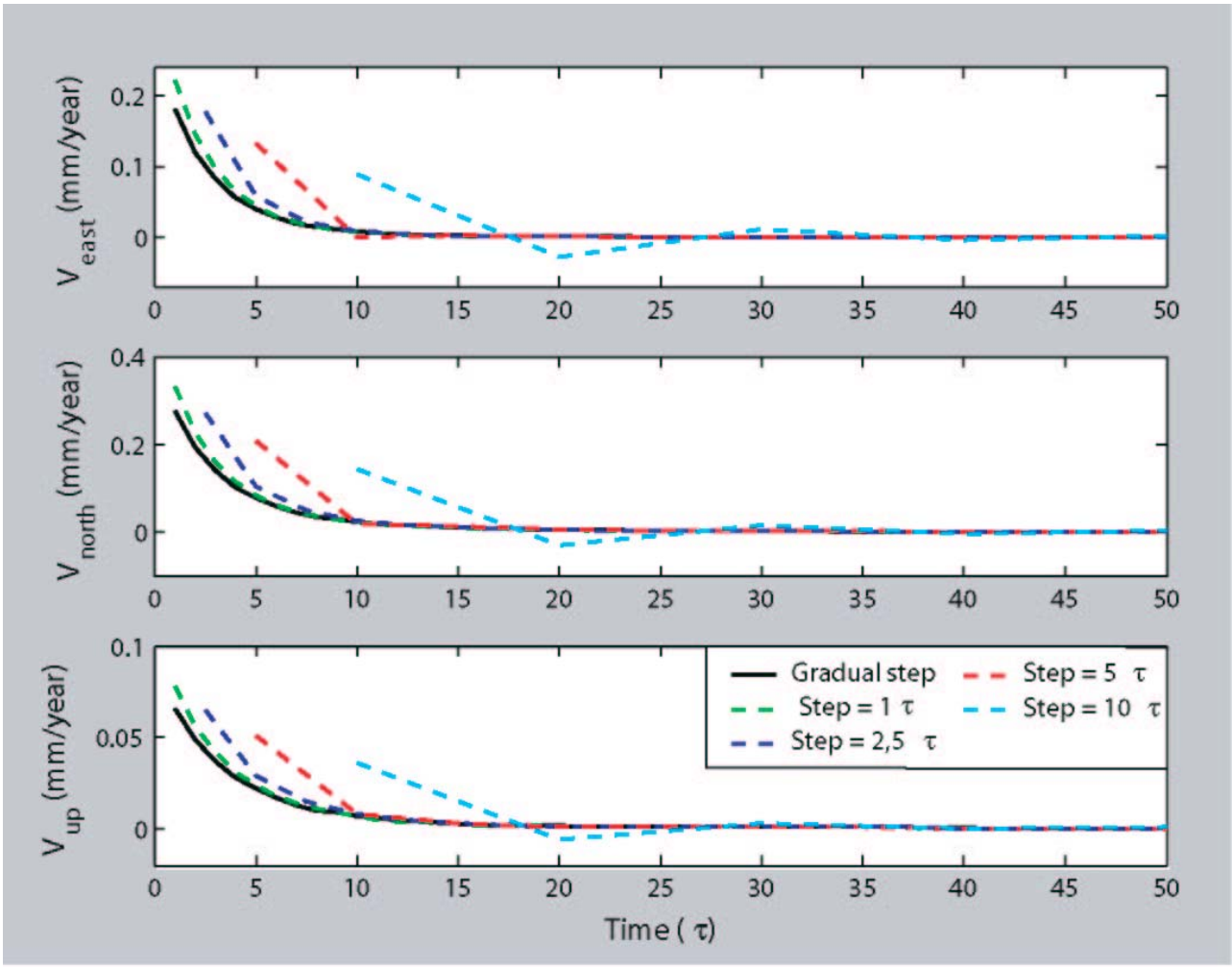

Figure 1.

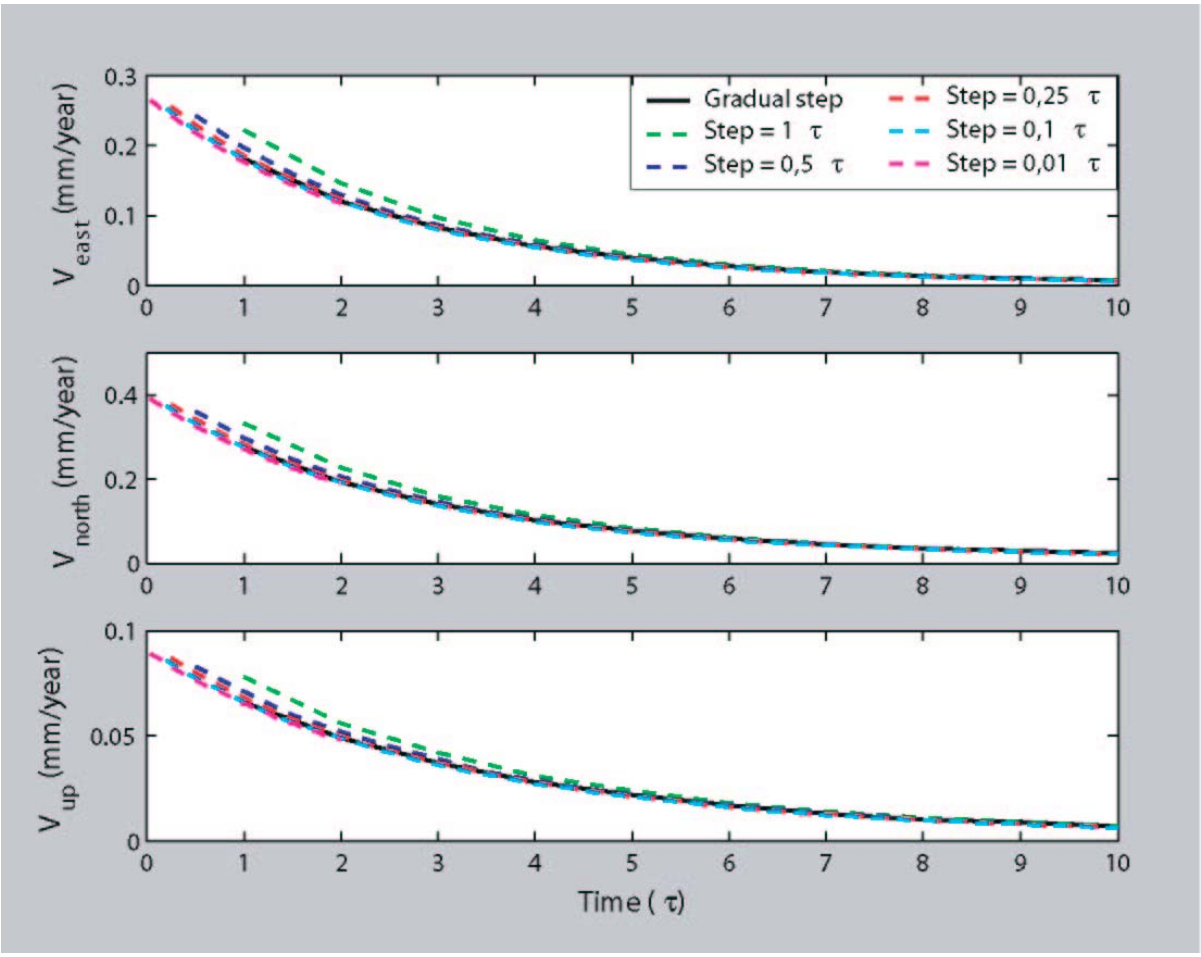

Figure 2.

Figure 3 shows that our Finite Element approach can reproduce an analytic solution to a visco-elastic relaxation problem [*Thatcher and Rundle*, 1984].

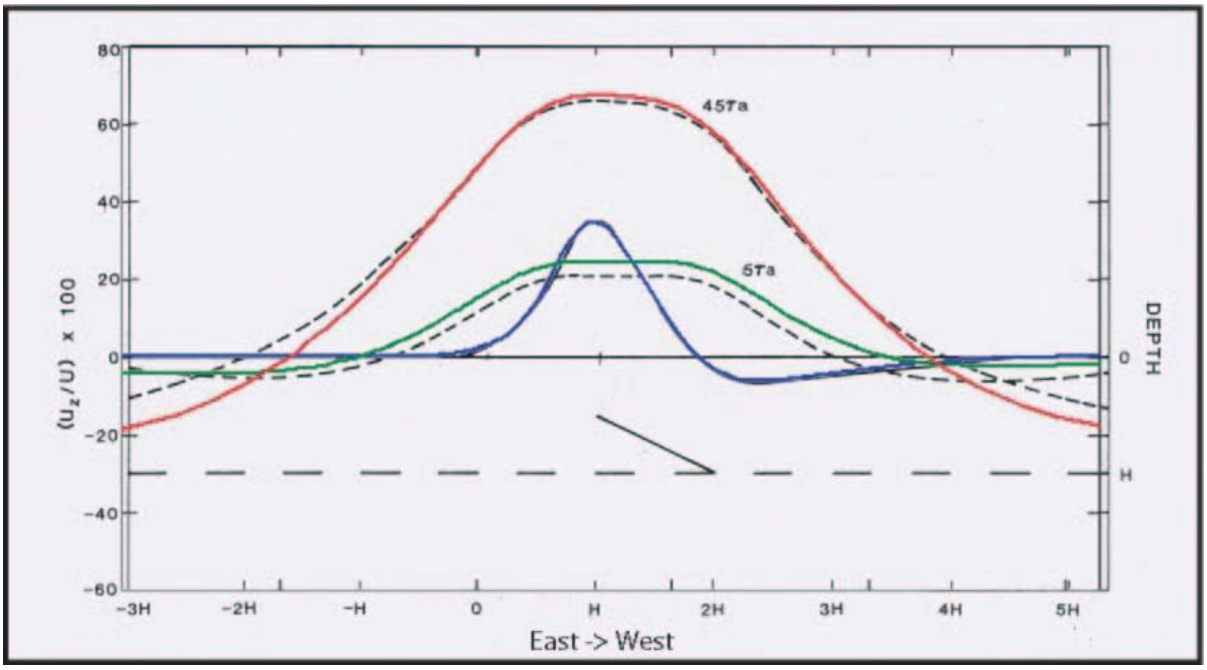

Figure 3.

Figure 4 shows that our Finite Element approach can reproduce the Coulomb Failure Stress field produced by the 17 June 2000 earthquake in Iceland [*Arnadottir, et al.*, 2003].

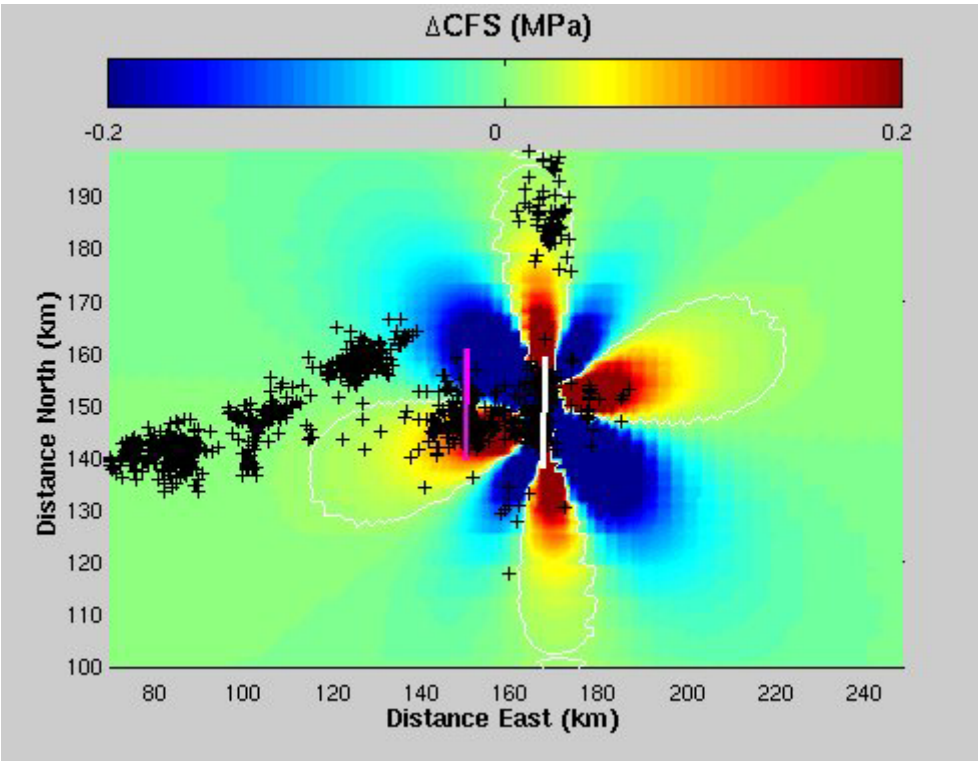

Figure 4.

We have submitted an abstract to the EGU meeting in Vienna (see below) in the PREPARED special session and will attend the PREPARED workshop.

References

Arnadottir, T., et al. (2003), Coulomb stress changes in the South Iceland Seismic Zone due to two large earthquakes in June 2000, Geophys. Res. Lett., 30, doi:10.1029/2002GL016495.

Thatcher, W., and J. B. Rundle (1984), A viscoelastic coupling model for the cyclic deformation due to periodically repeated earthquakes at subduction zones, J. Geophys. Res., 89, 7631-7640.

Abstract

Three-dimensional Finite Element calculations of co- and postseismic displacement and stress fields for hazard evaluation in the South Iceland Seismic Zone

Loïc Dubois,[1] Kurt L. Feigl,[1] Dimitri Komatitsch,[2] and Thora Árnadóttir[3]

(1) CNRS UMR 5562 Toulouse, France (2) University of Pau, France (3) Nordic Volcanological Centre, Institute Of Earth Sciences, Reykjavik, Iceland

(Loic.Dubois@ldtp.cnes.fr)

In June 2000, two magnitude 6.5 earthquakes ruptured two faults 17 km apart in the South Iceland Seismic Zone (SISZ). In addition to the co-seismic recordings , two geodetic datasets have recorded

the resulting post-seismic deformation on two different time scales: InSAR data over months and GPS over years. To explain the observed deformation, earlier models have made simple assumptions about the rheology and the geometry, such as an homogeneous elastic half-space for the coseismic model and horizontal visco-elastic layers for the post-seismic model. However, previous seismic studies have underlined the heterogeneous rheology and geometric complexity of the SISZ. Here, we attempt to account for these issues realistically using the finite element method (FEM). Extending recent FEM modeling on subduction zones to the transform zone SISZ, we use the TECTON code. By comparing our modeled displacement fields with observations, we evaluate the sensitivity of our model to parameters such as rheological characteristics (shear modulus, Poisson's ratio and viscosity) for the different lithospheric layers as well as to geometrical considerations (e.g., the dip of the interfaces between these layers). Our approach can also map static Coulomb stress for hazard evaluation as part of EU projects on risk management (PREPARED, RETINA and FORESIGHT).

Appendix 2

D79 Delivery report for workpackages 4.1 and 5.1
Catalogue of relocated earthquakes

Data

A catalogue of roughly nineteen thousand (19,180) relocated earthquakes in southwestern Iceland from the year 2000 is delivered for workpackages 4.1 and 5.1. The earthquakes are located using the relative location methods described in the First Periodic Report (Slunga et.al. 1995). The study area is divided into areas A-O, as shown in figure 1, and the method applied to events in each box seperately, using data only from stations with accurate timing. Where boxes overlap, duplicate events are removed, keeping the locations based on the greater number of groups, i.e. having greater location accuracy. In summary,

260 (1,36%) events in the catalogue are in one group,

896 (4.67%) events in the catalogue are in two groups,

1160 (6.04%) events in the catalogue are in three groups, and

16864 (87.93%) events in the catalogue are in four or more groups.

The time-span chosen for each box varied, depending on the number of events and the distribution of events in the boxes. A minimum magnitude limit was assigned according to the magnitude distribution of each box. Most events had a magnitude well above the allocated limit of each box, as described next.

Area	Time-span	minimum magnitude
A	June-December	0.01
B	June-December	0.01
C	January-December	-1
D	January-December	-1
E	January-December	-1
F	January-December	-1
G	June-December	-1
H	June-December	-1
I	June-December	-1
J	June-December	-1
K	June-December	-1
L	June-December	-1
M	June-December	-1
N	January-December	-1
O	January-December	-1

Catalogue file format

Description of fields in data distribution files: mlt

Field	
1-36	Event id, absolute (dir/id)
37-47	Event latitude [degrees]
48-59	Event longitude [degrees]
60-69	Event depth [km]
70-77	Median uncertainty in absolute latitude [km] (*)
78-85	Median uncertainty in absolute longitude [km] (*)
86-93	Median uncertainty in absolute depth [km] (*)
94-101	Median uncertainty in relative latitude [km] (*)
102-109	Median uncertainty in relative longitude [km] (*)
110-117	Median uncertainty in relative depth [km] (*)
118-125	Minimum "rms"-value of uncertainty in relative location [km] (1)
126-129	Nunber of groups event belongs to.
130-134	Origin time -year
135-137	Origin time -month
138-140	Origin time -day
141-143	Origin time -hour
144-146	Origin time -minute
147-154	Origin time -second
155-162	Local magnitude calculated from seismic moment according to (2)(**)

(1) Minimum rms relative location uncertainty is calculated according to
ru_rms = 0.333333*sqrt(relerrlat*relerrlat + relerrlon*relerrlon + 0.5*relerrdep*relerrdep)

where *relerrlat* is relative uncertainty in latitude, *relerrlon* is relative uncertainty in longitude and
relerrdep is relative uncertainty in depth.

(2) m = log10(Mo) - 10

Mlw = m	if	Mlw <= 2.0
Mlw = 2.0 + (m-a)*0.9		2.0 < Mlw <= 3.0
Mlw = 3.0 + (m-a-b)*0.8		3.0 < Mlw <= 4.6
Mlw = 4.6 + (m-a-b-c)*0.7		4.6 < Mlw <= 5.4
Mlw = 5.4 + (m-a-b-c-d)*0.5		5.4 < Mlw <= 5.9
Mlw = 5.9 + (m-a-b-c-d-e)*0.4		5.9 < Mlw <= 6.3
Mlw = 6.3 + (m-a-b-c-d-e-f)*0.35		6.3 < Mlw

where Mo = seismic moment in Nm and
a = 2, b = 1/0.9, c = 1.6/0.8, d = 0.8/0.7, e = f = 1

For additional information see:
Ragnar Slunga, Peter Norrman, Ann--Christine Glans, 1984: Seismicity of Southern Sweden. - Stockholm : Försvarets Forskningsanstalt, July 1984. - 106 p. FOA report ; C2 C 20543-T1.

(*) The median of uncertainties from all groups the event is found in.

(**)Magnitudes >= 4 may be poorly estimated.
Magnitudes of the largest events can be severely underestimated. If so, their magnitudes get the suffix *.

Small events riding on top of waves from the large events are often overestimated. In such cases the local magnitude, calculated according to (3), is used and the magnitude gets the suffix L.

Magnitude is replaced by a ** in the last column where neither moment- nor local magnitude could be properly estimated.

-9.99: No waveforms available for magnitude estimation.

(a) M = log10(amp) + 2.1 * log10(dist.-in-km) -4.8,
where amplitude is estimated in a 10 second window around the S arrival.

Reference

Slunga, R., Rögnvaldsson, S. Th., Böðvarsson, R., 1995. Absolute and relative locations of similar events with application to microearthquakes in southern Iceland, Geophys. J. Int., 123, 409-419.

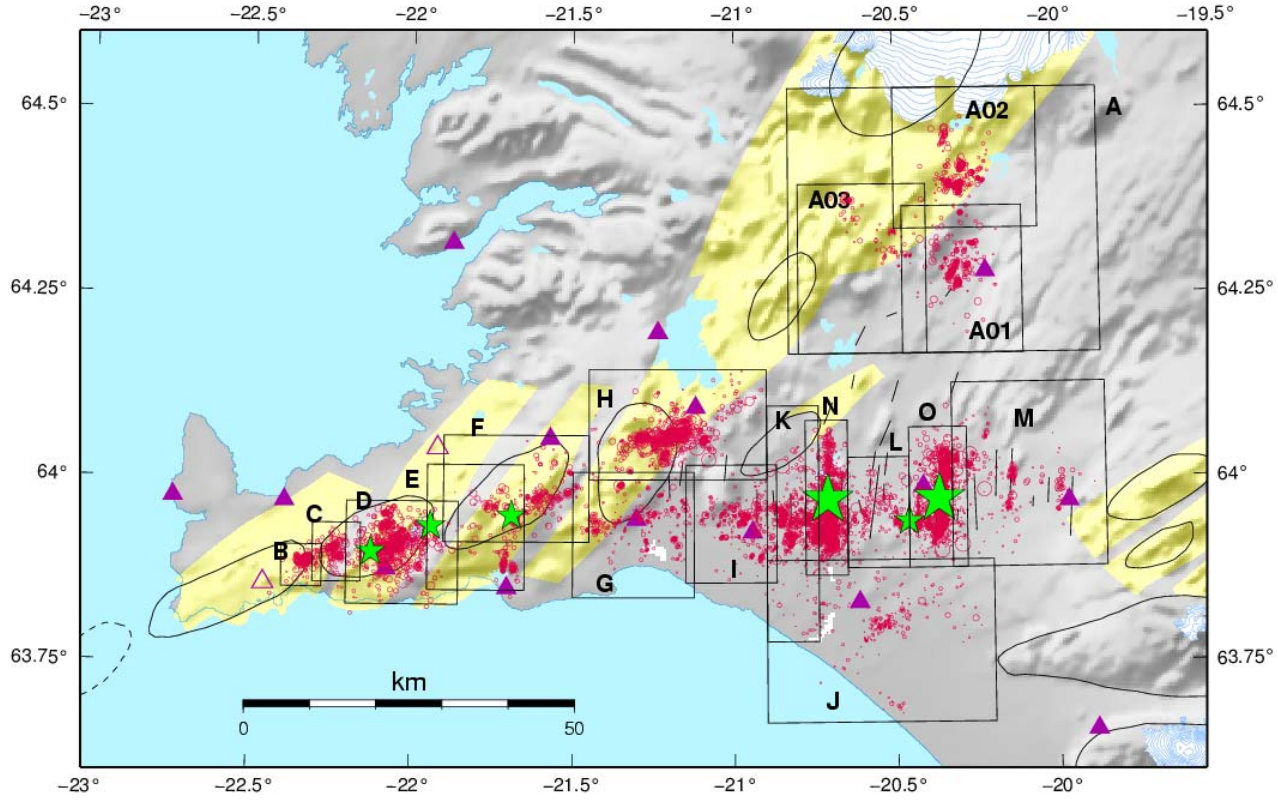

Figure 1. *Map of southwest Iceland showing the locations of boxes used for grouping epicentres. The red circles show epicentral locations, and the green stars signify earthquakes greater than magnitude 5. Seismic stations are shown as purple triangles (filled triangles: stations still in use).*